University of Essex

Biological Sciences at the University of Essex

Cell surface interactions of Coxsackie A9 virus

Marina Ioannou

A thesis submitted for the degree of Doctor of Philosophy in Molecular Medicine

School of Biological Sciences

University of Essex

October 2017

After climbing a great hill, one only finds that there are many more hills to climb.

–Nelson Mandela

This thesis is dedicated to all people, as a reminder that one can achieve anything he sets his heart to, no matter how big or small he feels.

Table of Contents

Acknowledgements

My PhD journey has been an amazing roller coaster experience full of all kind of emotions;, frustration, self-doubt, stress, happiness, joy, hard work and dedication. I am blessed to have had the opportunity to embark on a PhD, the highest academic qualification one can achieve. I thank God Almighty for this opportunity and for all His blessings and grace, the strength, power and patience He granted me to successfully end my journey.

I would like to express my deepest appreciation to Professor Glyn Stanway whose guidance, patience, encouragement, constant feedback and evaluated criticism made this PhD work possible.

To Dr. Nusaiba Baeshen, Dr. Ashjan Shami, Dr. Ali Khrid, Dr. Cheryl Eno-Ibanga and Mr. Osamah Hasan who have shared the same lab these 4 lovely years of my PhD and made this experience unique and unforgettable, for all their help and guidance, all the happy moments, all the lab meetings and for all the memories, a special debt of

gratitude is due. It has been an amazing journey and I wouldn't have asked for better people to share it with. Cheers to 5.14 family.

Special thanks to Mrs. Natalie Grey and Mrs. Hannah Adams for all their technical help and happy environment.

A special note of thanks to my dearest friend and lab member Dr. Cheryl; we've spend endless nights proof reading, supporting and encouraging each other, not only in lab life but also in personal. Thank you for the memories, may God bless you with abundance of happiness and joy in your life.

I am grateful to my parents and family for their financial support that allowed me to pursue my dreams but also for their patience, encouragement, endless love, guidance and prayers.

Last but not least, a huge thank you to my lovely hubby Mr. Christos Kaniklis. Only you know my daily struggles and fights, sleepless nights and hard work that went to this research. You have been next to me

through ups and downs supporting me and loving me and I will be forever grateful. Love you

Abstract

An understanding of how viruses interact with their receptors is vital as this step is a major determinant of host susceptibility and disease. Coxsackievirus A9 (CAV9), an enterovirus, harbours an integrin- recognition motif, RGD (Arg-Gly-Asp), in the capsid protein VP1 and although modes of transmission and pathogenesis are still largely unknown, this motif is believed to be primarily responsible for integrins αvβ6 and αvβ3 binding. The conservation of the RGD +1 position in CAV9 and other picornaviruses showed evidence that this is related to viral tropism and infectiousness of the virus. CAV9 has also been reported to interact with the heparan sulphate/heparin class of proteoglycans (HSPG). This thesis describes work designed to improve our understanding of the involvement of a) the RGD motif and more specifically the RGDX position in CAV9 infection, using a large panel of different RGDX variants and a number of cell lines not previously used in CAV9 research b) the significance of possible interactions between CAV9 and HSPG in infection. Several CAV9 variants were tested in a panel of 8 different cell lines. Infection in each cell line was observed to follow either an RGD- dependant or RGD- independent pathway, although the results did not fully correlate with the receptor expression found on the cell lines used. The RGDX position was found to be critical for efficient infection in cells when an RGD-dependent pathway is used. To understand which integrin is likely to be involved in entry, into one of the RGD-dependent cell lines, A549, blocking antibodies against αvβ3 and αvβ6 were used. Neither antibody gave full protection against CAV9, as has been reported previously, suggesting that other integrins might also be used. Two new HSPG-binding CAV9 mutants were discovered, showing that binding to HSPG can be

achieved by several mechanisms. Binding to HSPG was found to be significant in some cells, but not others, again illustrating the complexity of interactions between CAV9 and the cell surface. The results obtained have greatly improved our understanding of how CAV9 infects cells. This will be useful in the design of antivirus drugs and also gives a framework for the modification of CAV9 or other RGD containing picornaviruses for specific targeting of cancer cells for oncolytic therapy.

Abbreviations

A549	Human Lung Adenocarcinoma Epithelial Cell Line
Arf6	ADP-ribosylation Factor 6
Bp	Base pair
CAR	Coxsackievirus and Adenovirus Receptor
CCP	Clathrin-coated Pit
CCV	Clathrin-coated Vesicle
cDNA	Complementary DNA
CMC	Carboxymethyl Cellulose
CME	Clathrin-Mediated Endocytosis
CNS	Central Nervous System
CPE	Cytopathic Effect
CAV	Coxsackie virus A
CAV9	Coxsackievirus A9

CVB	Coxsackie virus B
DAF	Decay Accelerating Factor, known as CD55
DMEM	Dulbecco’s Modified Eagle's Medium
DMSO	Dimethyl Sulfoxide
DNA	Deoxyribonucleic Acid
E11	Echovirus 11
Echovirus	Enteric Cytopathogenic Human Orphan Virus; ECHO
ECM	Extracellular Matrix
EDTA	Ethylenediaminetetraacetic Acid
eIF4GI	Eukaryotic Translation Initiation Factor 4GI
ELFO	Electrophoresis buffer
ERBV	Erbovirus
EV	Enterovirus
FACS	Fluorescence Activated Cell Sorting
FBS	Foetal Bovine Serum

FMD	Foot-and-Mouth Disease
FMDV	Foot-and-Mouth Disease Virus
GAG	Glycosaminoglycan
GMK	Green Monkey Kidney Epithelial Cells
GPI	Glycosylphosphatidyl Inositol
GRP78	Glucose-regulated Protein 78
HAV	Hepatitis A Virus
HAVcr1	Hepatitis A Virus cellular receptor 1
HeLa	Human Epithelial Cervical Cancer Cell Line (Henrietta Lacks)
HEVs	Human Enteroviruses
HFMD	Hand-Foot-and-Mouth Disease
HLA	Human Leucocyte Antigen
HPeV	Human Parechovirus
HPV	Human Papillomavirus
HRV	Human Rhinovirus

HS	Heparan Sulphate
HSPG	Heparan Sulphate Proteoglycan
HSV	Herpes Simplex Virus
ICAM-1	Intracellular Adhesion Molecule-1
IFN	Interferon
Ig	Immunoglobulin
IgG	Class G Immunoglobulin
IRES	Internal Ribosome Entry Site
Kb	Kilo base
L-protein	Leader Protein
LDLR	Low Density Lipoprotein Receptor
MAb	Monoclonal Antibody
MCF-7	Human Breast Adenocarcinoma Cell Line
MDA-MB-231	Human Breast Adenocarcinoma Cell Line
MDA-MB-435	Human Melanoma Cell Line

MHC	Major Histocompatibility Complex
mRNA	Messenger RNA
N-terminus	Amino-terminus of Protein
NEAA	Non-essential Amino Acids
ORF	Open Reading Frame
Oril	Origin of replication internal
OV	Oncolytic Virotherapy
PBS	Phosphate Buffer Saline
PC-3	Human adenocarcinoma prostate cancer cell lines
PE	Phycoerythrin, Fluorescent Dye
PFU	Plaque Forming Unit
PSGL-1	Human P-selectin Glycoprotein Ligand-1
PV	Poliovirus
PVR	Poliovirus Receptor, known as CD155

RD	Human Rhabdomyosarcoma Cell Line
RGD	Arginine-Glycine-Aspartic acid
RNA	Ribonucleic Acid
RT	Room temperature
RT-PCR	Reverse Transcription Polymerase Chain Reaction
SA	Sialic Acid
SCARB2	Human Scavenger Receptor Class B Number 2
SCR	Short Consensus Repeat
ss	Single Strand
SVDV	Swine Vesicular Disease Virus
TMEV	Theiler’s murine encephalomyelitis virus
UTR	Untranslated Region
VCAM-1	Vascular Cell Adhesion Molecule 1
VLDL-R	Very Low Density Lipoprotein Receptor
VP	Viral Protein

VPg	Viral Protein Genome-liked
WT	Wild Type
β2M	β2-microglobulin

List of original publications

- Ioannou, M., Hughes, P, and Stanway, G. (in preparation) **Tropism of Coxsackie virus A9 depends on the +1 position of RGD (arginine- glycine- aspartic acid) motif found at the C' terminus of its VP1 capsid protein.**

- Ioannou, M., Baechen, N., Ivanova, M, and Stanway, G. (in preparation) **Analysis of heparan sulphate binding to Coxsackievirus A9.**

List of Figures

List of Tables

Chapter 1. Review of the Literature

1.1.Introduction

The family of *Picornaviridae* (commonly known as picornaviruses) is considered to be the oldest known to man, as a written record dating back to 3700 BC was found in Memphis, the capital city of ancient Egypt. A hieroglyph shows a temple priest called Ruma exhibiting the typical clinical characteristics of paralytic poliomyelitis due to poliovirus infection (Figure 1.1). Interestingly, in 1905 when the tomb of a young Pharaoh named Siptah, who ruled Egypt from 1200 – 1193 BC, was excavated, his mummified body showed also signs of paralytic poliomyelitis. His left leg was emaciated and his foot was tightly extended like a horse's hoof (Elder *et al.*, 2005; Faraj, 2006). The first 'modern day' discovery of a virus was announced in 1892 by a Russian botanist Dmitri Iosifovich Ivanovsky. Ivanovsky was unaware of the significance his discovery at that moment, but he noticed that a filterable agent (i.e. smaller than a bacterium) could cause disease in a healthy tobacco plant. Friedrich Loeffler and Paul Frosch made another striking discovery in 1898 when they detected a minute agent able to pass through a bacteria-proof filter causing disease in cattle (Smith, 1943). It was later identified as Foot- and- mouth- disease virus (FMDV), a picornavirus.

Picornaviruses that infect humans are now known to form one of the largest virus groups with more than three hundred virus types. They include significant pathogens such as rhino-, polio-, echo-, coxsackie-, hepato-, kobu- and parecho- viruses that cause wide range of disease symptoms. A large number of agriculturally-important animal pathogens have also been found to be picornaviruses, including FMDV, swine

vesicular disease virus, teschoviruses, avian encephalitis virus and duck hepatitis virus. Despite the economic importance of picornaviruses, there are no widely-used, effective antivirals. At present, there are vaccines directed against two human picornaviruses, poliovirus and hepatitis A virus. The oral, attenuated vaccines against the 3 poliovirus serotypes, which has been widely-used for many years, is being replaced in most countries by inactivated vaccines, as part of the strategy leading to poliovirus eradication. The inactivated polio vaccines and the hepatitis A vaccine are based on formaldehyde inactivated whole viruses (Sanders *et al.*, 2015).

The interaction between a virus and its receptor is a potentially important target for antivirals. Despite the fact that scientists have identified more than ten cellular receptors involved in picornavirus infection, their role in cellular infection has not been characterized for all picornavirus types. A sub-set of enteroviruses, together with many human parechoviruses and FMDV have experimentally been shown to bind and use integrin receptors in cellular infection, via an arginine-glycine-aspartic acid (RGD) motif in the virus particle. An understanding of the role of this motif in infection is important for understanding pathogenesis and potentially for antiviral design.

Figure 1.1: A hieroglyph artefact from Memphis, Egypt, dating back to 3700 BC.

This is the first written record of a virus infection showing Ruma, a temple priest with typical clinical characteristics of paralytic poliomyelitis (Major, 1954).

1.2.Viruses

1.2.1. Introduction to viruses

Viruses are known as small infectious agents that only replicate inside living cells- host cells. Because viruses can only replicate in their host cells there is a lot of debate amongst scientist on whether viruses are alive or not. As viruses do not have a required degree of biochemical autonomy or metabolic activities to produce molecules or metabolic energy, they are usually considered to be not alive (Villarreal, 2004). Viruses consist of a genome of either RNA or DNA (single or double stranded) which is enclosed by a protective capsid protein coat and sometimes is surrounded by an outer membrane (envelope). This structure is referred as a virion (Gelderblom, 1996). Most viruses were thought to have a diameter ranging from 20 nm- 200 nm and an overall very compact structure, but over the past few years larger viruses, including mimivirus and megavirus, have been discovered with a capsid of 400 nm and an overall diameter up to 800 nm when the network of fibrils projecting from the capsid are included (Klose *et al.*, 2010). The viral envelope is a lipid bilayer with glycosylated (trans-) membrane virus protein spikes, which are important in defining the host range and are major antigenic determinants of the virion (Gelderblom, 1996). These glycoprotein spikes present on the viral envelope help the viral attachment to the surface of target cells by interacting with specific receptors, and are also critical for fusing the envelope with the cell membrane or endosomal membrane, to allow virus entry and uncoating of the genome (Chazal & Gerlier, 2003). In viruses lacking an envelope (naked viruses), the

capsid proteins include receptor binding domains. Virus particles include a genome of one kind of nucleic acid which can be dsDNA, ssDNA, dsRNA or ssRNA. ssRNA viruses differ according to whether the genome RNA acts as messenger RNA (mRNA) for translation of the viral proteins or not. Thus, a positive sense RNA (+RNA) acts as mRNA, while negative sense RNA (-RNA) needs to be copied by an RNA- dependent RNA polymerase enzyme for the production of mRNA complementary to the RNA of the virus for viral protein synthesis**.** Retroviruses have a ssRNA genome, but this needs to be copied to dsDNA and integrated into the host cell genome, in the early stages of replication, while pararetroviruses have a dsDNA genome, which is transcribed to give a ssRNA copy which is then copied to dsDNA during replication (Nisole & Saïb, 2004).

1.2.2.Classification of viruses

In the early years when viruses started to be discovered they were named after the disease they caused, the affected body sites where the virus was isolated, after cities, rivers etc. or even after the scientists who first isolated them (Lwoff *et al.*, 1962). Serotype was, and still is, a major way of defining the immediate group of viruses to which a virus belongs. As no broader system for classifying viruses was present, in the early 60s Lwoff and Tournier suggested that classification of viruses should be according to the classical Linnaean hierarchical system of phylum, class, order, family, genus and species which resulted in viruses being grouped based on their properties and their genome and not the cells they infect (Lwoff *et al.*, 1962). The four important criteria used for the classification were morphology (symmetry of the protein shell, presence or absence of lipid membrane), size of the virion, chemical composition and

mode of replication (type of host) (Mahy & Van Regenmortel, 2010). Viruses can be divided into three groups according to their nucleocapsid morphology and capsomere arrangement: rod shaped viruses with helical symmetry, spherical viruses with icosahedral symmetry and, pleomorphic viruses with complex structure. In the early 70s David Baltimore proposed an alternative classification system based on the nature of the viral nucleic acid rather than physical and biological criteria. The Baltimore classification originally divided the viruses into six groups (Baltimore, 1971) and the seventh group was added in the following years. Baltimore not only divided viruses to these groups according to their genome but also according to their translational mechanism and importance of viral mRNA. As viruses can have DNA or RNA as genetic material the first two classes of viruses are the ones possessing a DNA genome, Class I for double- stranded (ds) DNA and Class II for single- stranded (ss) DNA viruses. Class III consists of dsRNA viruses, Class IV includes ssRNA viruses where the viral mRNA is identical to virion RNA (Baltimore, 1971). Class V includes viruses with ssRNA complementary to mRNA, Class VI consists of ssRNA viruses that require a reverse transcriptase to convert +RNA to DNA. Although class VII viruses have dsDNA genome they also require a reverse transcriptase during replication.

As more sequence data became available, it became clear that some of the previously used criteria are not reliable in classification and now classification is mainly based on sequence identities. Nowadays, the International Committee on the Taxonomy of Viruses (ICTV) is responsible for the classification of viruses. ICTV curates a database showing relationships among viruses (Büchen-Osmond, 2003). There are more than 30,000 different viruses known and according to ICTV there are 122 different families;

37 families belong to 8 different orders and 85 viral families have not been assigned to an order yet ***(www.ictvonline.org*** as on 20.09.17***).*** Orders are, *Bunyavirales Caudovirales, Herpesvirales, Ligamenvirales, Mononegavirales, Nidovirales, Picornavirales* and *Tymovirales. 735 genera and 4404 species are recognised* (Adams *et al.*, 2017). Order names and families are italicized and end in Latin suffix –*virales* and –*viridae* respectively, while genera end in –*virus*, subfamilies end in – *virinae* and species have a common English name, including the word -*virus*.

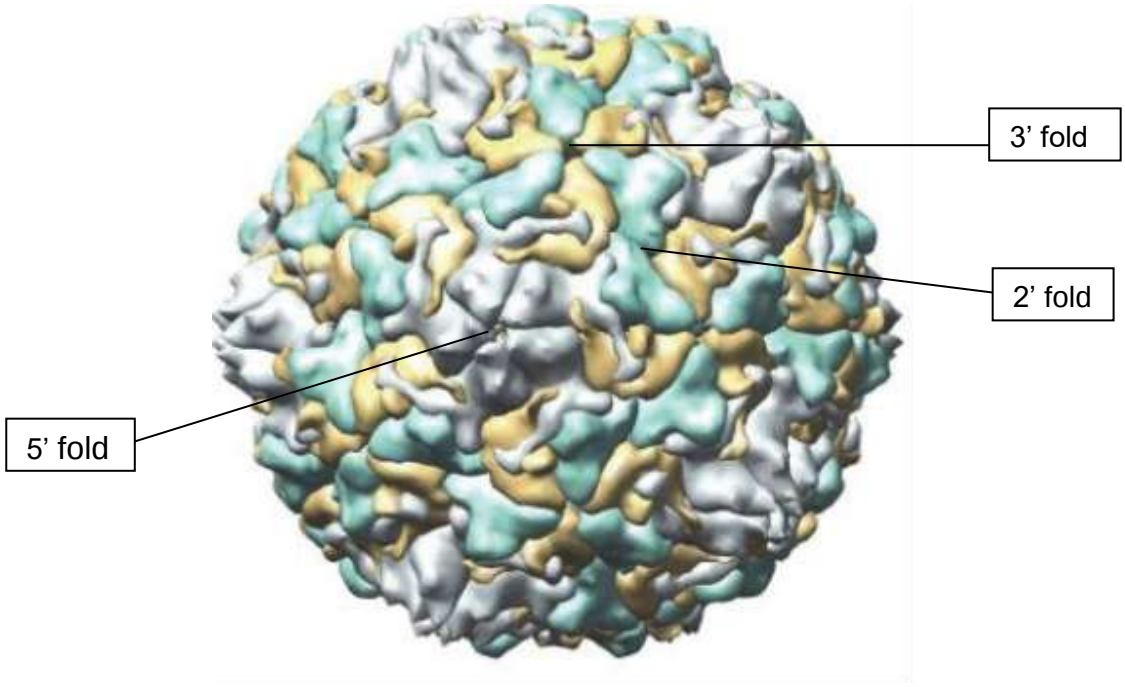

Figure1.2: Model of the crystal structure of a typical picornavirus, coxsackievirus A9. (Hendry *et al.*, 1999)

VP1, VP2 and VP3 are shown in grey, turquoise and gold respectively. The three different axes of symmetry are the 5’ fold, 3’ fold and 2’ fold as shown above.

1.3.Picornaviruses

1.3.1.Introduction to picornaviruses

Picornaviruses are non- enveloped (naked), positive sense ssRNA viruses with an icosahedral protein capsid with a diameter of 30 nm approximately (**Figure 1.2**). Their range of biological, physical and genetic characteristics classifies them in a family of RNA viruses, the *Picornaviridae*. The *Picornaviridae* family is one of the largest taxonomic families in the history of viruses and 'home' to some of the smallest known viruses. Their name derives from '*pico*'; a prefix in denoting one million- millionth (10^{-12}) i.e a very small quantity, and '*rna*' for their type of genetic material. The *Picornaviridae* family (order *Picornavirales*) compromises 31 genera (*Ampi-*, *Aphtho-, Aqua-, Avisi-, Avihepato-, Cardio-, Cosa-, Dicipi-, Entero-, Erbo-, Galli-, Harka-, Hepato, Hunni-, Kobu-, Mergi-, Mischi-, Mosa-, Osci-, Parecho-, Pasi-, Passeri-, Potamipi-, Rabo-, Rosa-, Sakobu-, Sali-, Sapelo-, Seneca-, Sicini-, Tescho-, Torchi-,* and *Tremoviruses*) where each genus is sub- divided into species which include the individual viral serotypes (Knowles *et al.*, 2012a; Adams *et al.*, 2015, 2016) (http://www.picornaviridae.com). They cause a wide variety of diseases. Classification of the picornaviruses used to be according to their biophysical properties, pathogenesis and antigenic properties (Hyypia *et al.*, 1997) while nowadays their genomic sequence is the primary key for their taxonomy. However, some picornavirus names relate to the tissue they tend to infect; for example '*Hepatovirus*' derives from hepatos a Greek word for liver, *Enterovirus* from enteron a Greek word for intestine and *Aphthovirus* from

aphtha which in Greek means vesicles in the mouth. According to Knowles et al., (Knowles *et al.*, 2012b) the number of known picornaviruses has increased by 40% in the last two decades and due to the lack of insufficient detection methods, control measurement against most picornaviruses exist only in theory. No approved drugs exist against picornaviruses although pleconaril and fluoxetine have been used to treat individual cases (Wildenbeest *et al.*, 2011; Gofshteyn *et al.*, 2016). Only three viruses are controlled by vaccines; poliovirus, hepatitis A virus and FMDV. Picornaviruses are Class IV viruses as they consist of a positive (+) single stranded RNA which functions as mRNA for protein synthesis once it is released into the host cell (Carter & Saunders, 2007).

1.3.2.Medical and economic importance of picornaviruses

Picornaviruses can infect both animals and humans; however human infections have only been reported (up to date) by members of the genera *Enterovirus, Cardiovirus, Cosavirus, Aphthovirus, Parechovirus, Hepatovirus, Salivirus and Kobuvirus* (King *et al.*, 2011). Rhinoviruses infect humans more frequently than any other virus, poliovirus has paralysed or killed millions of people over time and foot-and-mouth-disease virus threatens livestock all over the world with outbreaks causing huge economic loses (Salguero *et al.*, 2005; Whitton *et al.*, 2005). In terms of clinical significance in humans, enteroviruses and rhinoviruses (both members of the *Enterovirus* genus) are the most clinically important picornaviruses and cause a huge number of infections every year. Infections caused by enteroviruses vary in severity from asymptomatic to aseptic meningitis, encephalitis, paralysis, pneumonia, myocarditis and possibly even diabetes

type I (Stanway *et al.*, 2000; McMinn, 2002; Sawyer, 2002; Harvala *et al.*, 2003; Hober & Sauter, 2010; Hober & Alidjinou, 2013). Rhinoviruses are mostly responsible for common cold infections (up to 80% of these illness are associated with rhinovirus infection). The medical implications of rhinovirus infection are not, however, limited to the common cold. Rhinovirus can be associated with upper respiratory tract syndrome, acute otitis in children, (where 25% of affected children have evidence of virus in the middle ear fluid (Pitkäranta *et al.*, 1997)), and lower respiratory tract syndrome. They make the symptoms of asthma, cystic fibrosis in children and chronic bronchitis in adults more serious (Turner, 2007).

1.3.3. Structure of the virion

Picornaviruses are composed of a protective protein shell, the capsid which is made of 60 copies of each structural protein VP1- VP4 (Hogle *et al.*, 1985; Rossmann *et al.*, 1985) or in the case of parechoviruses and a few other genera VP0, VP1 and VP3 (Stanway *et al.*, 1994). This protects the RNA genome from degradation by nucleases and contains sites needed for interaction with cell receptors. Since picornaviruses have a very small genome they use several copies of the same protein for assembling into a symmetric, icosahedral structure where all subunits occupy the same environment. The VP4 capsid protein is the smallest protein with around 70 residues and X- ray crystallography revealed that it lies on the inside of the capsid (Rossmann *et al.*, 1985; Muckelbauer *et al.*, 1995) while VP1, VP2 and VP3 are composed of approximately 270 amino acids. These are each folded into eight- stranded antiparallel β- sheet structures and form the outer surface of the virus (Hendry *et al.*, 1999). Many

picornaviruses, have a characteristic deep cleft called the canyon approximately 2 nm deep around each of the twelve pentamers, (Rossmann *et al.*, 1985; Carter & Saunders, 2007). These canyons are found to be lined by the C- terminus of the VP1 and VP3 capsid proteins separating the 'surface- orientated protrusion' of VP1 from VP3 (Tuthill *et al.*, 2010) and play a significant role in viral attachment as they contain the attachment sites of the virus.

Interestingly, in some picornaviruses such as enteroviruses, a lipid molecule called a pocket factor was identified within a hydrophobic pocket in the VP1 β- barrel. This pocket is located underneath the canyon (Hogle *et al.*, 1985; Rossmann *et al.*, 1985; Hendry *et al.*, 1999). The pocket factor is known to provide capsid stability and is removed during interactions with the receptor, as a key step in uncoating. Drugs have been designed to replace the pocket factor in the hydrophobic pocket and to bind tightly so that they cannot be displaced during interactions with the receptor, so preventing uncoating (Plevka *et al.*, 2013). VP1 is also suggested to be involved in triggering RNA release (Ren *et al.*, 2013).VP1 is located at the 5'- fold axes and is the major surface accessible protein (Oberste *et al.*, 1999) while VP2 and VP3 alternate around the 3'- fold axes (Tuthill *et al.*, 2010) **(Figure 1.2 and 1.3)**.

Five copies of each capsid protein forms a pentagon- shaped pentamer, while twelve copies of pentamers result in the formation of a complete icosahedral viral capsid (Carter & Saunders, 2007). Loops between β- strands are variable and are found mainly in the surface of the virus where they define antigenic properties, as some of the loops contribute to specific antigenic neutralization sites (Oberste *et al.*, 1999).

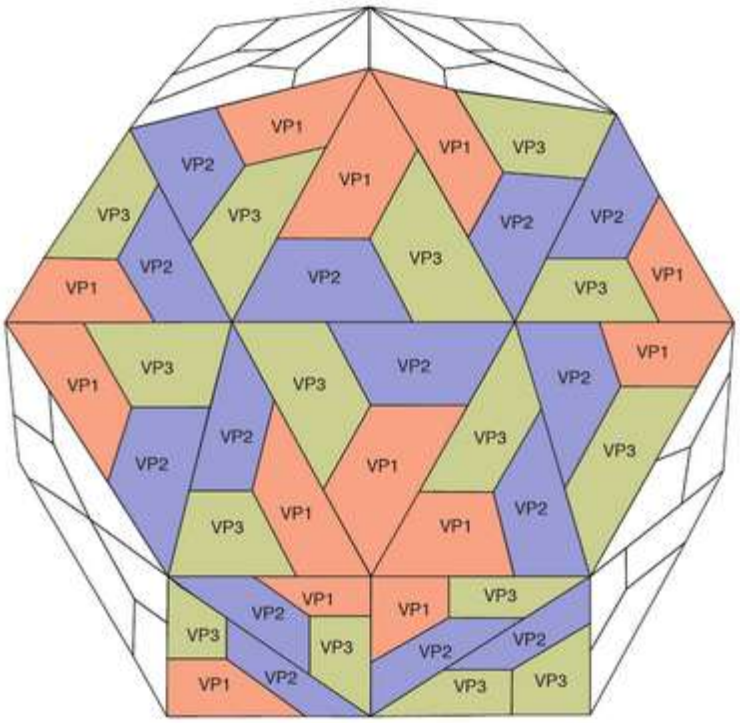

Figure 1.3: Icosahedral Picornavirus Particle.

All picornaviruses have icosahedral capsids approximately 30 nm diameter with triangulation number pseudo T= 3. The capsid is composed of 60 repeated subassemblies of proteins, each containing three major subunits, VP1 (shown in pink), VP2 (shown in blue) and VP3 (shown in green). A fourth protein, VP4, is not exposed on the surface of the virion but is present in each of the 60 repeated units that make up the capsid. (Taken from (Cann, 2012)).

1.3.4. The viral genome

The picornavirus genome organization is highly conserved and is a key characteristic of the family (**Figure 1.4**). Picornaviral ssRNA varies in length between approximately 7000-9700 nucleotides in different genera. The RNA is positive sense hence it is itself infectious and serves as a messenger RNA inside the host cell (Carter & Saunders, 2007; Palmenberg *et al.*, 2010). At the 5' end of the genome there is a small peptide called VPg (Viral Protein of the genome) covalently bonded via a tyrosine hydroxyl and phosphodiester bond (Tuthill *et al.*, 2010). The 3' end is polyadenylated (has a Poly-A tail) and this tail varies in length among species (Palmenberg *et al.*, 2010). The viral genome consists of three regions: the 5' untranslated region (5' UTR), the open reading frame (ORF) or coding region and the 3' untranslated region (3' UTR) (Tuthill *et al.*, 2010). The 5' UTR is a very complex region approximately 600-1200 nucleotides long containing structural elements important for replication and translation. The first ~100 nucleotides of the enterovirus and rhinovirus 5'-UTR contains a 'cloverleaf' structure which is an absolute requirement for viral RNA replication. The second important feature of 5'- UTR is the internal ribosome entry site (IRES) which directs the initiation of translation process (Lin *et al.*, 2009).

On the other hand, the specific function of the 3' UTR is still unknown, although it has been implicated in both translation and replication. In enteroviruses it contains a tertiary structure known as kissing interaction (Mirmomeni *et al.*, 1997).

In the best- studied picornavirus, poliovirus, the ORF region encodes a single polyprotein which contains 11 final proteins named 1A (VP4), 1B (VP2), 1C (VP3), 1D

(VP1), 2A, 2B, 2C, 3A, 3B, 3C and 3D (**Figure 1.4**) (Hyypia & Stanway, 1993). After translation, cleavage of the polyprotein is achieved through the action of proteinases such as $2A^{pro}$, $3C^{pro}$, and $3CD^{pro}$ where $3CD^{pro}$ can be further cleaved into $3C^{pro}$ and $3D^{pol}$ (Kerkvliet *et al.*, 2010). $3D^{pol}$ is an RNA- dependent RNA polymerase responsible for synthesis of first negative sense RNA (–ss RNA), then positive sense (+ss RNA) (new virus genome). The RNA-dependent RNA polymerase is estimated to make an error of one or two bases every time the genome is copied, which is the key factor of the high mutational rate and evolution of the virus (Solomon *et al.*, 2010). In poliovirus and other enteroviruses, co-translational cleavage by $2A^{pro}$ is the first (primary) cleavage of the polyprotein and results in the release of the precursor protein P1. P1 is cleaved by $3CD^{pro}$ then produces VP1, VP3 and the immature VP0. After assembly, VP0 is auto-cleaved producing VP2 and VP4. In the P2 region, 2B and 2BC are responsible for altering the membrane of infected cells, while 3AB is involved in the inhibition of cellular protein secretion. $3CD^{pro}$ performs the cleavage of P1 and $3C^{pro}$ cleaves the majority of the polyprotein (Lin *et al.*, 2009). Although poliovirus has mostly similar features to other viruses in the family not all picornaviruses encode exactly the same proteins (Hughes & Stanway, 2000).

The 5’ UTR

The 5’ UTR is a structurally complex part of the picornavirus genome, made up of several secondary and tertiary RNA structures (Martínez-Salas, 2008; Lin *et al.*, 2009). The 5’ UTR is 600- 1200 nucleotides long in different picornaviruses and has been reported to be significant in translation (Pelletier & Sonenberg, 1985) and RNA replication (Rohll *et al.*, 1994). It also plays role in defining virulence/ attenuation, for

example a key attenuating mutation is present in the 5'UTR of all 3 attenuated poliovirus vaccine strains (Evans *et al.*, 1985). Within the 5'UTR there are two well-defined functional domains important for virus replication (Palmenberg *et al.*, 2010). The 5′ UTR's largest part forms the internal ribosome entry site (IRES), a large domain made up from several secondary structures, which is important in the cap- independent initiation of translation (Martínez-Salas, 2008; Fernández-Miragall *et al.*, 2009; Tuthill *et al.*, 2010). It acts as a 'landing pad' for ribosomes to initiate translation (Pelletier & Sonenberg, 1985; Jang *et al.*, 1988). Most 5' ends of cellular mRNAs have a cap structure which acts as the binding site for eIF4F cap binding complex, required in early translation events, and translation of these mRNAs is therefore cap- dependent. Interestingly, picornaviral RNAs lack the cap structure and therefore cannot undergo cap- dependent translation resulting in the dependence on the IRES for a cap-independent initiation process. Potentially this gives picornaviruses a way of interfering with cellular mRNA translation, by inactivating the cap- dependent mechanisms (e.g. by cleaving components of the cap binding complex), while translation of its genome is not affected.

CREs

The CRE motif was first discovered within part of the HRV-14 VP1 encoding region that seemed to be required for virus RNA replication (McKnight & Lemon, 1998). It was later found to be necessary for uridylylation of VPg to produce the primer needed for genome replication (Paul *et al.*, 2000). All picornaviruses require such a CRE, but its location is not conserved among different viruses. It is made up of a single stem loop structure in each case.

The polyprotein

The genome is translated into a single polyprotein, which is subsequently cleaved into mature protein products by the action of viral proteases encoded within the genome (**Figure 1.4**). The polyprotein itself is divided into three regions, P1, P2, P3 where P1 contains the structural proteins (VP1, VP2, VP3 and VP4) required for capsid formation, while proteins P2 and P3 are processed into the proteins 2A, 2B, 2C, 3A, 3C, 3C and 3D (non-structural proteins) required for genome replication and manipulation of the infected cell (Stanway, 1990; Hyypia *et al.*, 1993; Tuthill *et al.*, 2010)

The Leader Protein

The encoded Leader protein (L^{pro}) is located just before the structural protein encoding region and it differs in structures and functions among different picornaviruses. It is only found in some of the picornaviruses, such as aphthoviruses, cardioviruses, erboviruses, sapeloviruses, senecaviruses, kobuviruses and teschoviruses (Stanway *et al.*, 2005). In aphtho- and erbo- viruses the L protein has proteolytic properties (Hinton *et al.*, 2002) and as well as cleaving itself from the polyprotein it also cleaves the eIF4GI and eIF4GII components of the eIF4F cap binding complex, which leads to the shut off of host translation. In cardiovirus the L protein is not a protease but is involved in inhibition of interferon production while in kobuviruses is essential for RNA replication and assembly (Sasaki *et al.*, 2003).

The structural Proteins

The structural capsid proteins of picornaviruses are encoded in the N- terminal part of the polyprotein (P1 region) and the capsid itself is made of 60 protomers of each viral protein; VP0, VP1 and VP3 as seen in parechoviruses, kobuviruses and avihepatoviruses where cleavage of VP0 does not occur (Castelló *et al.*, 2011) or VP1, VP2, VP3 and VP4 as seen in the rest of picornaviruses. VP1, VP2 and VP3 are surface proteins and have the same core structure, an 8-stranded antiparallel β-barrel, while VP4 is the interior part of the capsid with some secondary structures and is much smaller in size (Carter & Saunders, 2007). Some of these regions of the proteins on the surface of the capsid are variable between different viruses and this is a major factor in determining the antigenic properties of the virus and defining serotypes.

Receptor attachment sites are located on the surface of the capsid. In some genera, such as *Enterovirus*, these receptor attachment sites are located in canyon structures surrounding the 5 fold axis. Amino acids in the canyons of polioviruses and rhinoviruses bind to the amino-terminal domain of receptors, which also prompts the instability and uncoating of the capsid (De Palma *et al.*, 2008; Lin *et al.*, 2009).

The non-structural Proteins

2A is a small protein encoded within the P2 region of the genome and is found in all picornaviruses but with some major differences among subgroups (Hughes & Stanway, 2000). In enteroviruses and sapeloviruses the 2A protein ($2A^{pro}$) is 149 amino acids long and is a chymotrypsin- like protease, except that the active site serine, usually found in these proteases is replaced by a cysteine. It is responsible for the cleavage at

the P1-P2 (VP1-2A) junction, the first step in polyprotein processing (Stanway & Hyypiä, 1999; Hughes & Stanway, 2000). $2A^{pro}$ is also involved in shut off of the host-cell macromolecular synthesis by cleaving eIF4GI (eukaryotic translation inhibition factor 4GI) and also the Poly (A) binding protein (PABP) with the help $3C^{pro}$. $2A^{pro}$ has been associated with the virus- induced cytopathic effect and in others along with $3C^{pro}$, it induces apoptosis via both classic and autophagy pathways (Joachims *et al.*, 1995; Barco *et al.*, 2000; Calandria *et al.*, 2004; Lin *et al.*, 2009).

In several picornaviruses, including aphtho-, tescho-, and erbo- viruses, 2A has a characteristic NPGP motif and in these specific viruses 2A is only 16, 16 and 22 amino acids long respectively. In other cases, such as cardioviruses, 2A is longer, but has the same motif. The NPGP motif is involved in 2A/2B “processing” through an unusual mechanism, ribosome skipping, where during translation no peptide bond is made between the G and P at the 2A/2B boundary (Donnelly *et al.*, 2001).

A number of picornaviruses, including parecho-, kobu-, avihepato-, avisi-, galli-, megri-, passeri- and tremoviruses have a 2A with Hbox and NC motifs (Hughes & Stanway, 2000). These proteins are related to a family of cellular proteins involved in the control of cell growth, but the function of these virus 2As is not known. Other distinct types of 2A have been found in more recently isolated viruses and some viruses can have more than one type of 2A.

2B is a small hydrophobic protein which, together with its precursor **2BC** has been suggested to be responsible for changing the membranes of infected cells as well as

increasing the cell membrane permeability to possibly facilitate the release of newly formed virions (Barco & Carrasco, 1995; Aldabe *et al.*, 1996). In some picornaviruses it disrupts the Golgi and blocks protein secretion (de Jong *et al.*, 2008)

2C is one of the most highly conserved proteins in picornaviruses. It has a role in several processes during replication, including membrane rearrangement and encapsidation and was found to have NTPase activity which is considered essential for the synthesis of the negative sense viral RNA during replication (Belsham & Normann, 2008). Structure analysis showed that it is a member of the superfamily III helicases group of the AAA+ ATPases (Sweeney *et al.*, 2010). A recent study has demonstrated that 2C in EV-71 does have a helicase activity (Xia *et al.*, 2015).

3A, like **2B**, is a small hydrophobic membrane binding protein and it inhibits cellular protein secretion and is involved in remodelling cellular membranes proteins during viral infection (Lin *et al.*, 2009). Furthermore, 3A plays a role in positive sense RNA synthesis as part of the precursor 3AB (Teterina *et al.*, 2011).

3B protein, also known as VPg (viral protein genome) is a small peptide, no more than 22 amino acids in most picornaviruses and it serves as a primer for the synthesis of both positive and negative sense viral RNA after it is uridylylated by $3D^{pol}$ (Pathak *et al.*, 2007; Lin *et al.*, 2009).

3C is a protease ($3C^{pro}$) and is the main protease in all picornaviruses responsible for P2 and P3 cleavages during processing of the polyprotein (Lin *et al.*, 2009). The $3CD^{pro}$ precursor is needed for the VP0/VP3 and VP3/VP1 P1 cleavages (Ypma-Wong *et al.*,

1988). $3CD^{pro}$ also binds to the cloverleaf RNA structure at the 5' end of the enterovirus genome and this interaction is needed for viral replication (Lin et al., 2009).

3D is the viral RNA- dependent RNA polymerase $3D^{pol}$ and it plays a key role in viral genome replication, making it a target site for antiviral drug development (Gong & Peersen, 2010). $3D^{pol}$ can uridylylate VPg and use VPg- pUpU as a primer during viral replication (Paul *et al.*, 2003). The $3D^{pol}$ has been reported to be the most conserved protein within the picornavirus genera members (Stanway, 1990).

The 3' UTR

The 3' UTR region is usually much shorter than the 5" UTR, e.g., only about 30- 100 bases in enteroviruses, although in a few picornaviruses it is several hundred nucleotides long (http://www.picornaviridae.com/ Accessed: 18.09.17). It has been reported to be important in negative strand synthesis and in enteroviruses it contains secondary and tertiary structures which seem to be necessary for efficient synthesis of new RNA (Todd & Semler, 1996; Mirmomeni *et al.*, 1997). A highly conserved structure was discovered in the 3' UTR of three different families of +RNA viruses; *Astroviridae*, *Coronaviridae* and *Picornaviridae* (*Erbovirus* genus) suggesting a common ancestral origin and thus usefulness of the structure (Jonassen *et al.*, 1998; Robertson *et al.*, 2004). This structure and a second well-conserved structure, have recently been identified in several other *Picornaviridae* genera (Boros *et al.*, 2012).

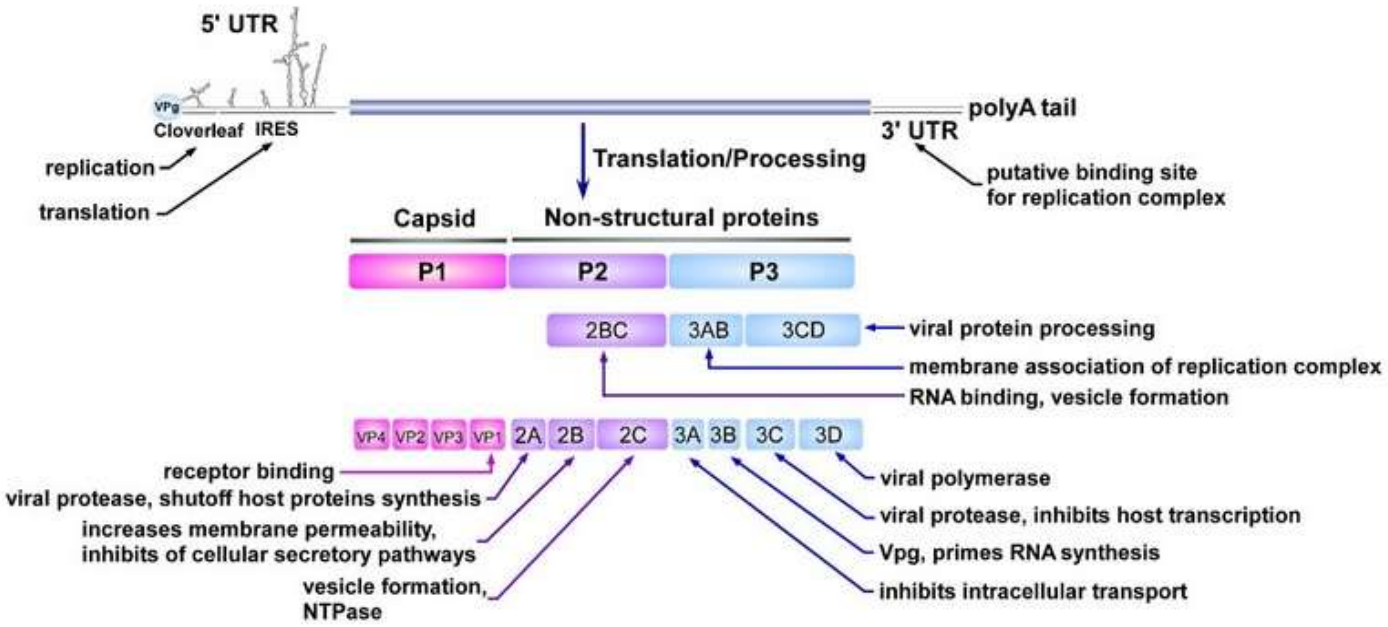

Figure 1.4: Schematic diagram of the enterovirus genome and the location and function of proteins within the encoded polyprotein.

A small protein (VPg) is covalently attached to the 5' end of the genome. The 5' UTR is followed by a single polyprotein encoding region and followed by a 3' UTR and a poly (A) tail. The 5'UTR contains a cloverleaf structure near to the 5' end, which is involved in RNA replication, and an IRES (internal ribosome entry site), a complex region made up of several RNA secondary structures, which is involved in translation of the genome to give the virus polyprotein. The polyprotein encodes proteins 1A- 3D, named by their location in three main precursors, (P1-P3) which are the first products of cleavage of the polyprotein. 1A, 1B, 1C and 1D are usually named VP4, VP2, VP3 and VP1 respectively. The 11 mature polypeptides are shown, together with three main cleavage intermediates 2BC, 3AB and 3CD. (Taken from (Lin *et al.*, 2009)).

1.3.5. The infection cycle of picornaviruses

Following entry of the virus into the cell, the life cycle of picornaviruses occurs in the cytoplasm of the host cell and the replication cycle is usually around 8 hours, depending on pH, temperature, cell type and the specific virus (**Figure1.5**). Natural hosts of picornaviruses are mostly mammals but individual viruses have a limited host range (Solomon *et al.*, 2010).

1.3.5.1.Attachment and Entry

The first stage of picornavirus infection is mediated by the interaction of the virus with specific receptors on the membrane of the cell. This receptor specificity plays a crucial role on the determination of virus- tissue tropism and pathogenesis amongst picornaviruses (Tuthill *et al.*, 2010). For many enteroviruses, the receptor binds at a depression in the capsid called the canyon, which surrounds the five- fold axis of symmetry. In these viruses, binding of the receptor into the canyon is thought to induce conformational modifications to the capsid necessary for uncoating and genome release into the cytoplasm once the virus has reached the appropriate cellular location (Carter & Saunders, 2007; Tuthill *et al.*, 2010). These changes include release of a “pocket factor” located in a hydrophobic space underneath the canyon, which is needed to allow uncoating to occur (Rossmann *et al.*, 2002). Viral genome release into the host cell can be achieved by either direct transfer of the RNA through the plasma membrane where the capsid remains on the cell surface, or, more usually, the intact virus particle is carried into the cell via a cellular endocytosis pathway (Mercer *et al.*, 2010). These pathways are most commonly clathrin -mediated endocytosis (CME), caveolin-

mediated endocytosis, lipid raft- dependant entry, macropinocytosis and others that remain poorly understood (Mercer & Helenius, 2009; Heikkilä *et al.*, 2010; Mercer *et al.*, 2010; Merilahti *et al.*, 2012).

1.3.5.2.Particle uncoating and Genome release

The second stage of picornavirus infection is uncoating, and it differs for different picornaviruses. Nonetheless, in all cases the final result is the externalization of the RNA genome from the capsid and its 'safe' delivery into the cytoplasm of the host cell in an intact and infectious form (Tuthill *et al.*, 2010; Ren *et al.*, 2013). The uncoating phase remains poorly understood but some in depth studies in a few picornaviruses revealed that they can be achieved through changes in the pH (due to endosomal acidification) as seen in the cases of aphtho- and cardio- viruses or some other less understood processes (Smyth & Martin, 2002; Tuthill *et al.*, 2010). It is thought that in enteroviruses the RNA is released through a pore close to the 2- fold axis (Shingler *et al.*, 2013).

1.3.5.3.Translation and RNA synthesis

As soon as the RNA is free in the cytoplasm the VPg protein at the 5' UTR of the genome is removed by a cellular enzyme and the genome is translated into a polyprotein which is then cleaved into viral proteins necessary for replication and assembly. In poliovirus, autocatalytic cleavage of the polyprotein is achieved via the action of two viral proteins: $2A^{pro}$ which catalyses cleavage between VP1/2A and $3C^{pro}$ or its precursor $3CD^{pro}$ which catalyses all other necessary cleavages (De Palma *et al.*, 2008).

Synthesis of the viral genome occurs in replication complexes on membranous vesicles that contain cell and viral proteins (Carter & Saunders, 2007). The first step in RNA replication is the production of negative- sense RNA copies of the virus genome, achieved by the 3D RNA-dependent RNA polymerase ($3D^{pol}$). The negative sense molecules are then used as template for synthesis of positive- sense RNA. During infection, the host cell's cellular protein synthesis can be inhibited by the action of the $2A^{pro}$ in enteroviruses, L^{pro} in aphthoviruses or $3C^{pro}$ in some picornaviruses. These cleave components of the cap- binding complex, including the translation initiation factor eIF4G and so inhibit cap- dependent translation (Ryan & Flint, 1997). This host-cell shut- off does not interfere with picornaviruses protein synthesis, as this does not depend on exactly the same cell factors. Instead, picornaviruses use their own mechanism for protein synthesis via the IRES in the 5' UTR, which allows a cap-independent initiation process (Belsham & Sonenberg, 1996; Kaku *et al.*, 2002). Once capsid proteins and genomic RNA are synthesized in sufficient amounts the new viral particles are assembled and released (Wu *et al.*, 2010).

1.3.5.4.Assembly and Release

Once synthesized, the genomic viral RNA is encapsidated by capsid proteins to form new virions (Hogle, 2002). This is guided by an interaction between 2C, which is located in the replication complex, and the capsid protein VP3 (Liu *et al.*, 2010). Assembly is usually initiated by the release of P1 capsid precursor from the polyprotein. In a spontaneous process, the capsid proteins VP0 (precursor of VP2 and VP4), VP1 and VP3 assemble to form a protomer, 5 copies of which later forms a pentamer, 12 copies of which in turn assembles to form a provirion (van der Linden *et al.*, 2015). The

last step before release is the maturation of the virion by RNA- induced cleavage of VP0 into VP2 and VP4, resulting in a newly formed infectious viral particle. It has been proposed that the process of maturation may be enhanced by the acidic environment in autophagosome- like vesicles (Richards & Jackson, 2012).

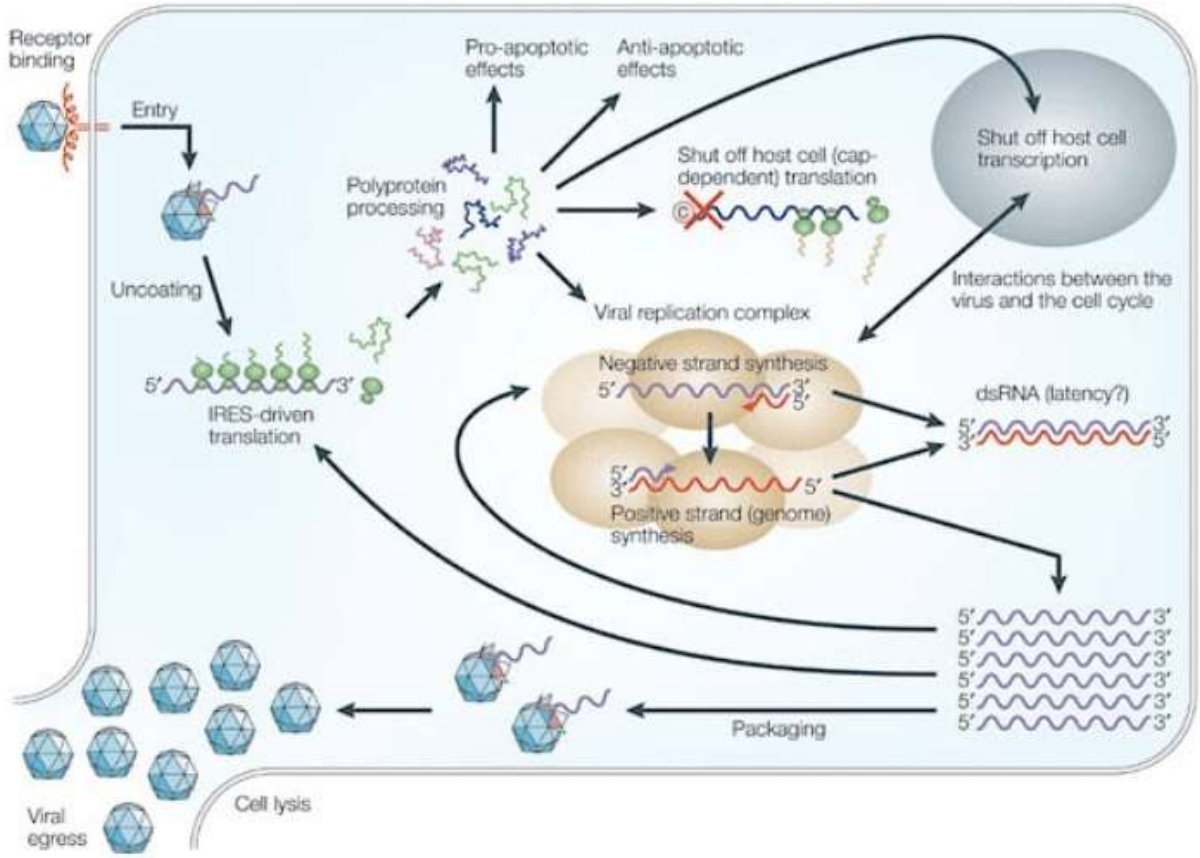

Figure 1.5: The life cycle of a typical picornavirus.

The replication cycle is initiated by binding of the virus to its receptor and internalization into the cell. The virion undergoes uncoating and the viral genome is released and translated into a single polyprotein, which is processed to give several proteins. These include capsid proteins, needed to form new virus particles, and proteins which manipulate the cell (e.g. affect apoptotic pathways or inhibit cellular protein synthesis) or replicate the virus RNA by making negative sense copies, followed by positive sense virus RNA. Newly synthesized positive-stranded RNA molecules can then either enter another round of translation and replication (not depicted) or they can be packaged into the viral capsid proteins to form new infectious virus particles which are released upon cell lysis and through several non-lytic mechanisms. Positive-sense viral RNA is shown in purple and negative-sense RNA in red. (Taken from (Whitton *et al.*, 2005)).

1.4. Host recognition and interaction of picornaviruses

Viruses can only infect cells to which they can bind thus the identification and characterization of cell receptors are key components in understanding the host range of a virus, susceptibility of individuals to infections, tissue tropism pathogenesis and potentially antiviral therapy (Coffin, 2013). Receptors are fundamental not only for viral entry itself, but some molecules instead, or also, act to concentrate viral particles to the cell surface prior to interactions with other receptor molecules, promote entry or uncoating by initiating conformational changes in the virus, induce fusion at the plasma membrane in the case of enveloped viruses, and may have a role in intracellular signalling for viral uptake into the cell. As a family, picornaviruses have been found to utilize a number of receptors of a wide variety of different types and in some cases more than one molecule is used as a receptor (Tuthill *et al.*, 2010). Even very similar picornaviruses using essentially the same region of the virus particle (e.g. the canyon) to interact with a receptor may recognise different receptors (**Figure 1.6**). In these cases, receptor specificity may be defined by subtle differences in sequence or arrangement of the capsid proteins making up the canyon (Plevka *et al.*, 2012).

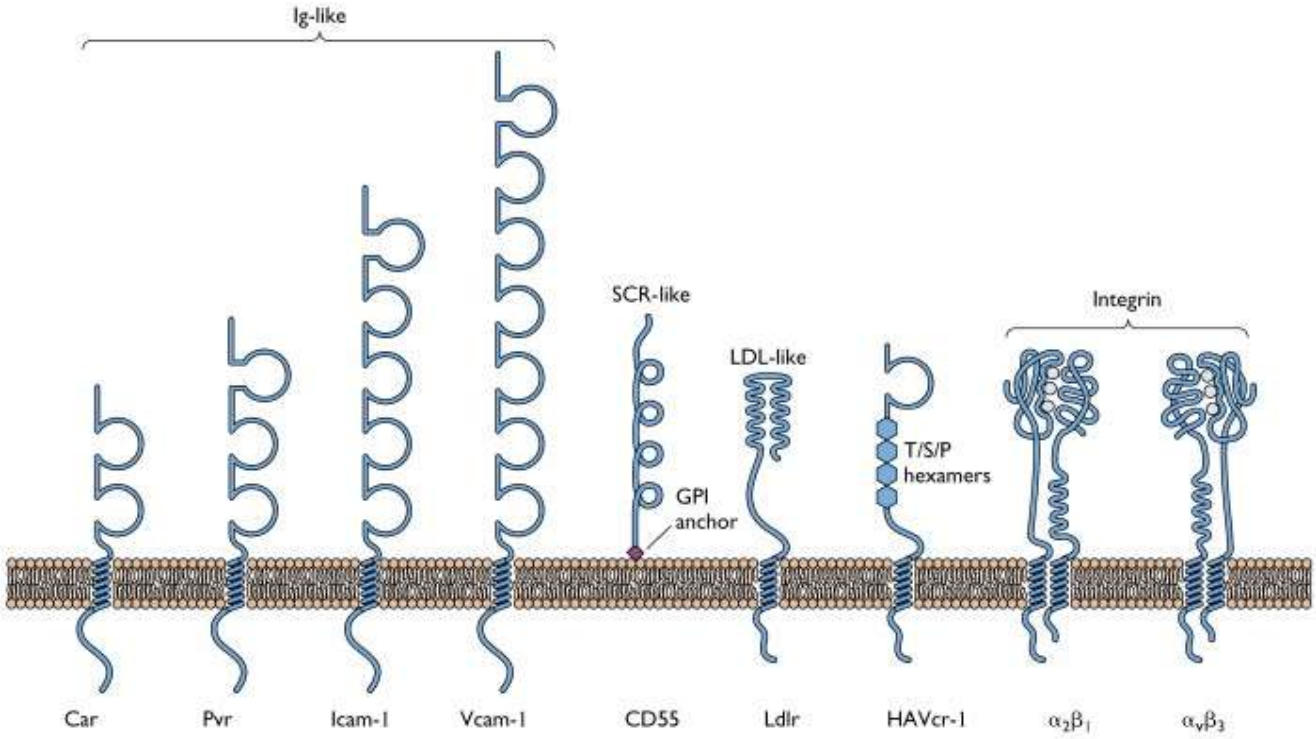

Figure 1.6: Schematic diagram of different proteins known to be picornavirus receptors.

Members of the Ig superfamily: CAR, coxsackie–adenovirus receptor; PVR, poliovirus receptor; ICAM-1, intracellular adhesion molecule type 1 and VCAM-1, vascular cell adhesion molecule type 1. Integrins α2β1 and αvβ3 (similar to αvβ3, integrin αvβ6 is RGD dependent and most likely the preferred receptor for several RGD- containing picornaviruses); DAF (CD55), decay-accelerating factor; GPI, glycosylphosphatidylinositol; HAVcr-1, hepatitis A virus cellular receptor 1; LDL-like, low density lipoprotein; LDLR, low density lipoprotein receptor; SCR-like, short consensus repeat; T/S/P, threonine/serine/proline (Taken from(Flint *et al.*, 2009)).

Immunoglobulin superfamily

Many picornavirus receptors are known to be cell- surface molecules of the immunoglobulin superfamily (IgSF) (Rossmann *et al.*, 2002)**.** These are transmembrane proteins and have extracellular regions comprising of two to five amino- terminal immunoglobulin (Ig)- like domains (Lin *et al.*, 2009). Poliovirus receptor (PVR), intracellular- adhesion molecule 1 (ICAM-1) and coxsackievirus- adenovirus receptor (CAR) belong to this superfamily and act as receptors for polioviruses, a major group of rhinoviruses and coxsackie B viruses (CBVs) respectively (Shafren *et al.*, 1999; Xiao *et al.*, 2001). Although they have up to five Ig- like domains only the first Ig-like domain (the N-terminal- most domain, located furthest from the membrane) is the one that triggers the penetration of the virus into the cell, via its insertion into the canyon of the virus (Rossmann *et al.*, 2002; Tuthill *et al.*, 2010). Interactions with IgSF receptors also seem to trigger particle disruption to allow RNA release after entry of the virus into the cell.

Low- density lipoprotein receptor (LDL-R) and Decay accelerating Factor (DAF)

Viruses can also use non- IgSF cell receptors which bind outside of the canyon (Lin *et al.*, 2009). These include low- density lipoprotein receptor (LDL-R) and the decay accelerating factor (DAF or CD55). DAF (**Figure 1.7**) is a glycoprotein that belongs to a family of proteins that protect cells from complement- mediated lysis (Bergelson *et al.*, 1994) and is found on most cell surfaces (He *et al.*, 2002). Unlike many other receptors, DAF is not a transmembrane protein and is instead anchored to the membrane with a glycosylphosphatidylinositol (GPI anchor). It serves as a cellular

receptor for several echoviruses (Plevka *et al.*, 2010)**,** enterovirus 70 and as an initial cellular receptor for CAV21 and CBV1, CBV3 and CBV5 (Spiller *et al.*, 2002). Binding of DAF with echoviruses does not involve penetration into the canyon, but instead DAF lies across the surface of the virus particle, close to the two fold axis of symmetry, and occupies a 'surface- exposed 'region of the capsid (Bhella *et al.*, 2004). DAF is made up mainly of 4 short consensus repeats (SCR) and SCR2, SCR3 and SCR4 are involved in binding to the virus particle involving parts of VP1, VP2 and VP3 (He *et al.*, 2002). Interestingly, CAV21 binds to DAF without being able to enter and infect cells and needs to bind to ICAM-1 to promote infection (Xiao *et al.*, 2001). DAF also does not trigger any conformational change in the capsid (Tuthill *et al.*, 2010). Instead, it seems to recruit the virus to the cell surface and acts as a primary receptor while a receptor needed for infection, e.g. ICAM-1 in the case of CAV21 and CAR in the case of CBV1, CBV3 and CBV5, is needed for triggering infectious entry. Interestingly, the importance of DAF is due to the fact that it triggers signalling- dependent transport of virus- receptor complex to tight junctions between cells where the CAR receptor is found (Tuthill *et al.*, 2010).

Low density lipoprotein receptors (LDL-R) are located on the outer surface of many different cell types, where they bind circulating low- density lipoproteins (LDLs) primary carriers of cholesterol, and transport them into the cell (Goldstein & Brown, 2009). LDL-Rs serve as receptors for a minor group of human rhinoviruses (HRVs). Binding is achieved via a ligand binding domain at the N- terminus of LDL-R (Vlasak *et al.*, 2005). Five LDL-R molecules bind around and very close to the five- fold axis of symmetry rather than in the canyon of the virus (Hewat *et al.*, 2000).

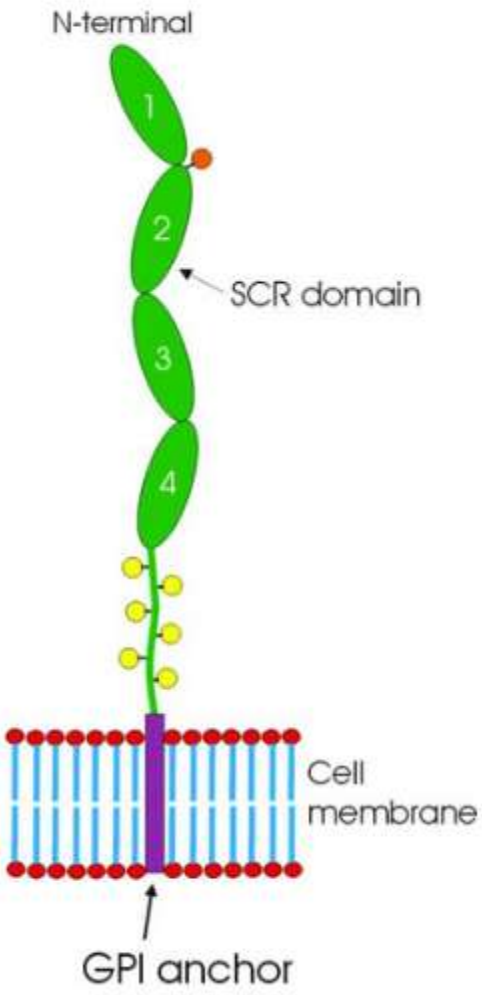

Figure 1.7: Schematic diagram of DAF structure.

The green ellipses represent the 4 short consensus repeat (SCR) domains. The yellow circles are O- linked and the orange circles are N- linked carbohydrate moieties. GPI, glycosylphosphatidylinositol (Taken from He et al., 2002)

Table 1.1 Summary of molecules used by different picornaviruses. (Based on Ehrenfeld et al., 2010; Stanway, 2013)

Viruses	Receptors										
	DAF	HSPG	β2-microglobulin	sialic acid	ICAM-1	CAR	PVR	LDLR	αvβ3	αvβ6	α2β1
Most Echo	✓	✓	✓		x	x	x	x	x	x	✓
CAV21	✓				✓	x	x	x			
CAV24				✓		x	x	x			
CBV	✓	✓			x	✓	x	x			
CAV9	x	✓	✓	x	x	x	x	x	✓	✓	x
EV70	✓			✓	x	x	x	x	x		x
EV71		✓		✓		x	x	x	x		x
E9						x	x	x	✓	✓	
E1			✓			x	x	x			✓
HPeV		✓				x	x	x	✓	✓	
HRV		✓			✓	x	x	✓			
HAV						x	x	x			
PV						x	✓	x			
EMCV		✓		✓		x	x	x			
FMDV		✓				x	x	x	✓	✓*	

✓- used as a receptor; **x**- not used as a receptor; blank-not tested; * FMDV also interacts with other RGD-dependent integrin. CAV-coxsackievirus A, CBV-coxsackievirus B, EV- enterovirus, E- echovirus, HPeV- human parechovirus, HRV-rhinovirus, HAV-hepatitis A virus, FMDV- foot and mouth disease virus, EMCV- Theiler's murine encephalomyelitis viruses.

Integrins as picornavirus receptors

Integrins are a family of integral membrane receptors that function as cell adhesion receptors (Ruiz-Sáenz *et al.*, 2009; Tuthill *et al.*, 2010; Merilahti *et al.*, 2012) and have key roles in normal cell physiology (Stewart & Nemerow, 2007). They were discovered in the mid 1980s and their name derives from their role in integrating the intracellular cytoskeleton with the extracellular matrix (Ruoslahti, 1991). Integrins are heterodimers of alpha (α) and beta (β) integrin subunits; each subunit is a glycoprotein and is composed of one large extracellular domain, a transmembrane helix and one small C-terminal cytoplasmic domain (Racaniello, 1990; Tuthill *et al.*, 2010). There are several different α subunits and β subunits and these can form many αβ combinations.Different α subunits are all homologous to each other, so are different β subunits, but there is no homology between α and β subunits. Both subunits are needed to bind the specific ligand. The α subunits are subdivided into two main groups according to structural differences: members of the group formed by α1, α2, αL, αM, αD and αX contain an inserted domain (I-domain). The group of α3, α5, α6, α7, α8, αIIb and αV undergo post translational cleavage resulting in a heavy and a light chain (Ruiz-Sáenz *et al.*, 2009). All the β subunits contain an I-domain that has a metal ion- dependent adhesion site (MIDAS) which serves as ligand binding only when the β subunit is associated with an α subunit that lacks this domain **(Figure 1.8)**. There are nineteen α and eight β subunits and by making different combinations results in a formation of a family with 24 members (Springer, 2002; Merilahti *et al.*, 2012) **(Figure 1.9)**.

Integrins are heavily involved in processes such as wound healing and are known to mediate cell adhesion, cell migration, growth, phagocytosis, inflammation and cell

differentiation and survival (Stewart & Nemerow, 2007) as a result of their ability to trigger endocytic pathways. Integrins also play a role in human diseases such as tumours, cancer and immunodeficiency disorders evidence of which have shown an altered integrin- mediated adhesion and migration (Huttenlocher & Horwitz, 2011). The role of integrins in initiation and progression of cancer makes them targets in cancer therapy. Expression of αv and β1 subunits have been associated with proliferation and metastasis and αvβ3 and αvβ6 with both proliferation and invasion (Ahmedah *et al.*, 2017). The αvβ6 integrin is an epithelial specific integrin that is expressed at low or undetectable levels in adult tissues but can be up- regulated during wound heallng, development, inflammation and cancer (Thomas *et al.*, 2006).

The cell biology of integrins is due to their ability to bind to a wide range of ligands that include: collagen, fibronectin, laminin, vitronectin, osteopontin, thrombospondin, ICAMs and plasma proteins, such as globulin and thrombine (Ruoslahti, 1991; Ruiz-Sáenz *et al.*, 2009) and the binding is universally divalent cation dependent (Ruiz-Sáenz *et al.*, 2009). Adhesion to a ligand can occur via the ligand- binding pocket which forms between the intersection of the α-chain and the βI domain, together with the divalent cations that bind to the α subunit chain. Based on their ligand recognition integrins can be broadly classified into four different categories: RGD binding, collagen binding, laminin binding and leukocyte specific binding receptors (Springer, 2002).

Some integrins can recognize an arginine- glycine- aspartic acid (RGD) tripeptide sequence in the native ligands, although only 8 out of 24 αβ combinations can achive this binding (Springer, 2002). As a result of this property, integrins are also exploited as efficient receptors for several important viruses including adeno-, rota-, hanta-, and

herpesviruses (Pellinen & Ivaska, 2006; Merilahti *et al.*, 2012) (**Table 1.1**)**.** A small number of picornaviruses also utilise RGD- dependent integrins. Integrins capable of recognizing the RGD motif found in these viruses are α5β1, α8β1, αvβ1, αvβ3, αvβ5, αvβ6 and αvβ8 (Johnson *et al.*, 2009a; Merilahti *et al.*, 2012). Coxsackievirus A9 (CAV9) and echovirus 9 (E-9) are two enterovirus types known to bind to integrins via an RGD motif (Nelsen-Salz *et al.*, 1999; Williams *et al.*, 2004), while several human parechovirus (HPeV) types also utilize an RGD to bind to integrins (Nelsen-Salz *et al.*, 1999; Boonyakiat *et al.*, 2001; Heikkilä *et al.*, 2009; Seitsonen *et al.*, 2010). One animal virus, FMDV, uses an RGD motif which is located in the highly exposed G-H loop of VP1 (Dicara *et al.*, 2008) while the other picornaviruses have their RGD motifs near the C- terminus of the VP1. The precise location of the RGD in the virus particle is not known in these latter cases as it is in a flexible region not visible by X- ray crystallography (Hendry *et al.*, 1999).

Not all integrins recognize and interact with the conserved RGD motif of viral proteins. There are multiple other non- RGD-binding integrins that drive virus entry and infection (Stewart & Nemerow, 2007). One such virus is echovirus- 1 (E-1), an enterovirus that binds to integrin α2β1 (Bergelson *et al.*, 1992). α2β1 was found to cluster on the surface of the cells after E-1 binding and this is needed for entry (Jokinen *et al.*, 2010). Other viruses who interact with non- RGD binding integrins include HIV-1 with integrin α4β7 (Cicala *et al.*, 2009), human cytomegalovirus (HCMV) (Feire *et al.*, 2010), Simian Virus 40 (SV40) (Stergiou *et al.*, 2013), and Ross River virus (La Linn *et al.*, 2005) with integrins α1β1, α2β1, α4β1, α6β1, α9β1 and αxβ2.

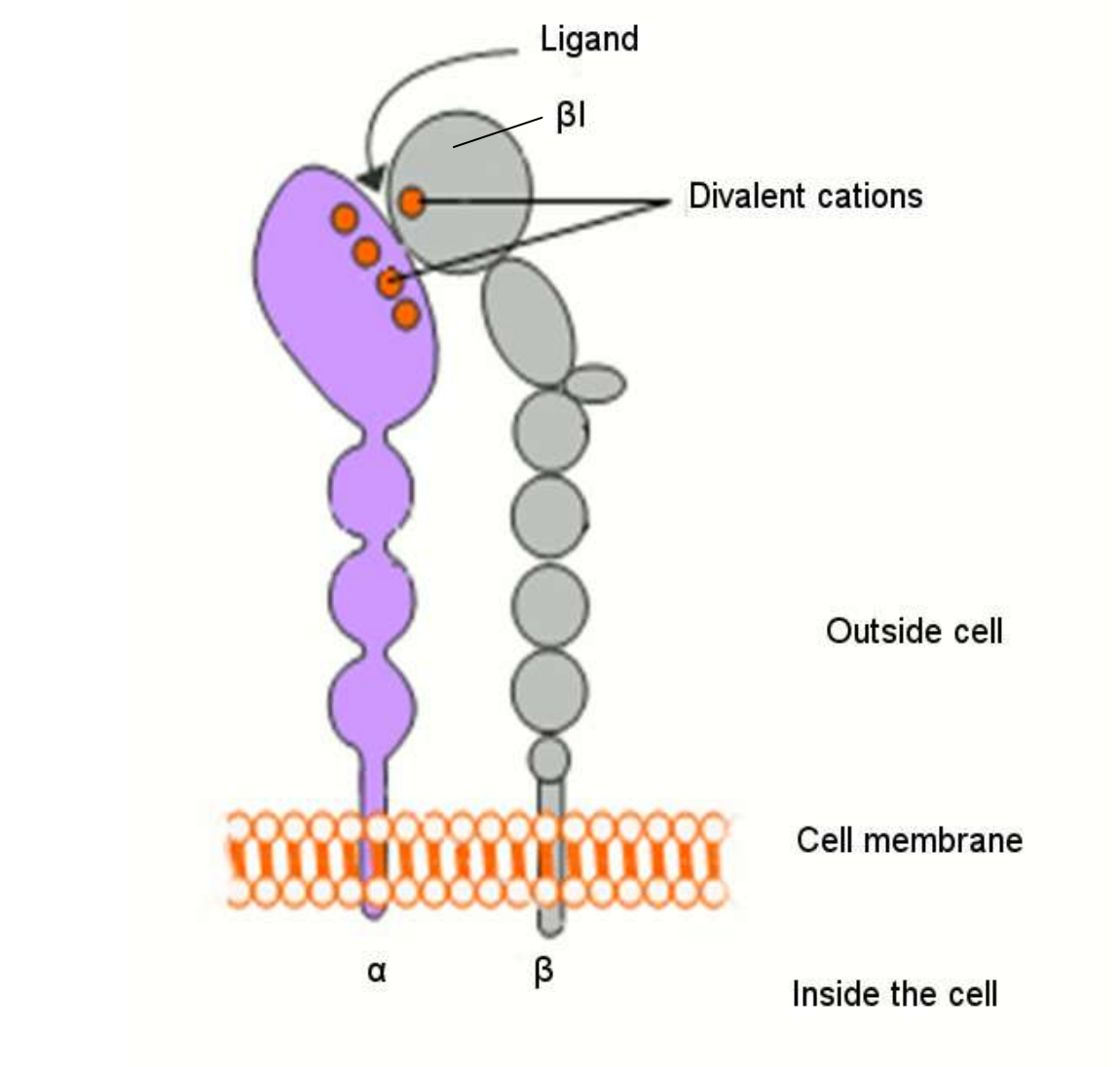

Figure 1.8: Schematic diagram of an integrin.

The alpha (α) and beta (β) subunits are glycoproteins and composed of extracellular, transmembrane and cytoplasmic domains. The ligand- binding pocket is located between the intersection of the α-chain and the βI domain of the β-chain, together with the divalent cations (orange cirles) that bind to the α subunit chain via a MIDAS domain. [Adapted from Barczyk et al., 2010].

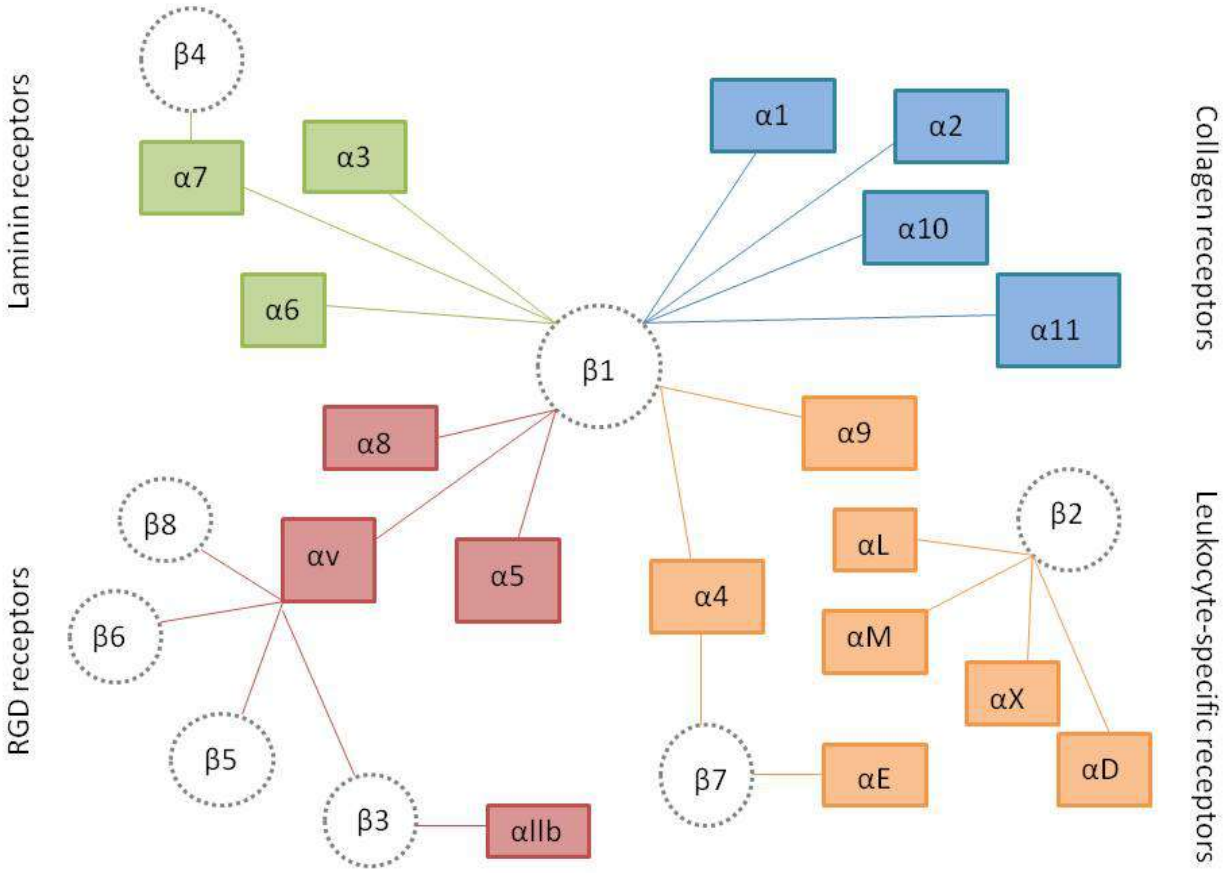

Figure 1.9: Known combinations of α and β subunits forming integrins and integrin receptor classification into four categories based on their ligand binding ability; RGD binding, collagen binding, laminin binding and leukocyte binding.

The β1-subunit can heterodimerise with twelve different kinds of α-subunits while most α-subunits pair up with one kind of β-subunit. [Adapted from (Barczyk *et al.*, 2010)].

Table 1.2: Integrins used by different viruses and their role in virus infection.

Virus	Intgrins	Role of integrns
Human adenovirus 2, 5	αvβ3, αvβ5, αvβ1, α5β1, α1β2, αMβ2	Cell entry, endosome escape
Human cytomegalovirus (HCMV)	α2β1, α6β1, αvβ3	Cell entry
Kaposi's sarcoma-associated herpesvirus (KSHV)	α3β1, αvβ3, αvβ5, α9β1	Cell entry
Epstein- Barr virus (EBV)	αvβ3, αvβ5, α5β1	Cell entry
Human immunodeficiency virus 1 (HIV-1)	α4β7, αvβ3, αvβ5, α5β1	Cell attachment
HPS-associated hantaviruses NY-1 and Sin Nombre virus (SNV)	αvβ3, αIIbβ3	Cell attachment, entry
Rotavirus	α4β1, α4β7, α2β1, αvβ3, αxβ2	Cell attachment, entry
Echovirus 1	α2β1	Cell attachment, entry
Echovirus 9	αvβ3	Cell attachment, entry
Human parechovirus 1 (HPeV1)	αvβ1, αvβ3, αvβ6	Cell attachment, entry
Foot- and- mouth disease virus (FMDV)	α5β1, αvβ3, αvβ6, αvβ8, αvβ1	Cell attachment, entry
Coxsackievirus A9	αvβ3, αvβ6	Cell attachment, entry
Murine polyomavirus	α4β1	Cell entry
Vaccinia virus	β1	Cell entry
West Nile virus	αvβ3, αvβ1	Cell entry
Simian virus 40	α2β1	Cell attachment, entry
Ross River (RR) virus	α1β1	Cell attachment, entry
Human papillomavirus	α6β4	Cell attachment
Ebola virus	α5β1	Cell entry

*Taken from (Hussein *et al.*, 2015)

Glycosaminoglycans: Heparan Sulfate

Heparan sulfate (HS), a glycosaminoglycan (GAG), is the most abundant linear carbohydrate polymer in the body (Ruiz-Sáenz *et al.*, 2009). It is composed of repeated glycosamine and hexuronic acid disaccharides, which are highly sulfated at various positions (Zhu *et al.*, 2011) giving it a negative charge. GAGs are covalently linked to proteins to give glycoproteins; heparan sulfate proteoglycans (HSPG) (Dasgupta *et al.*, 2011). There are three different groups of HSPG according to their location; membrane HSPGs such as syndecans and glycosylphosphatidylinositol-anchored proteoglycans (glypicans) (**Figure 1.10**), the secreted extracellular matrix HSPGs (agrin, perlecan, type XVIII collagen), and the secretory vesicle proteoglycan, serglycin (Sarrazin *et al.*, 2011).

Heparan sulfate (HS) is involved not only in animal development and homeostasis, but is also influences viral infection and pathogenicity as it has been found to serve as the attachment receptor for many important human pathogens among different families (Jinno-Oue *et al.*, 2001; Escribano-Romero *et al.*, 2004). Several important viruses are known to use cell surface HSPG during entry such as: herpes simplex virus (HSV) (Shukla & Spear, 2001; Bender *et al.*, 2005), human papillomavirus (HPV), hepatitis B virus (HBV), respiratory syncytial virus (RSV), some variants of foot- and- mouth disease virus (FMDV) (Jackson *et al.*, 1996) and human immunodeficiency virus type-1 (HIV-1) (Mondor *et al.*, 1998). The binding of a viral protein with HS is mainly via electrostatic interactions and has low specificity (Escribano-Romero *et al.*, 2004). This interaction can be explained as the amino acid residues of the viral proteins are positively charged in a three- dimensional array arrangement and are attracted to the

concentrated negative charge of the HS. The low- affinity of this binding was thought to serve the purpose of concentrating the virus along the cell surface in order to facilitate binding to a high- affinity, high- specificity receptor (Zhu *et al.*, 2011). Different viruses using heparan sulfate in this way have been observed during the years, such as flavivirus which was found to bind to HS firstly and then bind to a high- affinity receptor that facilitates endocytosis and membrane fusion. HSV type 1 was the first virus that was reported to use HS as a receptor. HSV viral glycoprotein B (gB) and glycoprotein C (gC) have been shown to interact with the negatively charged HS during the initial attachment phase (Laquerre *et al.*, 1998). Studies on FMDV revealed that HS binding is the initial event in cellular entry in some virus isolates and is a required step for efficient *in vitro* infection (Jackson *et al.*, 1996). Adaptation of FMDV to tissue culture cells showed that a mutation in VP3 replacing a histidine (found in field isolates) with an arginine, allows a high- affinity heparan sulphate binding site to form (Fry *et al.*, 1999). Although the role of HS in FMDV is not yet fully identified, speculations for the role include the idea that a weak binding to HS serves to increase the rate of integrin-mediated virus uptake (via the FMDV RGD motif) or other unidentified molecules involved in cell entry (Baranowski *et al.*, 2000).

Studies on CAV9 and other members of the species *Enterovirus* B (EV-B) found that some of these viruses share a common binding mechanism to HSPG (McLeish *et al.*, 2012). HSPG was found to interact with an arginine residue at the 132 position of the CAV9 VP1 protein. Non- binding CAV9 strains have a threonine at this position. This single mutation generates a patch of positive charges on the CAV9 surface as it is located immediately near the 5- fold axis (McLeish *et al.*, 2012; Plevka *et al.*, 2013).

This means that 5 copies of the amino acid are clustered due to the symmetry of the virus particle. An analysis of other EV-B species members showed that differences in HSPG use could also be correlated with the presence or absence of a positively-charged amino acid (lysine or arginine) at the equivalent position. Another way that HSPG- interacting regions can be exposed on the surface of the ligand is through positively charged amino acids in linear motifs. BBXB and BBBXXB (B- basic amino acid (lysine or arginine), X – any amino acid) have been defined as HSPG- interacting motifs (Cardin & Weintraub, 1989). Multiple passages of CAV9 Griggs *in vitro* on A549 cells produced a mutant virus with an S to R mutation at position 287 in VP1 capsid protein (S2871R) (Williams et al unpublished). The S2871R virus created a linear motif with four arginines including the first amino acid of the RGD motif, QRRRRGD rather than QSRRRGD, in the original virus, creating a highly positive charge of the virion capable of interacting with the negatively charged molecules of HSPG and possibly a BBXB type linear motif. In addition to A549 cells, the S2871R mutant was also able to bind to HSPG and infect MCF-7 cells (Ivanova & Stanway, unpublished) whereas the original virus fails to infect MCF-7 cells efficiently. The findings on CAV9 supported the evidence from FMDV, that HSPG binding is advantageous rather than necessary for infection as both the wild type and S2871R mutant can grow on A549 cells; HS may act as an initial receptor to concentrate the virus to the cell surface increasing the probability that virions and cells are close enough and facilitate subsequent interactions with other (co) receptors needed for the viral entry (Shukla & Spear, 2001) or HS may allow rapid cell binding, thereby more time for the FMDV or CAV9 to bind to integrins is gained (Jackson *et al.*, 1996).

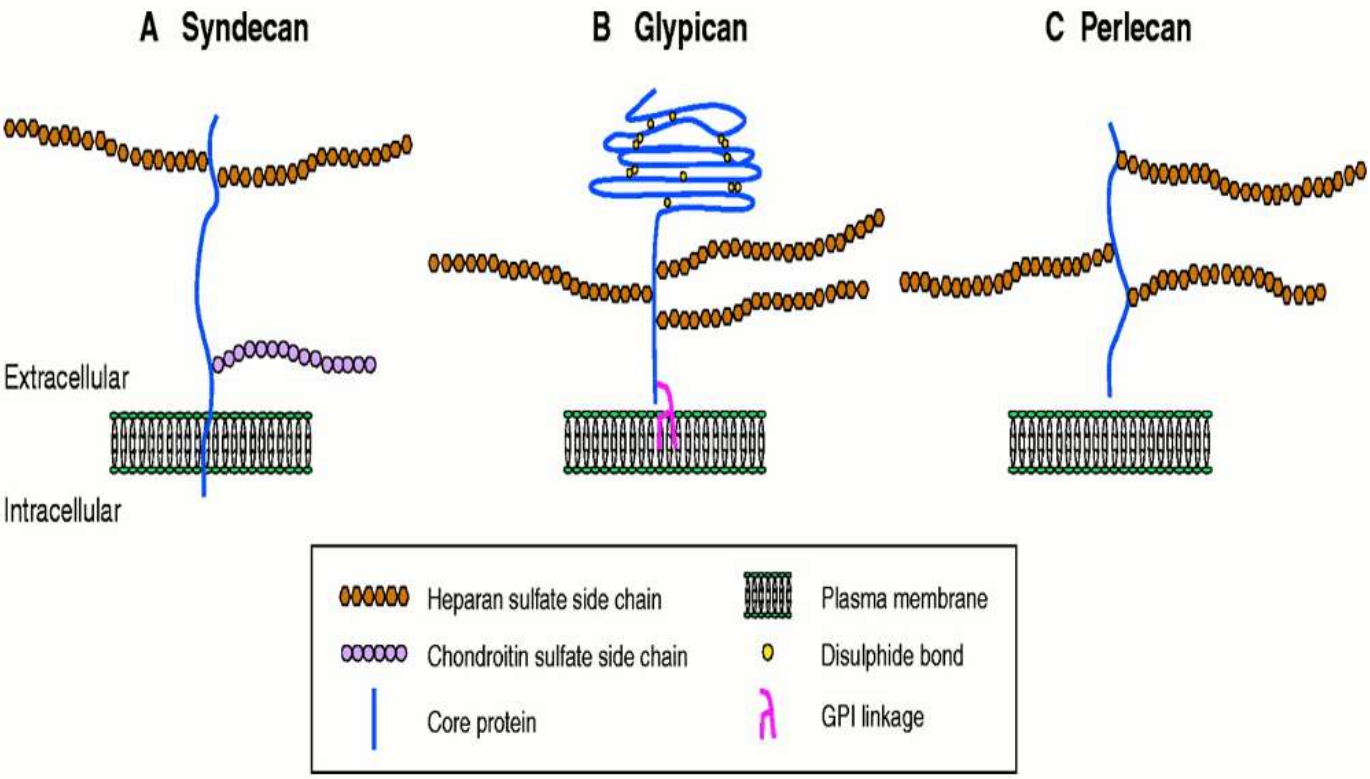

Figure 1.10: Structure of cell surface heparan sulfate proteoglycans (HSPG).

The three main classes of cell-surface heparan sulfate proteoglycans (HSPGs). (A) Syndecans are transmembrane proteins that contain a highly conserved C-terminal cytoplasmic domain. Heparan sulfate (HS) chains attach to serine residues distal from the plasma membrane. Some syndecans also contain a chondroitin sulfate (CS) chain(s) that attaches to a serine residue(s) near the membrane. (B) The glypican core proteins contain globular core proteins which are disulphide-stabilized and are linked to the plasma membrane by a glycosylphosphatidylinositol (GPI) linkage. HS chains link to serine residues adjacent to the plasma membrane. (C) Perlecans are secreted HSPGs that carry HS chains and bind to extracellular matrix and cell membrane proteins.(Taken from (Lin, 2004).

1.5.Mechanisms of Endocytosis for Picornaviruses

1.5.1.Overview of Endocytic pathways

Following binding to cell surface receptors, viruses still need to enter the cells by an endocytosis pathway, unless they have uncoated at the cell surface. Endocytosis pathways involve the virus being enclosed within a membrane delivered vesicle (**Figure 1.11**). Endocytosis is so popularly exploited by many viruses as it offers many important advantages: (i) a delayed immune response as there is no viral presence on the plasma membrane (ii) viruses can bypass obstacles such as the crowded cytoplasm and underlying actin skeleton (iii) it allows viruses to 'sense' their location within intracellular organells through pH changes caused by maturation of the endosomes (Mercer *et al.*, 2010; Schelhaas, 2010). For a prolonged period, clathrin-mediated endocytosis (CME) was thought to be the only pathway used for receptor mediated endocytosis, however extensive studies indicated that the process of endocytosis is much more diverse and complex. Relatively well- characterized routes in addition to CME are caveolin/raft dependent entry and macropinocytosis while less characterized pathways include phagocytosis and pathways dependent on Arf6 and flotillin (**Figure 1.11**). There are probably other pathways yet to be defined.

From a cellular perspective, endocytosis is used to transport cargo molecules from the cell surface or extracellular fluid. These cargos include membrane proteins, ligands, nutrients etc for recycling or degradation.

Although pathways differ in the formation of primary endocytic vesicles (PEVs), the nature of the cargo and the mechanisms of vesicle formation (Hansen & Nichols, 2009; Ghigo, 2010; Schelhaas, 2010) the steps involved in endocytosis are very similar. Cargo is endocytosed through PEVs and is usually delivered to early endosomes (EE), where sorting occurs. Cargo can then be routed to late endosomes (LE) and lysosomes for degradation, to trans-Golgi network (TGN), or to recycling endosomal (RE) carriers that are responsible for bringing cargo back to the plasma membrane (Grant & Donaldson, 2009).

The characteristics of the important endocytic pathways used by some picornaviruses will be discussed in the next sections.

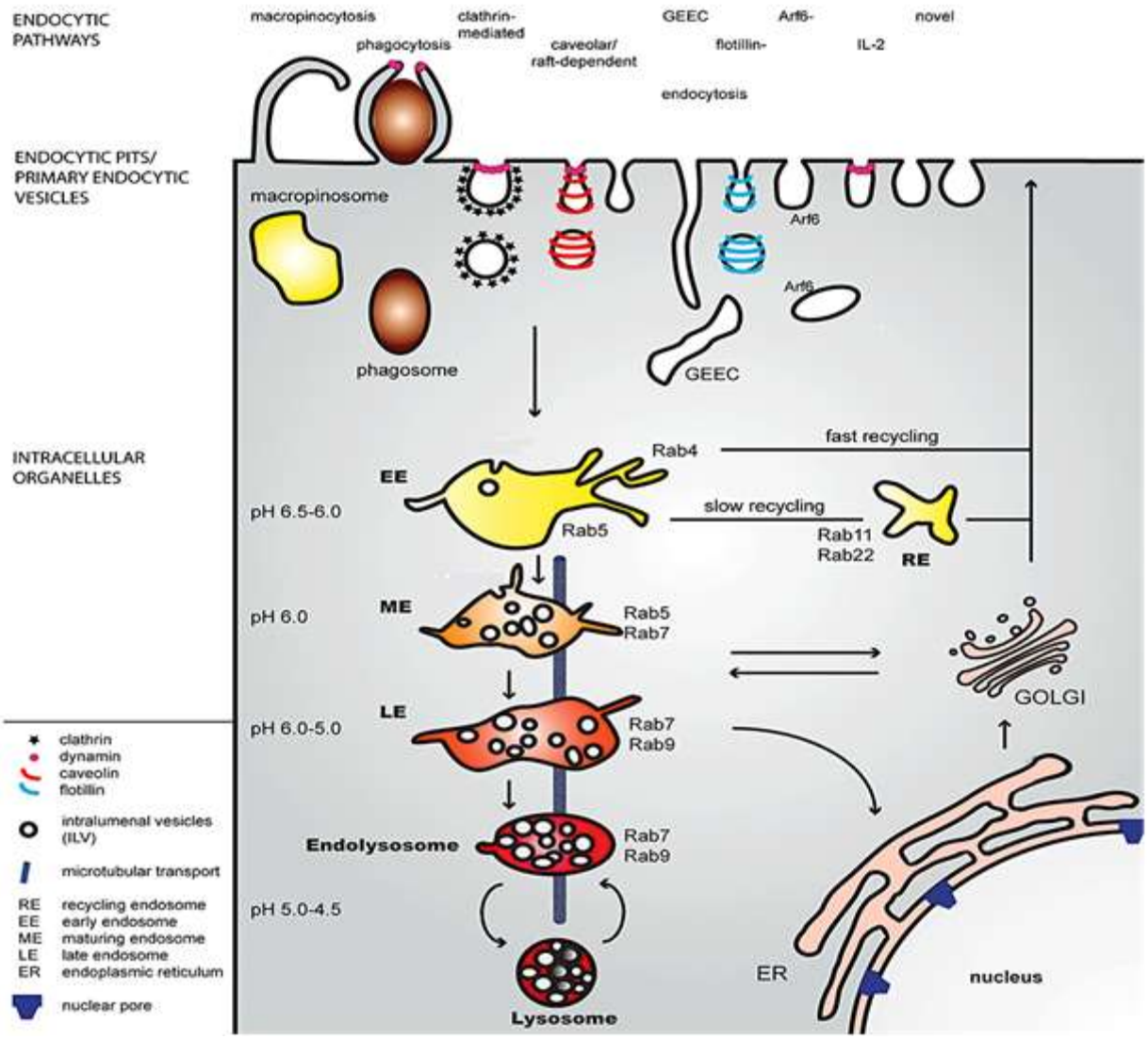

Figure 1.11: Endocytosis pathways.

A schematic depiction of the different mechanisms by which cargo can be internalized from the plasma membrane and their respective primary endocytic vesicles (PEV). The main intracellular trafficking connections are depicted in the bottom half. Different vesicles can be identified by the presence of different Rab proteins on their surface (Taken from (Schelhaas, 2010)).

1.5.2.Clathrin- dependant endocytosis

One of the best- characterized endocytic routes is that of clathrin- mediated endocytosis or CME; is a quick, efficient and constitutively active pathway in all mammalian cells (Ghigo, 2010). The unique characteristic of the pathway is the clustering of transmembrane receptors into clathrin- coated vesicles (CCV) that do not exceed 120 nm in size. The main use for CME is the uptake of essential nutrients (eg growth factors, iron- laden transferin, cholesterol- laden low- density lipoproteins) and the recycling of receptors (Takei & Haucke, 2001). The formation of the CCVs is a four-step process and requires the recruitment of several protein categories such as small G- proteins (Rab5, Arf6 etc), adaptor proteins (AP2, AP180 etc), accessory proteins (dynamin, amphiphysin, endophilin, actin etc), as well as phosphatidylinositol. However, the composition of CCVs is not always the same in all cells (Mercer *et al.*, 2010).

Viruses usually have a preference for this route for its rapidness and efficiency (Marsh & Helenius, 1989). The incoming viruses require conformational changes to their capsid proteins, thus within minutes after internalization, viruses are exposed to the acidic environment of endosomes to possibly trigger the steps in viral entry (fusion, penetration and uncoating) (Marsh & Helenius, 2006; Mercer *et al.*, 2010; Hussain *et al.*, 2011). The site of penetration depends on the pH threshold of the virus and it can be either in early endosomes (pH 6.5 to 6.0) or late endosomes (pH 6.0 to 5.5) (Marsh & Helenius, 2006). It is important to mention that low pH levels alone can sometimes not induce conformational change thus acid- dependent proteases may be needed in

some cases for viral capsid cleavages. Examples are Ebola virus (Miller *et al.*, 2012) and coronavirus (Zhou *et al.*, 2015). This pathway plays an important role in the internalization of several viruses, including some of the adenoviruses, vesicular stomatitis virus (VSV), influenza virus and Semliki forest virus (SFV), which were identified previously in clathrin- coated pits (CCPs) in the plasma membrane at early stages of internalization by transmission electron microscope (TEM) (Sieczkarski & Whittaker, 2002; Mercer *et al.*, 2010). FMDV is also internalised through this pathway (Berryman *et al.*, 2005) as well as HPeV1 where two studies have indicated that HPeV1 is endocytosed via the clathrin- mediated pathway (Joki-Korpela *et al.*, 2001; Merilahti *et al.*, 2012).

1.5.3. Caveolae- mediated endocytosis

Viruses have the ability to exploit more than one endocytic pathway as defined by the interactions between their receptors at the cell surface (Grove & Marsh, 2011). In contrast of CME, clathrin- independent endocytosis (CIE) comes in many forms but caveolin- mediated endocytosis is the best studied pathway amongst them. As its name suggests, this pathway is mediated by caveolae; flask shaped invaginations of the plasma membrane (Pelkmans & Helenius, 2002). These are 50-80 nm in diameter and can be found in many cell types. Their formation depends on lipids such as cholesterol and sphingolipids, lipid rafts, and proteins such as tyrosine kinases and phosphatases (Marsh & Helenius, 2006; Ghigo, 2010; Mercer *et al.*, 2010; Schelhaas, 2010). Synthesized in the endoplasmic reticulum, caveolin is oligomerized with the caveolin-associated proteins (e.g cavins) and lipids mentioned above to produce one caveolar

structure in a ratio of 1:144 caveolin molecules (Ghigo, 2010) in a still unclear mechanisms. Unlike CME, caveolar endocytosis is thought to be stimulated by a range of ligands and uptake involves caveolae and dynamin to form early endosomes or structures originally called caveosomes (Ghigo, 2010; Schelhaas, 2010). It is now thought that caveosomes are actually modified late endosomes or lysosomes and the term is not used any longer (Hayer *et al.*, 2010). Once the cargo is internalized it is transported through EE. LE and routed to ER or Golgi apparatus (Ghigo, 2010; Mercer *et al.*, 2010; Schelhaas, 2010). Caveolae seem to be used for entry by several viruses including polyomavirus and simian virus 40 (SV40).

1.5.4.Macropinocytosis

Macropinocytosis is considered to be a non- specific mechanism for internalization, as it is not related to any specific receptor. Macropinocytosis involves actin cytoskeleton rearrangement and during this process fluids and membrane are internalized into large vacuoles leading to the formation of membrane ruffles. The ruffles form as lamellipodia (planer folds), filopodia or blebs and are closed at the membrane ruffling sites forming a large vesicle known as a macropinosome. The formed closed vacuoles are no longer attached to the plasma membrane. Macropinosomes have the ability to become acidified and interact with early endosomes, like other vesicles produced by several different entry pathways (Sieczkarski & Whittaker, 2002; Mercer & Helenius, 2009). Examples of viruses entering the cell via the macropinocytosis pathway are vaccinia, virus HIV-1, adenovirus, CBVs, echovirus 1, Ebola virus and Kaposi's sarcoma-associated herpesvirus (Mercer & Helenius, 2009; Lim & Gleeson, 2011).

1.6. Coxsackie virus A9 of the *Enterovirus* genus

1.6.1.Enterovirus genus

The *Enterovirus* genus of the picornavirus family is home to many important human pathogens and can be characterized as among the most common causes of infections in mankind. Around 10-15 million symptomatic EV infections occur annually in the United States alone (Strikas *et al.*, 1986) and the highly prevalent rhinovirus infections are excluded from this figure. The *Enterovirus* genus is divided into 13 species; *Enterovirus* A, *Enterovirus* B, *Enterovirus* C, *Enterovirus* D, *Enterovirus* E, *Enterovirus* F, *Enterovirus* G, *Enterovirus* H, *Enterovirus* I, *Enterovirus* J, *Rhinovirus* A, *Rhinovirus* B and *Rhinovirus* C. These contain polioviruses (PVs), coxsackieviruses A and B (CAVs and CBVs), rhinoviruses (RVs) and echoviruses. ***Enterovirus A*** consists of 25 (sero) types; ***Enterovirus B*** consists of 63 (sero) types; ***Enterovirus C*** consists of 23 (sero) types; ***Enterovirus D*** consists of five (sero) types; EV-D68, EV-D70, EV-D94, EV-D111 (from both humans & chimpanzees) and EV-D120 (from gorillas). Human rhinovirus (HRV) 87 has been reclassified as a strain of EV-D68. ***Enterovirus E*** is comprised of group A bovine enteroviruses. Currently four types are recognised, EV-E1 to EV-E4. ***Enterovirus F*** is comprised of group B bovine enteroviruses. Currently six types are recognised, EV-F1 to EV-F6. ***Enterovirus G*** consists of a sixteen (sero) types: EV-G1 to EV-G16 and ***Enterovirus H***. In 2015 a novel virus was found in dromedary camels and it is proposed to place it within a new species, "***Enterovirus I***" (Woo *et al.*, 2015). ***Enterovirus J*** contains six simian enterovirus types (**Table 1.1**).

Enteroviruses are transmitted via the fecal-oral route or via respiratory transmission, depending on the type. EVs have two primary replication sites, the gastrointestinal tract and the respiratory tract, from where the virus can spread to the target organs via the blood circulation. This can result in severe, potentially fatal diseases.

1.6.2.Enterovirus pathogenesis

Enteroviruses (excluding rhinoviruses) are associated with a variety of infections varying from mild respiratory and gastrointestinal infections, herpangina, and hand-foot-and-mouth disease (HFMD), to more severe disease like poliomyelitis, pleurodynia, hepatitis, myo-peri-carditis, pancreatitis, meningitis, encephalitis, paralysis, neonatal sepsis leading to mortality, infections of the central nervous system (CNS) and type 1 diabetes (Harvala *et al.*, 2003; Roivainen & Klingel, 2009; Tracy *et al.*, 2011; Hober *et al.*, 2013; Tapparel *et al.*, 2013). Enteroviral primary replication process takes place in tissues of the respiratory tract or in the gastrointestinal tract, which is a result of their resistance in acidic pH conditions which allows them to withstand the acidic pH of the stomach (Hyypia & Stanway, 1993). Enterovirus infections are usually mild and limited to the site of infection, the gastrointestinal tract or respiratory tract. However, after the primary replication, the virus can sometimes enter the blood stream (viremia) which leads to infection of secondary target organs (Vuorinen *et al.*, 1999). During low- grade viremia, viral spread mainly occurs in reticuloendothelial tissue (e.g. liver, spleen, bone marrow, distant lymph nodes). In isolated incidences, infected individuals could progress to major viremia resulting in dissemination to target organs (e.g. CNS, heart, skin) often leading to necrosis or inflammatory lesions.

1.6.3.Coxsackieviruses

The first Coxsackie virus was isolated by Dalldorf and Sickles in 1948 in Coxsackie town, New York, (Dalldorf & Sickles, 1948). The virus isolated was first thought to be a

poliovirus and was isolated from children with suspected poliomyelitis. Extensive research in mice indicated that the virus was serologically different than poliovirus and since the first recognized human cases were residents of Coxsackie town Dalldorf and Sickles decided to name the virus Coxsackievirus. In subsequent years, outbreaks of different unexplained illnesses presenting with a variety of clinical symptoms resulted in the isolation of different Coxsackieviruses which were grouped into several serotypes within the *Enterovirus* genus. Newly discovered viruses were defined as coxsackieviruses, due to their ablity to infect new- born mice while polioviruses cannot. Echoviruses also cannot infect new- born mice and viruses with typical enterovirus properties e.g. size, buoyant density, acid stability, which were not coxsackieviruses or polioviruses, were called echoviruses.

Coxsackieviruses were divided into two subgroups, coxsackie A viruses (CAVs) and coxsackie B viruses (CBVs). CAVs consisted of 23 serotypes and CBVs of 6 serotypes (Moreau *et al.*, 2011). This division was based on the precise symptoms of the disease caused in new- born mice, but there are also some differences in the spectrum of human diseases caused by these two groups (Hyypia & Stanway, 1993). As more isolates became available and were studied more thoroughly, it became clear that there was much variation in the biological properties of different isolates belonging to the same serotype and this classification into coxsackieviruses and echoviruses was abandoned. New serotypes were just called enterovirus and given a number, although the names coxsackievirus A etc was kept for serotypes which have been already named in this way. Following this, sequence analysis showed that in fact viruses called

coxsackie A were not monophyletic and needed to be assigned to the three different species,EV-A, EV-B, and EV-C (Hyypia *et al.*, 1997).

Coxsackievirus infections are mostly mild or inapparent and humans are their only known natural hosts. Coxsackie A viruses are known to cause mainly rashes, vesicular lesions, and infection of muscles while Coxsackie B viruses cause viral pericarditis/ myocarditis, pleurodynia; infections of the CNS, pancreas and liver (Hyypia & Stanway, 1993; Yin-Murphy & Almond, 1996). Coxsackie virus A24 (CAV24) was the first known picornavirus to cause disease in the eyes and was discovered in Singapore in 1970 (Chan *et al.*, 2003; Oh *et al.*, 2003). A recent outbreak of Coxsackievirus A9 (CAV9) was recorded in Alberta, Canada in 2010 with increased cases of aseptic meningitis (Pabbaraju *et al.*, 2013).

1.6.4.Coxsackievirus A9

Coxsackievirus A9 (**Figure 1.12**) is the only CAV assigned to the species EV-B, together with the 6 CBV serotypes, the echoviruses and more recently- isolated numbered EV types (Hyypia & Stanway, 1993; Mirmomeni *et al.*, 1997; Hendry *et al.*, 1999; Harvala *et al.*, 2005). CAV9 is one of the 10 most commonly- isolated enteroviruses. During the determination of its complete sequence it was found that CAV9 has an insertion of approx 15 amino acids at the C- terminus of the VP1 protein where an arginine- glycine- aspartic acid (RGD) motif is found (Chang *et al.*, 1989, 1992). RGD motifs are known to have significant roles in cell- cell and cell- matrix interactions as well as in the recognition of the host cells by viruses via cell surface integrins (Ruoslahti & Pierschbacher, 1987). The RGD motif was conserved in all CAV9

isolates found over a 25 year period even though the C- terminal VP1 region is otherwise variable. This suggests that it has an important role in infection (Chang *et al.*, 1992). This result was confirmed by subsequent extensive analysis (Santti *et al.*, 2000; Merilahti *et al.*, 2012). Other viruses with an RGD motif able to bind to integrins include some HPeVs and all FMDV serotypes (Mateu *et al.*, 1996; Boonyakiat *et al.*, 2001; Burman *et al.*, 2006). Altering the RGD motif in these viruses showed that is important in infection (Mateu *et al.*, 1996; Boonyakiat *et al.*, 2001).

Interestingly, aligning the RGD region on the diverse picornaviruses where it is found, showed that there is strong conservation of the +1 position (RGDX, where X is usually L or M) and +4 position (RGD_ _ _ X, where X is usually L) **(Figure 1.13)**. In order to understand the viability of viruses possessing an RGD motif a number of mutant cDNAs containing either deletion or substitutions involving the RGD were constructed and used to study the viral infectiousness on different cell lines (Hughes *et al.*, 1995). Surprisingly, it was found that amino acid substitutions at the RGD +1 position could have a significant effect on growth efficiency of the virus but not in all cell lines. Indeed, the complete deletion of the RGD motif had no effect on infectivity on the rhabdomyosarcoma (RD) cell line suggesting that cells can be infected by a different mechanism that does not rely on the RGD motif; an RGD- independent mechanism. Although the RGD- independent entry is not very much understood, the RGD-dependent mechanism is thought to be via an integrin, with integrin αvβ6 being the major receptor for CAV9 (Williams *et al.*, 2004). Cryo EM analysis (**Figure 1.12**) shows that CAV9 forms a complex with integrin αvβ6 and that the integrin binds to the virus particle on the far side of the canyon from the 5-fold axis (Shakeel *et al.*, 2013).

As CAV9 can infect cells via both an RGD- dependent and RGD- independent mechanism, it may be that the acquisition of the VP1 RGD- containing C-terminus in CAV9 is a recent event, explaining the ability of CAV9 to be still internalized in a non-RGD dependent manner. This may be supported by the apparent involvement of β2 microglobulin (β2-M, a subunit of histocompatibility complex class I [MHC-I]) and GRP78 (glucose-regulated protein 78-kDa) as co receptors in the internalization process, which possibly play roles in a post- attachment step in several picornaviruses including CAV9 and several echoviruses (Ward *et al.*, 1998; Triantafilou *et al.*, 2000a, 2002, Heikkilä *et al.*, 2009, 2010; Shakeel *et al.*, 2013; Huttunen *et al.*, 2014)**.** Interestingly, studies indicate that the possible αV integrin receptors did not cointernalize with the virus in endosomes (Heikkilä *et al.*, 2010) and that the internalisation of CAV9 appears to depend on β2-M, dynamin and the Arf6 pathway but are independent of the clathrin and caveolin-1 pathways (Heikkilä et al., 2009; Heikkilä et al., 2010; Merilahti et al., 2012). On the contrary, CAV9 entry appears to be closest to macropinocytosis and more recent studies have suggested that in light and EM observations during CAV9 early infection, actin was strongly modulated on the plasma membrane and caused ruffling and large invaginations for the virus to gain entry (Huttunen *et al.*, 2014). In addition, treatment with EIPA showed a very strong inhibitory phenotype on CAV9 suggesting that macropinocytosis is indeed in use (Heikkilä *et al.*, 2010; Huttunen *et al.*, 2014). Entry then involves the virus being taken into non-acidic multivesicular bodies, in which uncoating occurs (Heikkilä *et al.*, 2010; Huttunen *et al.*, 2014).

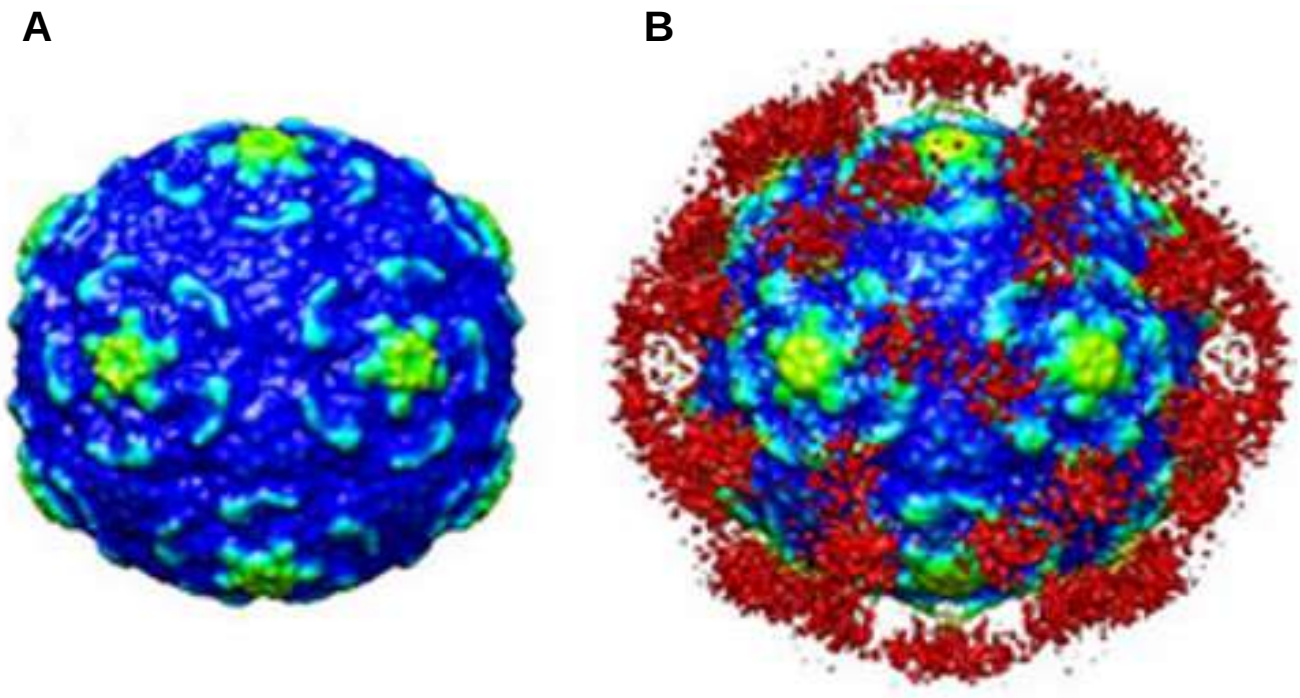

Figure 1.12: Icosahedral reconstructions of CAV9 in complex with integrin αvβ6. Radially depth-cued isosurface representations of the CAV9 capsid (A) and CAV9 capsid-integrin $\alpha_v\beta_6$ complex filtered to 10.3-Å resolution (B). Blue represents the shallowest parts of the surface and green the most prominent. αvβ6 is shown in red (Adapted from (Shakeel *et al.*, 2013)).

.

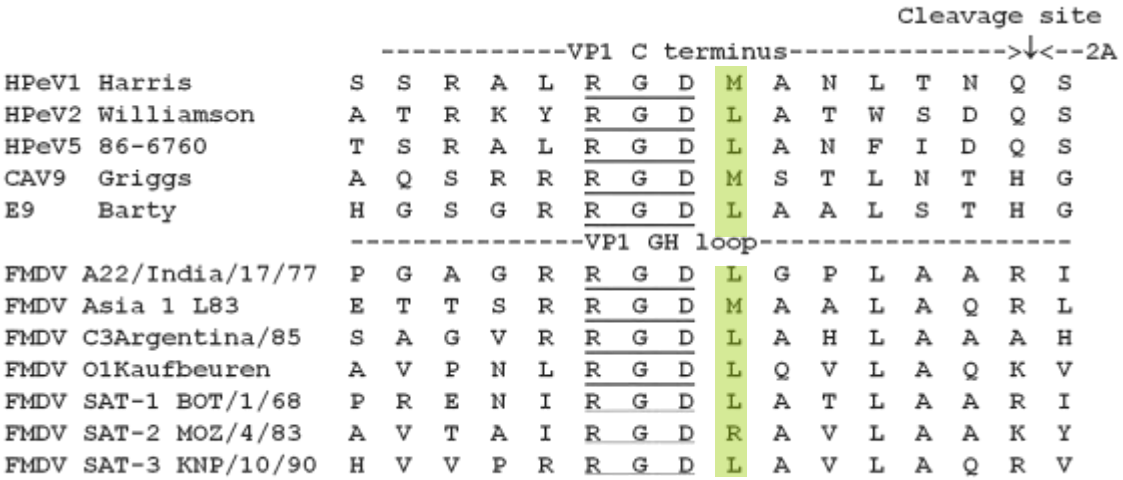

Figure 1.13: Sequence alignment of RGD containing viruses.

Sequence alignment of the VP1 region that contains the RGD motif in different picornaviruses. ((Boonyakiat *et al.*, 2001). The well-conserved RGDX position is highlighted in green.

Aim of the study

The knowledge of the precise sequences involved in binding to two distinct cellular receptors (integrins and heparan sulphate) makes CAV9 a very good model to explore the relationship between receptor interactions and cell tropism. This is important in understanding how viruses target specific cells and cause disease, as well as in the design of viruses for oncolytic therapy. Early studies on different RGD- containing picornaviruses (Hughes *et al.*, 1995; Jackson *et al.*, 2000; Boonyakiat *et al.*, 2001) showed that different amino acid substitution found near the RGD motif could affect receptor binding. These studies were limited in the number of virus mutants and cell lines used. More recently, the ability of CAV9 to interact with cell surface heparan sulfate has started to be investigated (McLeish et al., 2012; Merilahti et al., 2016).

This thesis describes work designed to improve our understanding of the involvement of a) the RGD motif and more specifically the +1 position in CAV9 cell using a large panel of different RGDX CAV9 variants b) the significance of possible interactions between CAV9 and heparan sulfate in infection.

Chapter 2. Materials and Methods

2.1. Materials

The project used a number of virus strains and cell lines as well as cell biology reagents. Those, together with their source are listed below to help others who may wish to perform similar work.

2.1.1.Virus Strains

Several CAV9 variants were used and these were generated previously from an infectious cDNA clone, pCAV9 (Hughes *et al.*, 1995) by transfection of RD cells. The titres of the stock solutions were measured and are given in **Table 2.1**.

- Coxsackievirus A9 wild-type (CAV9 wt; Griggs strain).
- S2871R (mutation of position 287 in VP1, Williams et al., unpublished); RGDA, RGDT, RGDR, RGDL, RGDS, RGDD, RGDG, RGDI, RGDF, RGDQ (mutants with a mutation in the position immediately downstream of the RGD motif in VP1 [i.e. VP1 position 293), Hughes et al., 1995 and Hughes, unpublished); CAV9 d4 (mutant lacking the RGD motif (Hughes *et al.*, 1995)).

2.1.2. Mammalian Cell Lines

A large panel of cell lines was used to study CAV9 cell tropism.

- A549- Human epithelial lung adenocarcinoma cell line
- GMK- Green Monkey Kidney epithelial cell line
- HeLa- Human epithelial cervical cancer cell line

- HT-29- Human epithelial colorectal adenocarcinoma cell line
- MCF-7- Human breast adenocarcinoma cell line
-
- MDA-MB-435- Human melanoma cell line
- PC-3- Human adenocarcinoma prostate cancer cell line
- RD- Human rhabdomyosarcoma cell line

These were obtained originally from ATCC and provided by Dr Merja Roivainen, THL, Helsinki, Finland (GMK); Dr Sisko Tauriainen, University of Turku, Finland (A549, RD); Dr Andrea Mohr (HT-29); Professor Nelson Fernandez (MCF-7, HeLa) and Professor Elena Klenova (PC-3, MDA-MB-435, MDA-MB-231) (University of Essex).

2.1.3. Tissue Culture Reagents

- Accutase solution (1x Accutase enzymes in Dulbecoo's PBS, 0.5 mM EDTA) (Sigma)
- DMEM- Dulbecco's Modified Eagle's Medium. High Glucose (4.5 g/L) with LGlutamine (Biosera)
- FBS- Fetal Bovine Serum (Research grade, Sigma)
- Gentamicin solution (50mg/mL) (Sigma)
- McCoy's 5A (modified) medium (1x) (Gibco)
- NEAA- MEM Non-essential Amino Acid Solution (100x) (Sigma)
- PBS- Phosphate Buffered Saline tablets (1x) (Fisher). 1 tablet of PBS was dissolved in 100 ml of water then autoclaved.
- Penicillin-Streptomycin solution (100x) (Sigma)

- RPMI-1640 Medium- Roswell Park Memorial Institute (Sigma)
- Trypsin-EDTA (1x liquid, 0.25% Trypsin 1mM) (Gibco)

2.1.4. General Chemicals/ Solutions

- Calcium chloride $CaCl_2$ (Sigma). A 20 mM solution was prepared and adjusted to pH 7.5 then autoclaved.
- DMSO- Dimethyl sulfoxide Hybri-Max, ≥99.7% (Sigma)
- EDTA-Ethylenediaminetetraacetic Acid anhydrous (Sigma)
- Magnesium chloride MgCl2 (Sigma). A 20 mM of solution was prepared and adjusted to pH 7.5 then autoclaved.
- TBS- Tris Buffered Saline (made up of 20 mM Tris+150 mM NaCl) (Sigma), and adjusted to pH 7.5 then autoclaved.
- Ammonium Chloride (Sigma). A 50mM solution was prepared and filter sterilised
- Sodium Chlorate (Sigma). A 500 mM solution was prepared and autoclaved.
- Protamine Sulphate (Sigma). 0.5 mg/ml and 2.0 mg/ml were dissolved in PBS.

2.1.5. Heparin and heparin- agarose

Heparin sodium salt, from porcine intestinal mucosa (Sigma) - heparin was dissolved in water to give a 50 mg/ml solution and filter sterilized using a 20 nm filter.

Heparin- Agarose, Type I (suspension in 0.5 M NaCl, 0.02% thimerosal) (SIGMA)

2.1.6. Antibodies

Several antibodies were used for cell surface receptor expression, integrin blocking or visualising infected cells.

- Human monoclonal Anti- Integrin αvβ3 antibody (CD51/61), conjugated with PE under optimal conditions (304406, Biologend).
- Mouse monoclonal Anti- Coxsackie A9 antibody (Millipore , MAB947).
- Mouse monoclonal Anti- IgG2a antibody, conjugated with PE under optimal conditions (Biolegend, 407107).
- Purified Mouse IgG1, κ Isotype Ctrl Antibody for αvβ3, conjugated with PE under optimal conditions (Biolegend, 400113).
- Purified Mouse IgG2a, κ Isotype Ctrl Antibody for αvβ6 (Biolegend, 400201).
- Mouse monoclonal anti- Integrin αvβ3 antibody (Millipore, MAB1976Z). [function blocking]
- Mouse monoclonal Anti-Integrin αvβ6 antibody [10D5] (Abcam, ab77906). [function blocking]

2.1.7. Plaque Overlay Medium and Crystal Violet Stain

- Agarose (general purpose, Fisher)
- CarboxyMethyl Cellulose (CMC, Sigma).
    - A 2 % CMC/agarose overlay was produced by adding 2.0 g of CMC and 2.0 g of agarose to 100 ml of distilled water then autoclaved.

- A 2 % Liquid CMC overlay was produced by adding 2.0 g to 100 ml of distilled water then autoclaved.

- A 0.1% w/v solution of Crystal Violet was produced by dissolving 0.5 g of Crystal Violet powder (ACROS Organics, Fisher) in 495 ml of distilled water + 5 ml of absolute ethanol.

2.1.8. Immunofluorescence Reagents

- 4 % Formaldehyde (FA): 40 % formaldehyde (Fisher) was diluted with x1 PBS to give a 4% solution.
- Antibody diluents: 1 % BSA, 0.05 % TWEEN® 20, 1x PBS
- Blocking Solution: 2 % FBS, 1 % Bovine Serum Albumin (BSA) (Sigma), 0.05 % TWEEN® 20 (Sigma), 1x PBS.
- Permeabilization buffer: 250 µl of Triton X-100 (0.25 %) (Fisher) was mixed with 100 ml of 1x PBS.
- VECTASHIELD HardSet Mounting Medium with DAPI (Vector Laboratories).
- Washing buffer: 100 mM glycine was prepared by dissolving 0.751 g of glycine (Fisher) in 100 ml of 1x PBS.

2.1.9. Extraction and Purification Techniques

A variety of extraction and purification kits were used for purifying DNA, viral RNA or PCR products (Qiagen). These included:

- QIAGEN- QIAquick PCR purification kit (50), using a microcentrifuge.
- QIAGEN- QIAquick Gel Extraction kit (50), using a microcentrifuge.

- QIAGEN- QIAamp Viral RNA Mini Kit (50), for purification of viral RNA (Spin Protocol) from tissue cultures.

2.1.10. Reverse Transcription Polymerase Chain Reaction (RT-PCR)

RT-PCR of purified samples containing CAV9 RNA was performed using a SuperScript III one-Step RT-PCR System with Platinum *Taq* DNA polymerase kit (Life technologies).

2.1.11. Primers

Oligonucleotides (Table 2.2) were used for RT-PCR and sequencing. They were obtained from Fisher on a 50 nmole scale and dissolved in sterile distilled water to give a 100 µM solution.

2.1.12. Agarose Gel Electrophoresis

Agarose gel electrophoresis was used to analyse and purify PCR fragments.

- Agarose (general purpose, Fisher)
- Electrophoresis buffer (ELFO buffer) (50x): A mixture of 242 g Tris base and 100 ml of 0.5 M EDTA (pH 8.0) was adjusted to pH 7.7 with glacial acetic acid and made up to 1 L with water.
- Loading buffer (5x): 25 ml of glycerol, 100 µl of 0.5 M EDTA pH 8 and 0.2 g of bromophenol blue were mixed and volume made up to 50 ml with sterile distilled water. For some DNA isolations, loading buffer without bromophenol blue was used

to avoid co-purification of DNA/bromophenol blue and make bands migrating to the approximate bromophenol blue position more visible.

- Loading buffer was added to DNA samples at a ratio of 1:5.
- DNA standard loading mixture for a 5 mm agarose gel lane: 1 µl GeneRuler 1 Kb DNA ladder (**Figure 2.3.** 0.5 µg/ µl), 1 µl 6x DNA loading dye, were mixed and the volume was made up to 6 µl with nuclease-free water (Thermo scientific).
- SafeView Nucleic Acid Stain (NBS Biologicals) was used at 5 µl/ 50 ml gel.
- TopVision Low Melting Point Agarose (Thermo scientific)

Table 2.1: Summary of CAV9 strains and the titres in PFU (plaque forming unit) of the stock solutions.

Strain	Titre (PFU/ml)
CAV9-Griggs (wt, RGDM)	$8.2x10^7$
CAV9 RGDL	$1.2932x10^8$
CAV9 RGDT	$1.8x10^7$
CAV9 RGDA*	$2.48x10^6$
***found to also have a Q2861R mutation**	
CAV9 RGDS	$2.6x10^7$
CAV9 RGDR	$5.4x10^7$
CAV9 RGDF	$1.6x10^8$
CAV9 RGDI	$1.6x10^7$
CAV9 RGDD	$1.7x10^7$
CAV9 RGDQ	$4.8x10^7$
CAV9 RGDG	$2.2x10^7$
CAV9 RGD del (d4)	$3.6x10^6$
CAV9 T132R mutant	$3.22x10^8$
CAV9 S2871R mutant	$1.61x10^8$

Table 2.2: The CAV9 specific primers used for RT-PCR.

Virus	Primers name	Orientation (5'- 3' →, 3' – 5' ←)	Primers sequence (5'→3')	Length (bases)
CAV9-wt	OL2055	Fragment 1-Fwd →	AGT CCT CCG GCC CCT GAA TG	20
	OL2079	Fragment 1-Rev ←	CTT CCA CCA CCA CCC CAC CGA	21
	OL2080	Fragment 2-Fwd →	GTG TGC TAA CGT GGT GGT GGG GT	23
	OL2081	Fragment 2-Rev ←	AGG TTC TTC ACT TCT CCT GGG ATG	24
	OL2082	Fragment 3-Fwd →	CTA TGC CGA CAC CGC ATC CAC	21
	OL2083	Fragment 3-Rev ←	TGG CTT CTT CCA CAT CCC CTT G	22
	OL2145	Fragment 4-Fwd →	ACG TGT TGG TAT CAG ACT GGT ATG	24
	OL2146	Fragment 4-Rev ←	CTT CCG TCC AGA AAA TGC TGG GGT	24
	OL2147	Fragment 5-Fwd →	TCG ACA AGA CCC CGG AAC AAC CCT	24
	OL2148	Fragment 5-Rev ←	TCG TGC TCA CAA GGA GGT CTC T	22

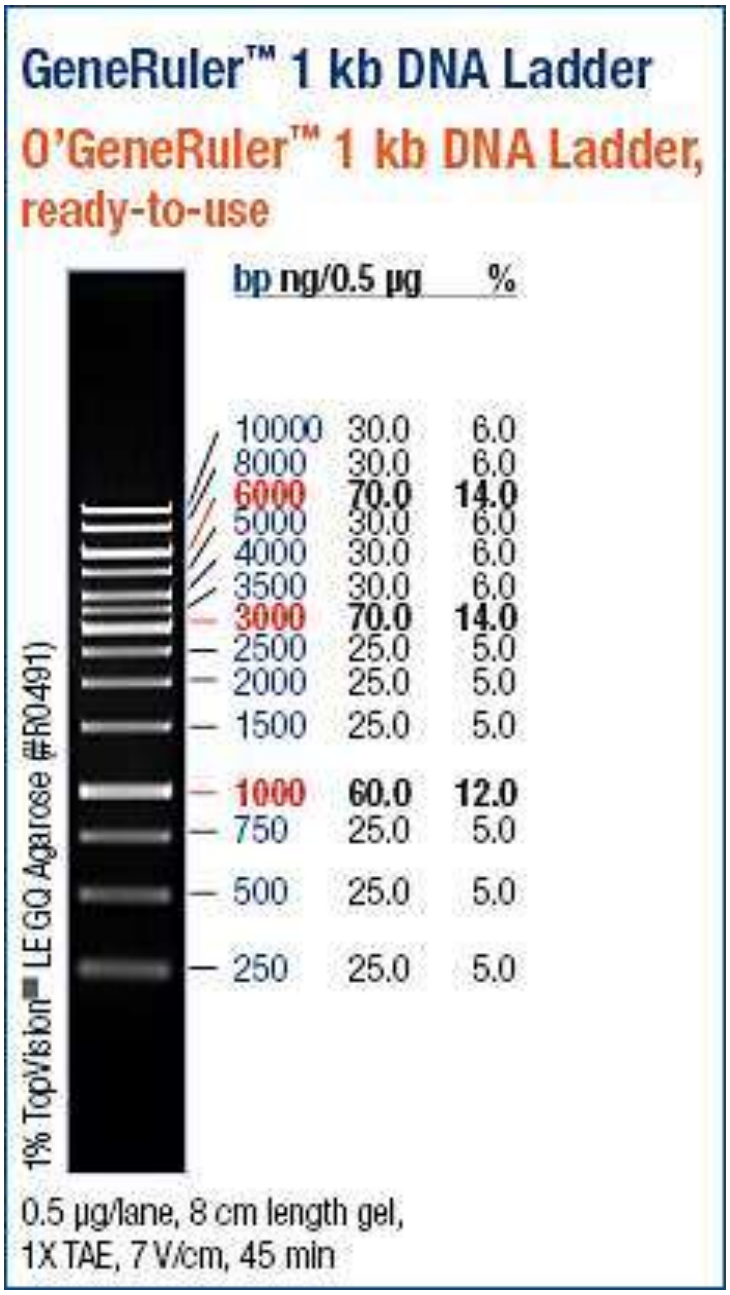

Figure 2.1: 1 kb DNA ladder used as a size standard.

The size of fragments and amount of DNA (ng) in each band when a 500 ng sample is loaded (Thermo scientific).

2.2. Methods

2.2.1. Cellular Biology and Virology

2.2.1.1. Cell Culture Maintenance

A549, GMK, MCF-7, MDA-MB-435, HeLa and RD cell monolayers were grown in 50 ml (25 cm^2) tissue culture flasks in DMEM supplemented with 10 FCS, 1 % NEAA and 5 µg/ml Penicillin-Streptomycin. PC3 cells were maintained in RPMI-1640 medium containing 10% FCS and 5 µg/ml Penicillin-Streptomycin. HT-29 cells were maintained in McCoy's 5A medium supplemented with 10% FBS and 5 µg/ml Penicillin-Streptomycin. To propagate the cells, growth medium was discarded carefully from confluent flasks prior to washing twice with 1x PBS; 500 µl of Trypsin- EDTA or Accutase were added and the cells were placed on a rocking platform shaker at room temperature for 3 minutes or until all cells were detached. In order to culture the cells in flasks, 5 ml of growth medium was added to the cell suspension and 1 ml aliquots were then placed into flasks containing 4 ml of fresh medium. Flasks were incubated at 37˚C in 5% CO_2 and passaged after ~80-100 % confluent cells monolayer was observed (3-5 days).

2.2.1.2. Cryopreservation of Mammalian Cells for Storage

Freezing: Cells were washed twice with 1x PBS and detached by using 500 µl of Trypsin- EDTA or Accutase. Cells were washed with 1 ml fresh medium and

centrifuged for 5 min at 1300 rpm. The cell pellet was re- suspended in 1ml FBS and 111 µl DMSO before being transferred into cryo-vials (Nunc). The cryo-vials were then wrapped in cotton wool and frozen at -80°C for 72 hours. For long-term storage, the cells were transferred into liquid nitrogen.

Thawing: Cells were removed from -80°C freezer or liquid nitrogen and immediately transferred to a 37˚C water-bath for a minute. Cells were pelleted (1300rpm; 5 min) and washed with 1 ml fresh medium. Cells were then transferred to a flask containing 4 ml of fresh medium and 1 ml of FBS and incubated at 37˚C 5% CO2 incubator.

2.2.1.3. Viral Plaque Assay

Tissue Culture flasks 25 cm^2: Once confluent cell monolayers were obtained, medium was discarded and 100 µl of each diluted virus were added to 1 ml of fresh growth medium prior incubation at room temperature on a rocking platform for 45 minutes. The cells were then covered with 4 ml of overlay made from warm DMEM (56 °C) and a 2 % solution of CMC and agarose (melted in a boiling water bath) at a ratio of 3:1 (DMEM: CMC/ agarose). Flasks were then incubated at 37˚C in a 5% CO_2 incubator for 3 days or until plaques were formed. Once the plaques were observed, the overlay medium was removed gently by washing twice with 1x PBS, and 0.1 % Crystal Violet stain was added. After 5 minutes the flasks were washed with PBS and the plaques were counted.

Tissue Culture 6-well plates: Once confluent cell monolayers were obtained, medium was discarded and 50 µl of each diluted virus were added to 500 µl of fresh growth medium prior incubation at room temperature on a rocking platform for 45 minutes.

Cells were then treated the same way with only exception of adding 2 ml of 2% CMC solution (without agarose) at a ratio of 1:2.

2.2.1.4. Viral Propagation

In order to amplify viruses, the medium was discarded from the confluent monolayers of cells and 1 ml of fresh growth medium was added. 10 µl of virus sample was added to cells and left for 1 hour at room temperature on the rocking platform allowing individual viral particles to adsorb to cells and initiate a spreading infection. After incubation, 3 ml of media was added and the flasks incubated at 37 ˚C in a 5% CO_2 incubator for 3-4 days to allow cytopathic effect (CPE) to progress. Virus was then released from cells by freeze-thawing three times and aliquots were stored at -80 °C for future plaque assays or plaque purification.

2.2.1.5. Viral Plaque Purification

Plaque assay was performed on cells of interest and plaques were left to fully develop. Individual plaques were selected and picked using a sterile micropipette tip by scratching through the CMC/agarose overlay. 10 µl of fluid was withdrawn and added to 200 µl of fresh media. If further viral propagation was desired, 100 µl from this mixture was transferred to fresh cell monolayers and the same steps were followed as described above.

2.2.1.6. Differences in CAV9 Tropism

GMK, A549, MCF-7, PC-3, HT-29 and RD cells were grown on 6- well plates for 3 days. All media were removed and 50 µl (5000 PFU) of the virus sample (CAV9-wt, RGDT, RGDR, RGDA, RGDL, RGDS, D4, RGDI, RGDG, RGDF, RGDQ, RGDD) were added to 500 µl of growth medium to each well. The plates were then were placed on a rocking platform shaker and incubated for 1 hour at room temperature. CMC and medium was prepared in the same way as described above and 2 ml were added to each well. The samples were then incubated at 37˚C in a 5% CO_2 incubator for 3-4 days prior staining with 0.1% Crystal Violet.

2.2.1.7. Effect of EDTA treatment

A549 and GMK cells were grown in 6- well plates in medium for 2 days to ~100% confluence. 50 µl (5000 PFU) of viral dilutions were added to the cells along with 500 µl of fresh medium or TBS supplement with divalent cations (TBS- CaMg) or TBS with20mM EDTA (TBS-EDTA) and incubated for 45 minutes at 4℃ to allow the virus bind to the cells but not get internalized. After incubation the cells incubated with media were washed two times with either fresh medium, TBS supplement with divalent cations (TBS- CaMg) or TBS with 20mM EDTA (TBS-EDTA). The cells incubated with the virus alongside the TSB-CaMg or TBS- EDTA, were washed twice with fresh media to remove any unbound virus and residue of the solutions. All plates were overlaid with CMC overlay medium as described previously and incubated in the 5% CO_2 incubator at 37˚C for 3-4 days prior staining with 0.1 % Crystal Violet.

2.2.1.8. NH_4Cl treatment to neutralise endosomal pH

A549 and RD cells were grown in 6- well plates in medium for 2 days to ~100% confluence. Media was supplemented with HEPEs buffer and NH_4Cl at a ratio of 7:1:2 (ml). Control media was supplemented with 2 ml sterile water instead of NH_4Cl. 1 ml of the control solution was added to control cells while 1 ml of the NH_4Cl solution was added to the treated cells and were incubated at 37˚C for 1 hour. 5000 PFU of each viral sample (RGDM/wt, RGDF and d4) were added to the cells and incubated for 45 min at room temperature on a rocking platform. The wells were washed with 1 ml media before the addition of CMC. The samples were then incubated at 37˚C in a 5% CO_2 incubator for 4 days prior staining with 0.1% Crystal Violet.

2.2.1.9. Inhibition of Infection with Soluble Heparin

A549, HeLa, MCF7 and RD cells were grown in 6- well plates for approximately 3 days. 90 µl 5000 PFU) of a virus dilution (RGDM/wt, S2871R, RGDR, T132R and Q2861R) was incubated with 10 µl of heparin (50 mg/ml) for 30 minutes at room temperature. 90 µl of virus plus 10 µl of water was used as a control. The virus- heparin solution was added to the cells along with 500 µl of fresh medium. The cells were then incubated for another 45 minutes at room temperature in a rocking platform. After incubation, the cells were overlaid with CMC overlay medium as described previously and incubated in the 5% CO_2 incubator at 37˚C for 3-4 days. Once the plaques were observed the cells were stained with 0.1% Crystal Violet.

2.2.1.10. Removal of viral particles using immobilised heparin

Heparin agarose, type I, (0.5 ml suspension) was centrifuged for 30 seconds at 3000 rpm. 1 ml of cell growth medium was added and after mixing well the solution was centrifuged for 30 seconds at 3000 rpm and the supernatant was discarded. The pellet was washed with medium and centrifuged in the same way three times. 0.5 ml (1000 PFU) of a virus sample was added and the sample was left on a rotary mixer at room temperature for 45 minutes. Then, the sample was centrifuged for another 30 seconds and the supernatant was stored at - 80˚C. The pellet was washed 3 times with medium, then 0.5 ml of 0.5 M NaCl in PBS was added and incubation continued for 30 minutes on the rotary mixer at room temperature. After the incubation period, the sample was centrifuged for 30 seconds and the supernatant was stored at - 80˚C. The binding to the immobilised heparin was then analysed by plaque assays on A549 cells.

2.2.1.11. Inhibition of Proteoglycan Sulphation with Sodium Chlorate

A549 and GMK cells were grown in 6- well in the presence or absence of sodium chlorate ($NaClO_3$) for 3 days to ~100% confluence. Media was supplemented with 50 mM $NaClO_3$ or water (control). The cells were then used for plaque assay using 5000 PFU of each viral sample (CAV9-wt, RGDR, S287R, Q286R and T132R). The plates were then were placed on a rocking platform shaker and incubated for 1 hour at room temperature. CMC and medium (± $NaClO_3$) was prepared in the same way as described above and 2 ml were added to each well. The samples were then incubated at 37˚C in a 5% CO_2 incubator for 3-4 days prior staining with 0.1% Crystal Violet.

2.2.1.12. Blocking of cell surface heparan sulphate with protamine sulphate

A549 and GMK cells were grown in 6- well plates for 3 days to ~100% confluence. Media was removed and cells were incubated in the presence of 0.5 mg/ml or 2.0 mg/ml protamine sulphate for two hours at CO_2 incubator at 37 ˚C. 1000 PFU of each viral sample (RGDM/wt, RGDR, S287R, Q286R and T132R) were added to the cells and incubated for 45 min at room temperature on a rocking platform. CMC and medium was prepared in the same way as described above and 2 ml were added to each well. The samples were then incubated at 37 ˚C in a 5% CO_2 incubator for 3-4 days prior staining with 0.1% Crystal Violet.

2.2.1.13.Flow Cytometry Analysis of Integrin Expression on Cells

The expression of integrins αvβ3 and αvβ6 on the cell surface was analyzed by flow cytometry and specific monoclonal antibodies (PE- labelled anti- human CD51/61, anti-integrin αvβ6 and PE anti- mouse IgG2a). PE conjugated mouse IgG1, κ Isotype Ctrl and IgG2a, κ Isotype Ctrl were used as controls for αvβ3 and αvβ6 respectively. Cell monolayers were washed with 1x PBS and detached using Trypsin-EDTA. Cells were re-suspended at 5x 10^5 cells/ ml. Then, centrifuged at 1300 rpm for 5 min before adding 95 µl of DMEM containing the appropriate mAbs; 5 µg/ml of anti- human CD51/51 (αvβ3), 5 µg/ml of anti- integrin αvβ6 (primary antibody) and 5 µg/ml PE anti-mouse IgG2a (secondary antibody), 5 µg/ml of Isotype controls IgG1 κ Isotype Ctrl (for αvβ3) and IgG2a κ Isotype Ctrl (for αvβ6). Incubations with antibodies were performed in the dark at 4 °C for 20 min. Cells were then centrifuged and the pellet was re-suspended in 200 µl of media prior fluorescence analysis. For each experiment, 20,000

events were counted and cell debris/ apoptotic cells gated out using a plot of forward scatter versus side scatter. Analysis was performed with FACS Calibur flow cytometry (Becton Dickinson; BD Accuri™ C6).

2.2.1.14. Blocking of Viral Infection with Monoclonal Antibodies

A549 and RD cells were grown on 13-mm sterile glass coverslips in 6- well plates for 1 day. After media was removed the cells were pre- treated with 1.0 µg of mAb against integrin αvβ6, αvβ3 or isotype controls along with 500 µl fresh media for 30 minutes at 37 °C prior to the infection. Then 5 µl of neat virus was added to each well and incubated at 4 °C for 30 min to allow binding of the virus to cell receptors. After this, the cells were incubated for a further 6 hours at 37 °C in the CO_2 incubator. All media was removed and the cells were gently washed 2x PBS before being fixed with 1 ml cold 4% paraformaldehyde (FA) for 20 min at room temperature. To stop the fixation reaction, cells were washed twice with 100 mM glycine prepared in 1x PBS for 5 min, then permeabilized for 20 min with 0.25% Triton X-100 followed by a wash with PBS for 10 min. Cells were then treated with blocking solution for 30 min at room temperature on the rocking platform. After removing any liquids from the wells, 50 µl of primary antibody against CAV9 (anti- CAV9) was added (at titre of 1:112; diluted with antibody diluent) and coverslips were covered with parafilm and incubated overnight (16 hrs) at 4 °C the following day, cells were first washed with 1x PBS, and secondary antibody (PE- labelled anti- mouse IgG) was added (titre of 1:200) to the cells and incubated in the dark for 2 hours at 4 °C. Cells were then washed with 1x PBS and mounted using mounting media containing DAPI on glass slides. The slides were examined by

fluorescence microscopy using BX41 microscope and the number of green- fluorescent cells were counted in 20 random fields.

2.2.2. Molecular Virology

2.2.2.1. Purification of Viral RNA from Tissue Culture

Extraction of the viral RNA was performed using a QIAamp viral RNA mini kit (QIAGEN). A volume of 140 µl of cell- culture supernatant containing viral particles was lysed in 560 µl AVL buffer (lysis buffer) in the presence of 5.6 µl carrier tRNA. 560 µl of ethanol (100%) was added to the RNA containing solution and mixed by pulse-vortexing for 15 s before the solution was applied to the provided silicate column and centrifuged at 8000 rpm for 1 min. Salt and pH conditions in the lysis solution prevent proteins and other contaminants from binding to the silicate disc. The viral RNA bound to the spin column was washed with buffers AW1 and AW2 to achieve a maximum contaminant removal. Finally, the viral RNA was eluted from the column by 50 µl of AVE Buffer and centrifugation (13000 rpm, 1 min). Viral RNA was stored at -80 °C or used directly for RT- PCR.

2.2.2.2. Reverse- Transcription Polymerase Chain Reaction (RT-PCR)

RT-PCR was performed using the Superscript III One- Step RT-PCR System with Platinum *Taq* (Lifetechnologies). cDNA was generated from 5 µl of purified RNA and amplified with 100 nmoles of forward and reverse primers (Table 2.2). The RT-PCR reaction was assembled in a thin- walled PCR tubes containing 1 µl of each forward and reverse primers, 1 µl RT-*Taq* mix, 5 µl of RNA, 25 µl of the provided reaction mix and 17 µl nuclease free water reaching a total volume of 50 µl. The reaction was run in a GeneAmp PCR System 9700 thermal cycler (Applied Biosystems). The settings of

the PCR are provided in Figure 2.2. The amplicons were then purified using a QIAquick Gel Extraction kit (QIAGEN) and commercially sequenced by Source Bioscience Life Sciences (Nottingham, UK).

2.2.2.3. Agarose Gel Electrophoresis

Agarose powder was mixed with 1x ELFO buffer to 10 mg/ml and heated until completely dissolved. 5 µl of Safe View was added to the mixture prior to its addition onto a casting tray. The gel was allowed to cool down and solidify at room temperature. The DNA sample of interest was mixed with clear loading buffer at a ratio of 5:1 and loaded to the gel alongside a DNA marker. Electrophoresis was carried out for 20 min at 150V. Gel was visualized using blue light and images were taken by a gel documentation and analysis system (SYNGENE InGenius3/ GeneSys software).

2.2.2.4. DNA Purification from Agarose Gel (Gel Extraction)

The desired DNA fragments were excised from the agarose gel using a clean scalpel and gel extraction and purification of DNA was performed using a QIAquick gel extraction kit. The embedded DNA in the agarose gel was removed by dissolving the agarose in QG buffer (lysis solution; 300 µl per 100 mg) at 50 °C for 10 min with intermittent vortexing, or until the gel had been completely dissolved. 100 µl of isopropanol was added to the samle. The mixture was then transferred into a QIAquick column provided and centrifuged for 1 min at 14000 rpm to allow the DNA to bind to the silicate disc. Residual agarose was removed by further washing of the column with 500

µl QG buffer. Precipitation of the sample was achieved by washing the column with 750 µl ethanol based PE buffer. Any residual ethanol was removed by full speed centrifugation for an additional minute. DNA was eluted from the column by addition of 30 µl EB buffer and centrifugation at 14000 rpm for 1 min.

2.2.3. Bioinformatics

2.2.3.1. DNA sequencing and Sequence analysis

The DNA samples of interest were commercially sequenced by Source BioScience LifeSciences, Nottingham. Each fragment was sequenced in both orientations using the specific primers used in the amplification process.

Sequencing raw data were accessed using the program Chromas Lite to visualise for any heterogenicity at each position. DNA sequences were translated into protein sequences using the online tool ExPASy (http://web.expasy.org/translate/) prior their alignment with ClustalW (http://www.genome.jp/tools/clustalw/). Multiple sequence alignment was also used to identify conserved sequences for primer design as well as comparison between different phenotypic viruses for identification of unique genotypes. Database searches were conducted using NCBI BLAST search facility (http://blast.ncbi.nlm.nih.gov/Blast). The BLAST program can be used to search sequence homology from all similar species represented in the database starting from 100% down to 1% similarity. Any sequence logos were produced using the weblogo (http://weblogo.berkeley.edu/logo.cgi).

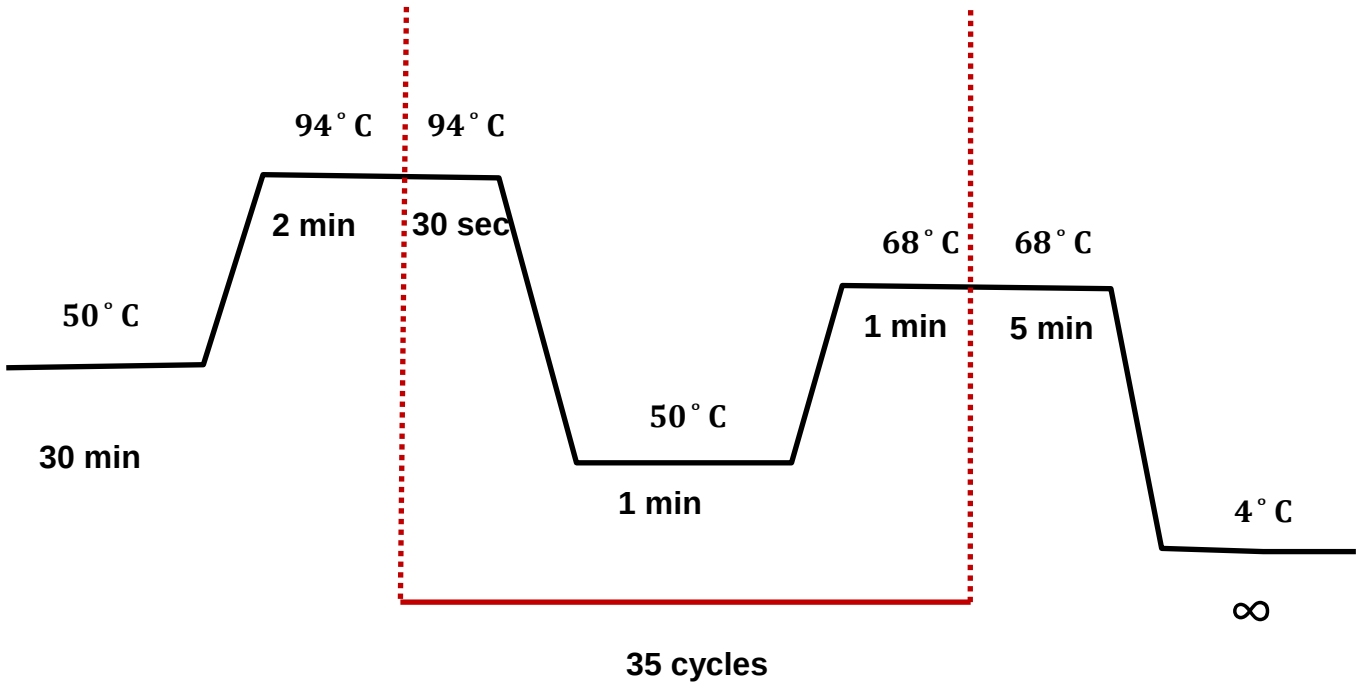

Figure 2.2: Parameters used for RT-PCR of CAV9 RNA.

The cycle starts at 94 ˚C to activate the polymerase enzyme followed by 35 cycles of denaturation at 94 ˚C to separate the two strands of DNA, annealing at 45-50 ˚C, where the primers bind to specific areas of the target gene, and DNA polymerase, extension at 68 ˚C. A final extension at ˚C confirms that strand synthesis has been completed, before the reaction is stopped by cooling to 4 ˚C. The annealing temperature depends on the melting temperature of the primers and the length of the 72 ˚C extension may vary based on the length of the amplified DNA fragment. pfu polymerase requires a time of 2 min per 1000 bases amplified.

Chapter 3. Coxsackie virus A9 tropism on different cell lines

Introduction

The interaction between a virus and its cellular receptor is potentially a key determinant of cell tropism and disease. Recombinants between coxsackieviruses A9 and B3 (CAV9, CBV3), which show different pathogenicity in new-born mice, showed that this usually correlated with the P1 region and so probably involved receptor interactions (Harvala et al., 2002). Interactions of CAV9 with its receptors occur through an RGD motif located at the VP1 protein at its C- terminus (Chang *et al.*, 1989; Hughes *et al.*, 1995; Williams *et al.*, 2004). Reported receptors for CAV9 are the integrins αvβ3 and αvβ6, although αvβ6 seems to have a higher affinity to the virus (Heikkilä *et al.*, 2009). Infection occurs in two different pathways, RGD- dependent and RGD- independent as mutant viruses lacking the RGD motif are still viable (Hughes *et al.*, 1995).

Sequence comparisons between a number of picornaviruses which have a functional RGD show that in these the RGD +1 position (RGDX) has limited variability and is nearly always M or L (Boonyakiat *et al.*, 2001). This chapter describes an extensive series of experiments to investigate the cellular interactions of CAV9 and its receptors. A panel of different CAV9 variants at the RGD +1 position were used to infect a panel of different cell lines to investigate whether the RGD+1 position is important for viral tropism and receptor interactions. A number of cell lines that have never been used for CAV9 infections were also used to determine the effect of these mutations as well as elucidate the two RGD- mechanisms and CAV9 tropism.

3.1.The RGD motif is highly conserved

The earlier conclusions about the conservation of the RGDX position were based on relatively few sequences from virus isolates. To find whether the same pattern emerges when the greatly increased number of sequences now available is explored, we analysed each of the RGD containing picornaviruses. We used a sequence containing the RGD motif in each case to do a BLAST search for all available sequences of that type (CAV9, E9, HPeV [a global analysis of all the RGD-containing HPeV types as only few sequences are available for some types] and each of the 7 FMDV types). The aligned output was exported into the program sequence logo. (http://weblogo.berkeley.edu/logo.cgi) **Figure 3.1, 3.2 & 3.3** show the sequence logo of these virus types in the RGD region of the VP1 capsid protein. The size of the letter(s) at each position indicates how frequent the amino acid occurs in that position. It can be seen that for CAV9, there is significant diversity surrounding the RGD motif, but the RGDX position is always L or M (**Figure 3.1**). There is also strong conservation of the RGD +4 position, where L is found in most cases while a few isolates have F. For the other enterovirus studied, E9, the situation is similar, but there is less variation. L is always found at the RGDX position and also at the +4 position. There is also strong conservation of the +2 position, where A is nearly always seen, suggesting that there are pressures to maintain a particular amino acid at other positions, not just RGDX and RGD +4. Two other enteroviruses, EV-B83 and EV-C99, contain the sequence RGD, but this is in a different context (RGDH and RGDG respectively) and this may not be functional or bind to a different integrin than CAV9 or E9.

An analysis of HPeV sequences shows a similar pattern to CAV9 and E9 (**Figure 3.2**). Like CAV9, some isolates have M and some L at the RGDX position, but L is preferred. As seen in E9, there is a strong conservation of A at RGD position 2, but the +3 position is less variable than seen in CAV9 and E9, and N is usually seen there. Surprisingly, most HPeV isolates have F rather than L at the RGD +4 position.

For FMDV types (**Figure 3.3**) there is a strong preference for RGDL in most cases, although some isolates of types A, Asia, and SAT3 have RGDM, and this is slightly preferred in type Asia. There are a few type C strains which have RGDS. SAT2 gives the most surprising result, as virtually all isolates have the sequence RGDR. The RGD +2 position also tends to be conserved within a type, and often A is seen, although type A isolates usually have RGD +2 G and type O isolates have RGD +2 Q.

The RGD motif is present in virtually all these viruses. There are a very small number of FMDV isolate sequences where RGD is not seen, but this could be due to sequence errors, or due to adaptation of the strains to tissue culture growth before sequencing as RGD-less variants are known to occur occasionally under these conditions (Baranowski *et al.*, 1998). The results show that for all these RGD-containing picornaviruses, although they belong to different genera and are therefore genetically diverse, there is a strong preference for L/M in the RGDX position and for L at RGD +4 as previously reported (Jackson *et al.*, 2000; Boonyakiat *et al.*, 2001; Al-Sunaidi *et al.*, 2007). This may suggests that the RGD motif in these dfferent viruses recognises the same range of integrins.

CAV9

E9

Figure 3.1: Sequence logo of CAV9 and E9 solates in the RGD region of VP1.

The size of the letter indicates how frequent the amino acid occurs in that position and the colours show different amino acid types (blue= basic, red= acidic, black= non-polar, green= polar, pink=polar, amide. There is a strong preference for M/L (methionine/ leucine) at the RGD+1 (position 32 in the sequence logo) and L at RGD+4 (position 35) in both viruses.

HPeV

Figure 3.2: Sequence logo of HPeV solates in the RGD region of VP1.

The size of the letter indicates how frequent the amino acid occurs in that position and the colours show different amino acid types (blue= basic, red= acidic, black= non-polar, green= polar, pink=polar, amide.. There is a strong preference for M/L (methionine/ leucine) at the RGD+1 (position 32 in the sequence logo) and F/L (phenylalanine/leucine) at RGD+4 (position 35).

FMDV Type A

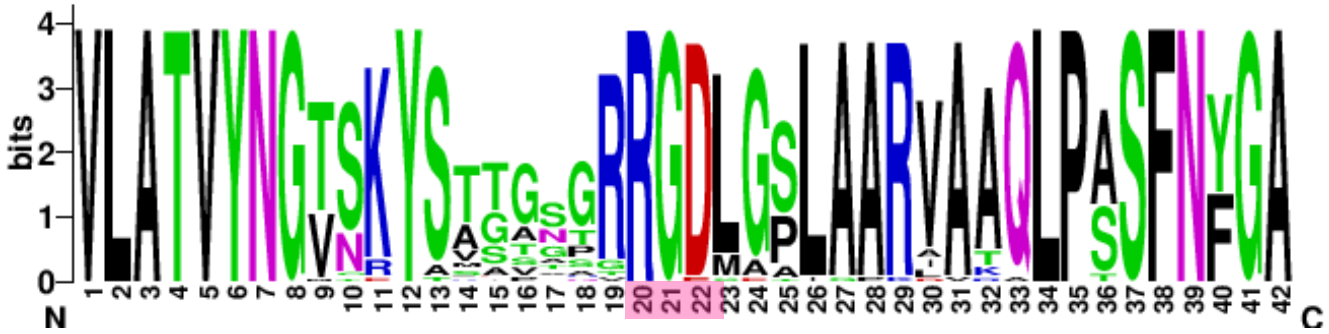

FMDV Asia

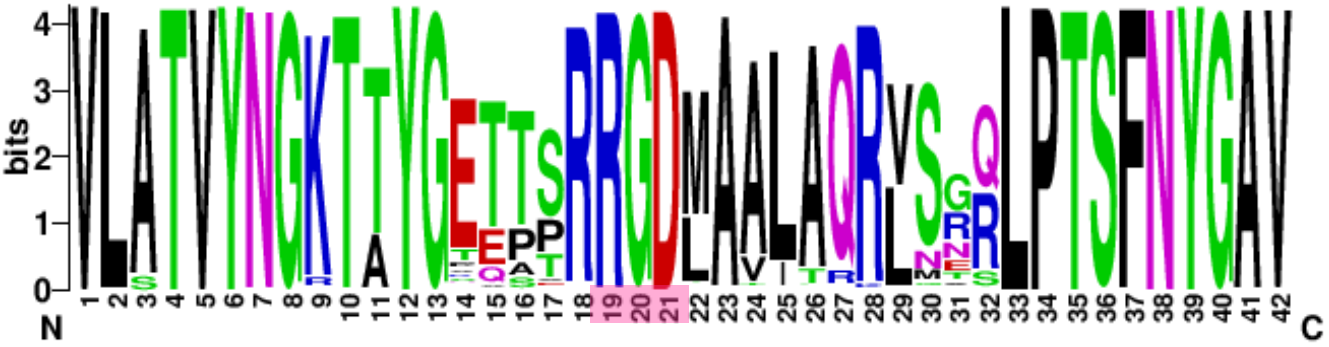

FMDV Type C

FMDV Type O

FMDV Type SAT 1

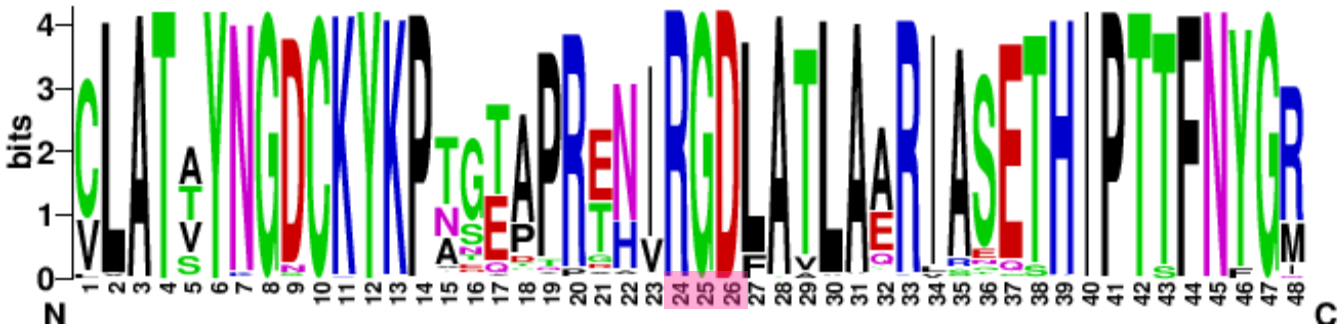

FMDV Type SAT 2

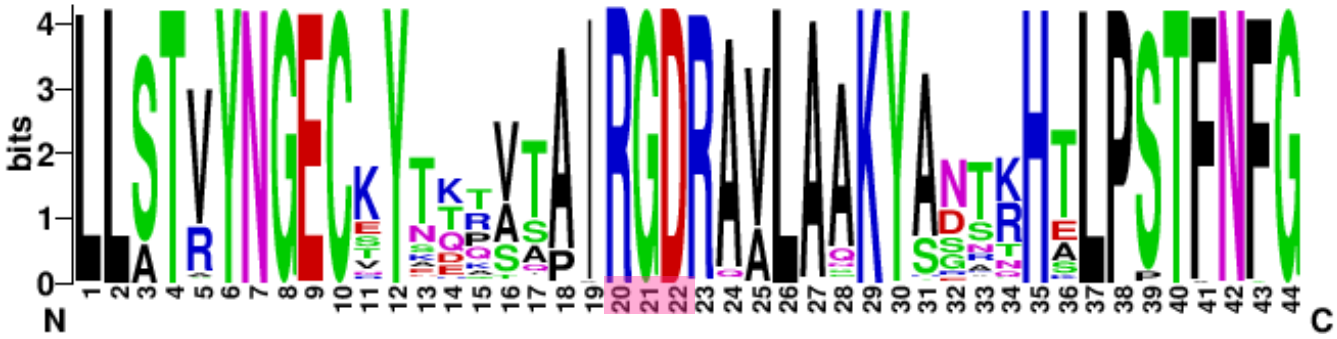

FMDV Type SAT 3

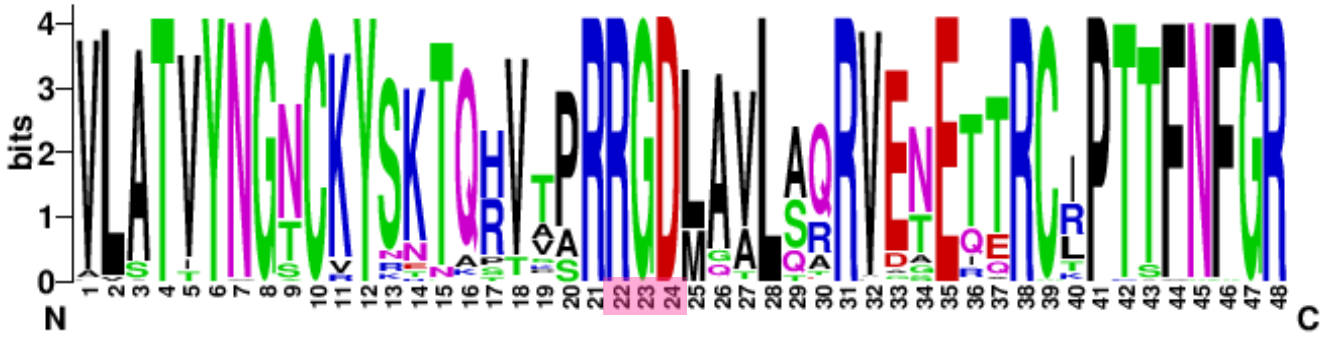

Figure 3.3: Sequence logo of the RGD- containing region in FMDV types.

The RGD motif is located in the VP1 GH loop. The height of each letter indicates how frequently the amino acid occurs at that position in the sequences available for different virus strains and the colours show different amino acid types (blue= basic, red= acidic, black= non-polar, green= polar, pink=polar, amide. For types Asia (390 sequences), C (40 sequences), SAT 1 (250 sequences), SAT 2 (451 sequences) and SAT 3 (77 sequences) all available sequences spanning the whole region were used. For types A and O, because of the very large number of closely related sequences which would reduce diversity, a sub-set of sequences was used. For type A this was the set of sequences (36) used in a study of viruses collected over a period of 75 years, representing the known antigenic diversity of type A (Ludi *et al*., 2014). For type O, a set of sequences (42) from viruses collected from 1952 to 2016 was selected, where each year was represented by only one strain.

3.2. Analysis of mutated CAV9 viruses on different cell lines

3.2.1. CAV9 tropism on A549, GMK, HeLa, MCF7, MDA-MB-435, PC3 and RD cells

Passaging CAV9wt Griggs (RGDM) on A549 lung carcinoma cells previously generated a mutant (RGDL) which was suggested to enhance the viral ability to infect the cells more efficiently (Ioannou & Stanway, unpublished). The mutation observed was surprisingly positioned immediately downstream of the RGD motif, at the position showing a strong preference for M/L in CAV9 isolates (**Figure 3.1**). A switch between these preferred amino acids possibly suggests that there may be subtle cell-specific pressures on this position, in addition to the clear preference of either M or L.

In order to further investigate the significance of this position in CAV9 cell tropism, a panel of previously constructed RGDX mutants (Hughes *et al.*, 1995) was used. These included several mutants not previously studied (Hughes, unpublished) as well as four previously reported mutants (Hughes *et al.*, 1995). Ten different CAV9 mutants at the RGD +1 position (RGDT, RGDR, RGDA, RGDL, RGDS, RGDI, RGDG, RGDF, RGDQ, and RGDD), a mutant completely lacking the RGD motif (d4) and the parental wild type Griggs strain (RGDM) were analysed. The different cell lines A549, GMK, HeLa, HT-29, MCF7, MDA- MB-435, PC3 and RD cells were tested.

Initially, all the mutant stocks were analysed by measuring the titres (Table 2.1). RD cells were used as CAV9 growth on these cells seems to be largely independent of the

RGD motif (Hughes et a;, 1995). Similar titres were observed suggesting that the viruses had grown similarly when the stocks were produced. Measuring the titre allowed a standard amount of each of the strains to be used in the subsequent plaque assay (5000 PFU). The mutant stocks were also sequenced in the VP1 C-terminal region and all showed that the expected mutation was present. The only unexpected result was that the RGDA mutant also contained a Q2861R mutation upstream of the RGD motif (QSRRRGDA> RSRRRGDA). This is close to the S2871R mutation which allows binding to heparan sulphate (Williams, unpublished).

Monolayers of each cell line were produced and plaque assays were performed. The results of the plaque assays are shown in **Figure 3.4**. It can be observed that for A549, GMK and PC3 cells infectivity is highly dependent on the RGD motif as the RGD deletion mutant (d4) gives poor infection on these cells. The different RGDX mutants show that the +1 position is a major viral tropism determinant in A549 and GMK cells, as only the RGDM/L plaques are large and clear in these cells, indicating that they infect the cells more efficiently. In addition, RGDM/L viruses give more plaques than the other strains, suggesting that they can bind to cells more efficiently to initiate an infection. For GMK cells, RGDD and RGDQ gave more plaques than the other mutants, but this was not seen for A549 cells. PC3 cells give a similar result to the A549 and GMK cells. Although in PC3 cells some other mutants give significant cell killing (particularly RGDQ and RGDF), the RGDM/L plaques are larger than those produced by other mutants. Efficient infectivity was observed in RD cells for all RGDX mutants, suggesting an RGD- independent mechanism operating in these cells. For MCF7 cells, most strains, including the wild type RGDM, grew poorly but RGDR shows slightly

larger plaques. Similar results were obtained for HeLa cells. No infection at all was observed in both HT-29 and MDA-MB-435 and cells.

The results show that for GMK, A549 and PC3 cells, the plaque assays are consistent with the strong conservation of M and L at the RGDX position. For RD, HeLa and MCF7 cells, the presence of the RGD motif and an optimal RGDX amino acid did not give an advantage, suggesting that infection is RGD- independent.

Plaque sizes are related to the efficiency of infection over several infectious cycles. To analyse infectivity more directly, cells were infected with equal numbers of virus particles and after a plaque assay the number of plaques was counted. This gives an indication of the efficiency of the initial infection. The results are shown in **Figure 3.5**. It can be seen that RD cells are infected far more efficiently than the other cells, even though infection of these cells is RGD- independent. HeLa and MCF7 cells are also infected in an RGD-independent way but infection is much less efficient than for RD cells. The RGD- independence can be seen as all the mutants infect similarly. For GMK and A549 cells, again the RGDM and RGDL viruses infect more efficiently than the other mutants. The same is true of PC3 cells.

The results again show that some cells are infected in an RGD- independent manner and some in an RGD- dependent manner and that the RGDX position is important in infection in these cells.

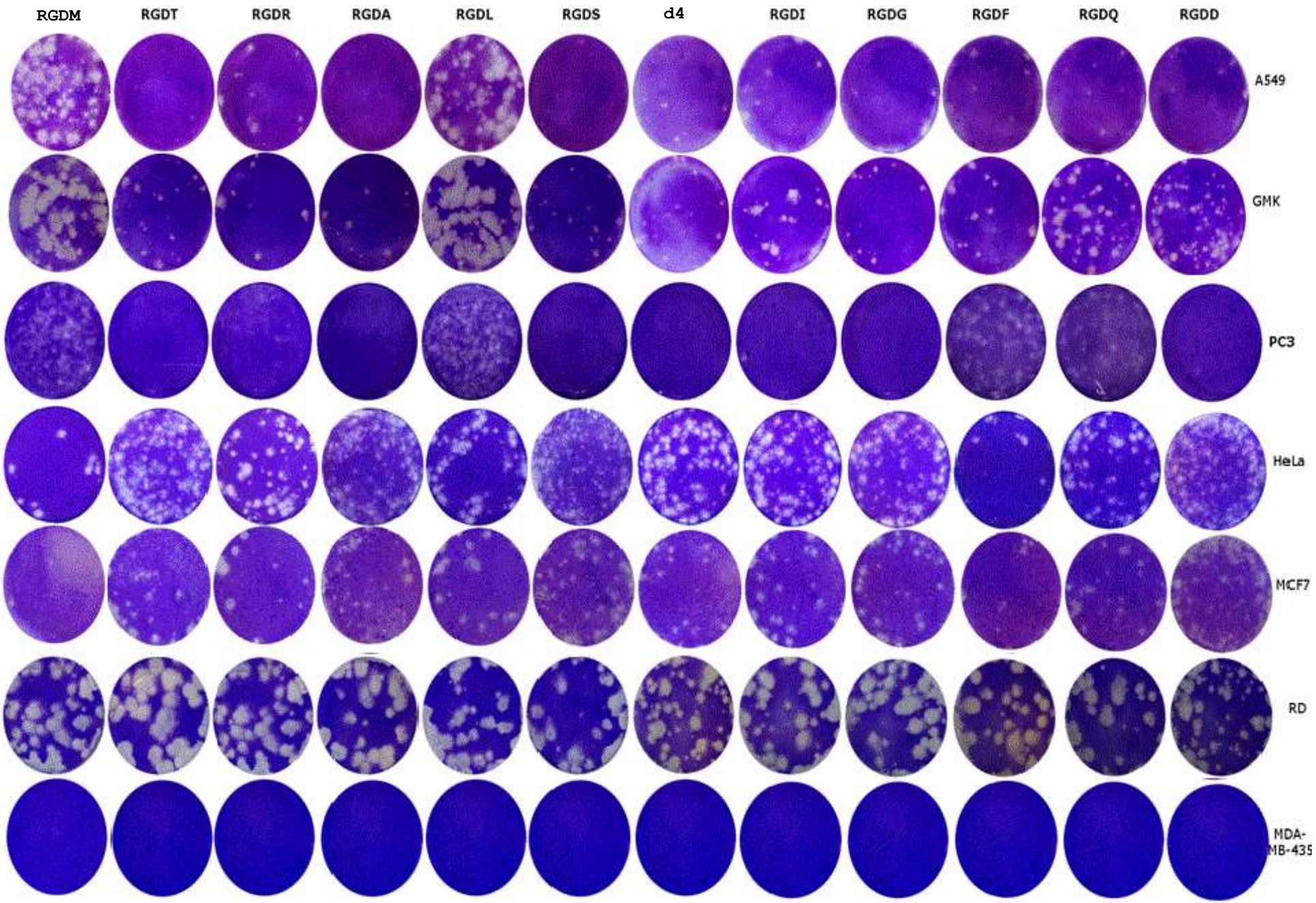
RGDM
RGDT
RGDR
RGDA
RGDL
RGDS
d4
RGDI
RGDG
RGDF
RGDQ
RGDD
A549
GMK
PC3
HeLa
MCF7
RD
MDA-
MB-435

Figure 3.4: Plaque assay of CAV9 mutants at the RGD+1 position.

Plaque assays were performed on A549, GMK, HeLa, MCF7, MDA-MB-435, PC3 and RD cells by incubating 5000PFU of each RGD+1 mutant viruses as well as the wt (RGDM) and the RGD deletion mutant (d4) for 4 days, followed by staining with Crystal Violet. Different RGD+1 mutants show that this position is a major tropism determinant in RGD-dependant cells, A549, GMK and PC3 cells. Only the RGDM/L mutants are able to infect these cells efficiently. On the other hand more equal infectivity of all viral samples was recorded in MCF7, HeLa and RD cells suggesting an RGD- independent mechanism of infection.

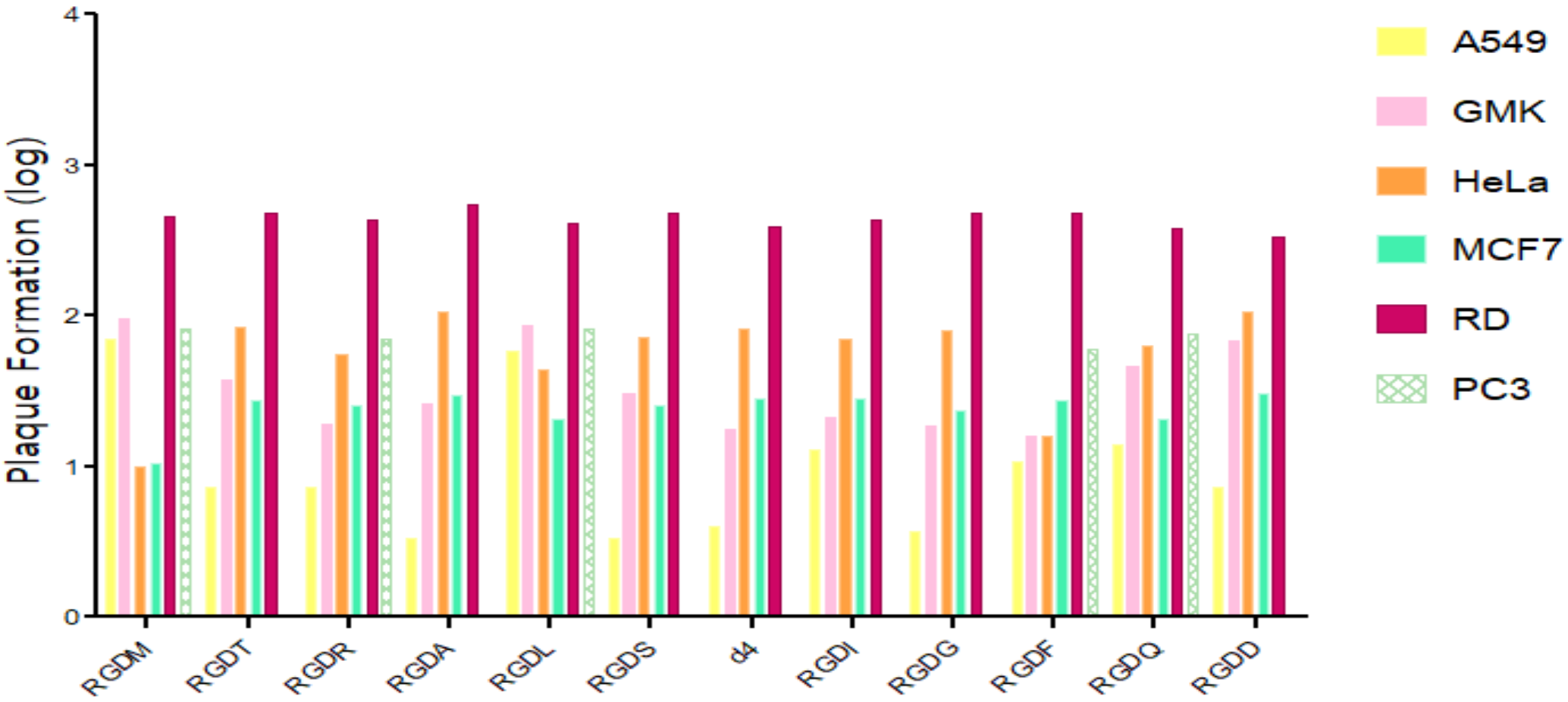

Figure 3.5: Plaque formation of CAV9 variants on A549, GMK, HeLa, MCF-7, RD and PC3 cell lines.

Monolayers of A549, GMK, HeLa, MCF-7, RD and PC3 cells were incubated with equal quantities of each mutant and these were allowed to bind at room temperature for 1 hour. Unbound viruses were removed and the cells were washed twice with growth medium. Plaque overlay was added and the cells were incubated for 4 days, followed by staining with Crystal Violet. The number of plaques was calculated from three independent experiments and expressed in a logarithmic scale.

3.2.2. Analysis of virus yield in different cells

The results shown in **Figures 3.4** and **3.5** demonstrate that the RGD motif plays a key role in infection in some cells and that the RGDX position is also important. To quantify this, an end point assay was performed. This measures the efficiency of infection of the mutant viruses and the successful production of viral particles. A549, HeLa, MCF7, PC3 and RD cell lines were used in a time course assay. Cells were grown on 25 cm^3 flasks for 3 days and viral samples (RGDM/L/R/F/Q & d4) were added to the cells at a ratio of 0.1:1 (virus: cell number in a flask). Virus infection was allowed to proceed for 0 h or 24 h then viruses present were released using the freeze and thaw method. The new viral samples were then used in a plaque assay on RD cells to quantify the newly produced viral particles. The result in **Figure 3.6** shows that, as expected from the plaque assay, viral productivity in A549 cells is highly dependent on the RGD motif and the RGDM/L viruses are able to produce significant quantities of new virus particles. Interestingly, RGDR also performed well in this assay, which was unexpected compared to the results shown in Figure 3.4 and 3.5. Although infection of PC3 cells was shown to be RGD- dependent (d4 is unable to produce new viruses) there seems to be a more relaxed selection for the +1 amino acid downstream the RGD motif and all mutants tested are able to successfully produce new viruses. For HeLa, MCF7 and RD cells all mutants are able to reproduce and although there is a variation in the amount of productivity, cells are infected in a largely RGD independent manner. RD cells are much more efficiently infected than MCF7 and HeLa cells.

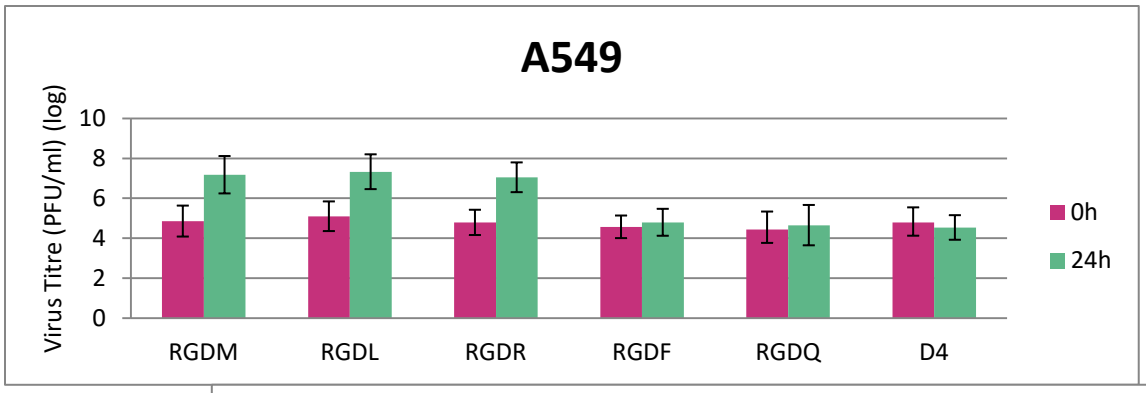
A549
Virus Titre (PFU/ml) (log)
10
8
6
4
2
0
RGDM
RGDL
RGDR
RGDF
RGDQ
D4
0h
24h

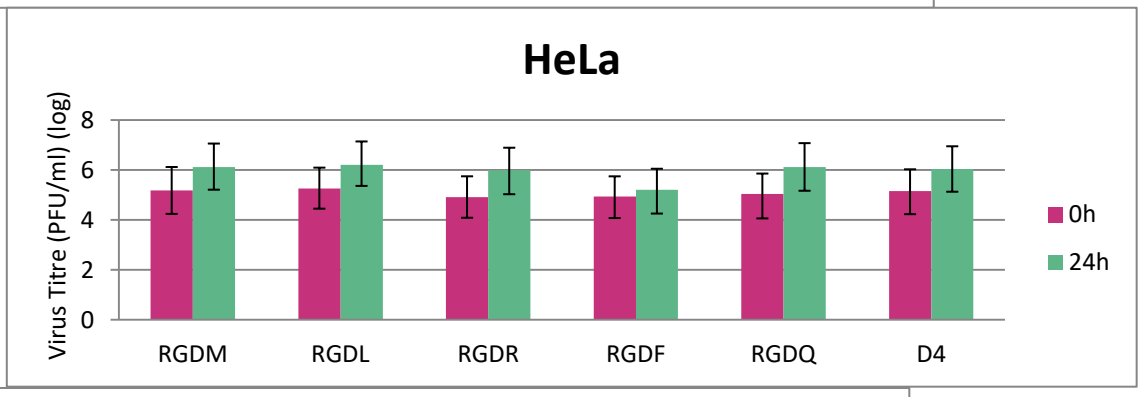
HeLa
Virus Titre (PFU/ml) (log)
8
6
4
2
0
RGDM
RGDL
RGDR
RGDF
RGDQ
D4
0h
24h

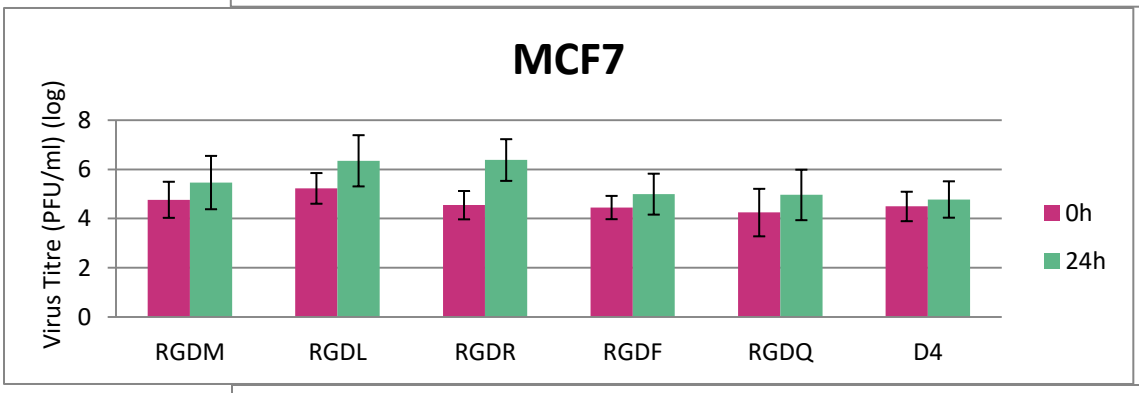
MCF7
Virus Titre (PFU/ml) (log)
8
6
4
2
0
RGDM
RGDL
RGDR
RGDF
RGDQ
D4
0h
24h

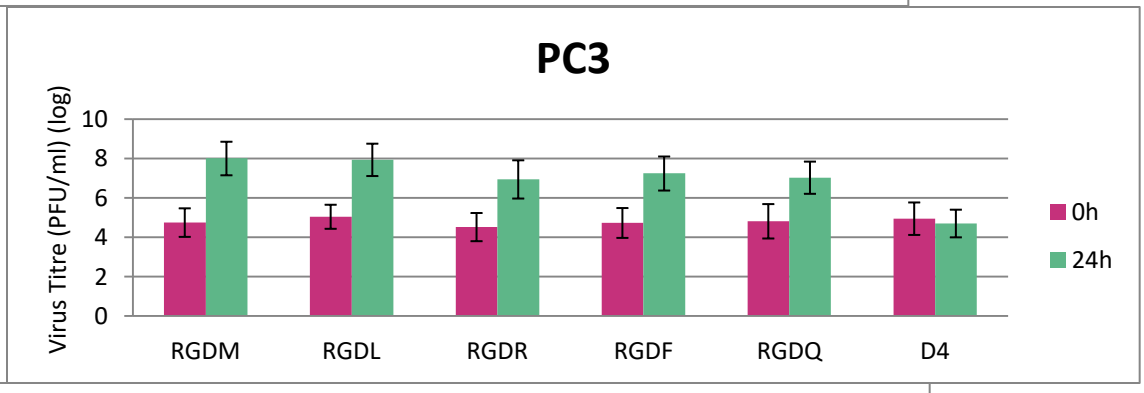
PC3
Virus Titre (PFU/ml) (log)
10
8
6
4
2
0
RGDM
RGDL
RGDR
RGDF
RGDQ
D4
0h
24h

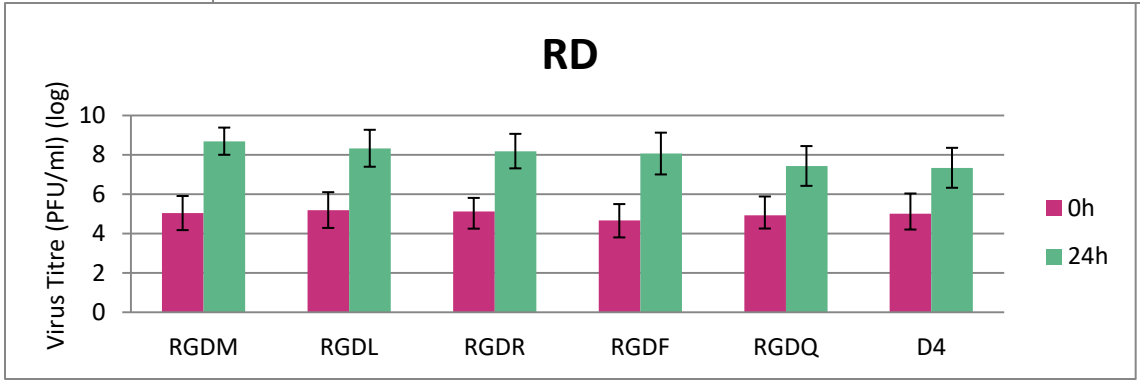
RD
Virus Titre (PFU/ml) (log)
10
8
6
4
2
0
RGDM
RGDL
RGDR
RGDF
RGDQ
D4
0h
24h

Figure 3.6: Viral particle production of CAV9 viruses on cell lines.

Monolayers of A549, HeLa, MCF-7, PC3 and RD cells were incubated with CAV9 mutant viruses including the RGDM wt for 0 and 24 hours prior collection of the newly formed viral particles. Samples were then analyzed by plaque assay on RD cells. Bar charts represent the average number of newly formed viral particles over 24 hours incubation against the number of viral particles added to each cell. Error bars represent the standard deviation from 3 independent experiments. All values are expressed in a logarithmic scale.

3.3. Analysis of avβ3 and avβ6 integrin expression on different cell lines by flow cytometry

CAV9 was previously reported to infect cells by exploiting interactions between the RGD motif and integrin αvβ3 (Roivainen *et al.*, 1991; Triantafilou *et al.*, 1999; Vuorinen *et al.*, 1999). It was later suggested that integrin αvβ6 is the major receptor for CAV9 (Williams *et al.*, 2004; Heikkilä *et al.*, 2009). In order to investigate the expressions of these two integrins on the cell lines used to study CAV9 infection flow cytometry was used. Confluent monolayers of the cells were treated with trypsin to detach them. They were then counted and then incubated with mouse monoclonal antibody against either αvβ3 or αvβ6. The anti-αvβ3 was PE-labelled and could be visualised directly, while the anti-αvβ6 antibody was used with a secondary antibody labelled with PE. The samples were then analyzed by flow cytometry (**Figure 3.7**). Isotype antibodies (the same isotype as the anti- αvβ3 or anti- αvβ6 antibodies) were used as negative control (grey histogram) while the pink histogram represents the antigen expression. The results are expressed in terms of mean fluorescence ratios in Table 3.1.

The expression of αvβ3 is greatest on GMK cells with a much lower level on A549, HeLa, MDA-MB-435 and RD cells and little to no expression on MCF-7, HT-29 and PC3. On the other hand the highest expression of αvβ6 is recorded in A549 cells with the other cell lines expressing it at very insubstantial levels. Even A549 cells express relatively small amounts of αvβ6. The A549 and RD results agree with a previous analysis, which indicated low but significant expression of both αvβ3 and αvβ6 on A549

cells and low expression of αvβ3 but no expression of αvβ6 on RD cells (Heikkilä *et al.*, 2009). Another study looking at these two integrins on A549, HT-29, MCF7 and PC3 cells reported no expression i.e. below the threshold of their definition on all these cells, except substantial levels of αvβ6 on HT-29 (Goodman *et al.*, 2012). This is the first time that GMK cells have been analysed in terms of expression of the two integrins and it is interesting that expression of αvβ3 is comparatively high, and that there seems to be so little αvβ6.

Comparing the expression of these integrins with the infectivity of the viruses (**Figure 3.8**) there is not always clear correlation. The two integrins tested are known to interact with RGD motifs but αvβ6 shows only low expression on A549 cells and little on GMK cells where infection is highly RGD- dependent. There is virtually no expression on PC3 cells where infection is also RGD-dependent. Similarly, expression of αvβ3 is very low on PC3 cells, but there is some expression on A549 cells and much more on GMK cells. However, in general there seems to be more expression of the integrins on cells where infection is RGD-dependent than on cells where infection is RGD-independent.

A]

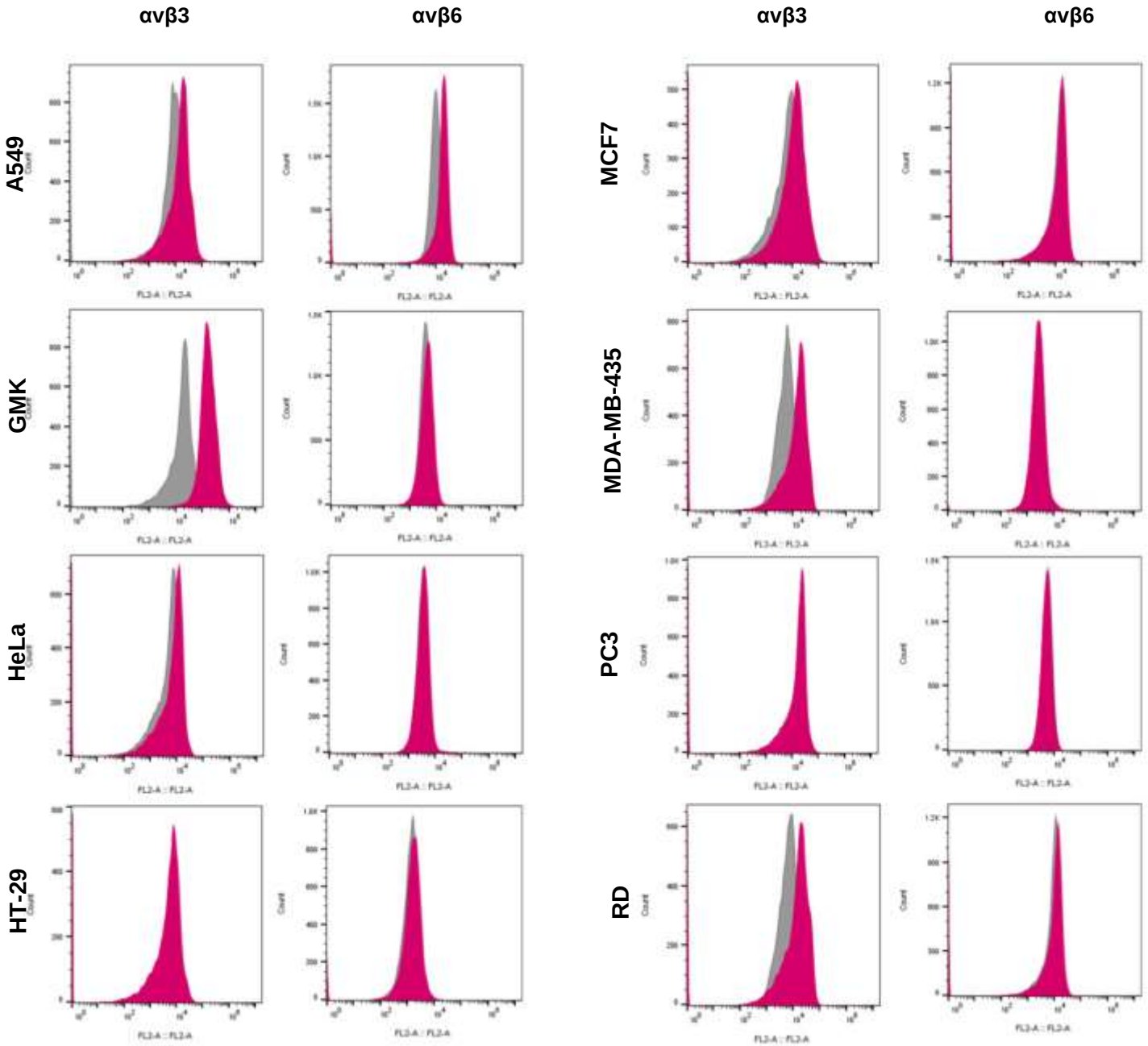

B]

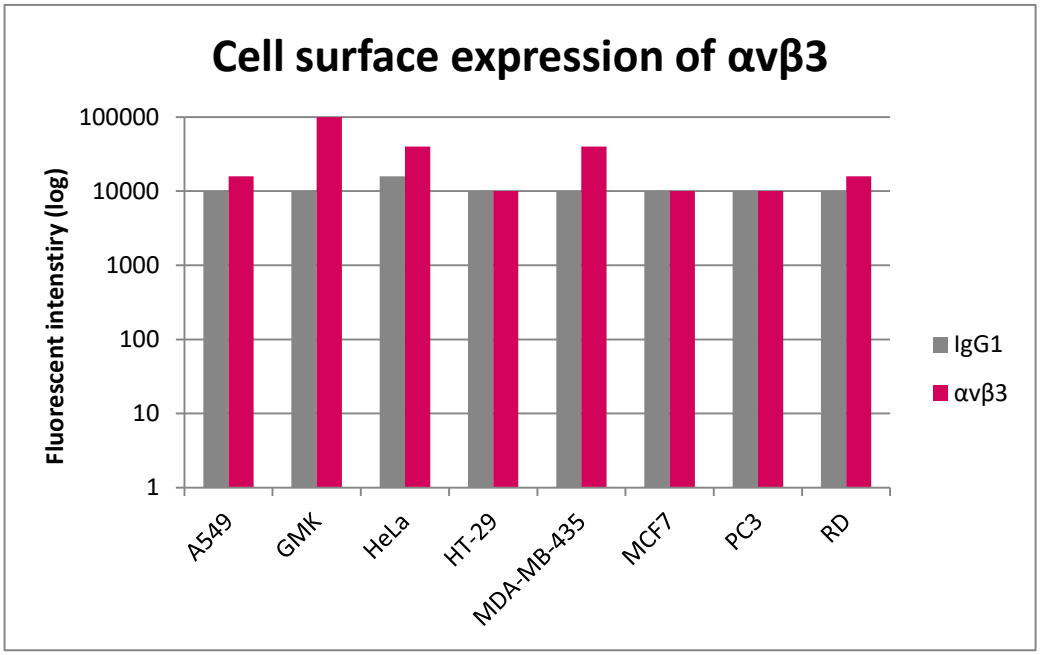
Cell surface expression of αvβ3
Fluorescent intenstiry (log)
100000
10000
1000
100
10
1
A549
GMK
HeLa
HT-29
MDA-MB-435
MCF7
PC3
RD
IgG1
αvβ3

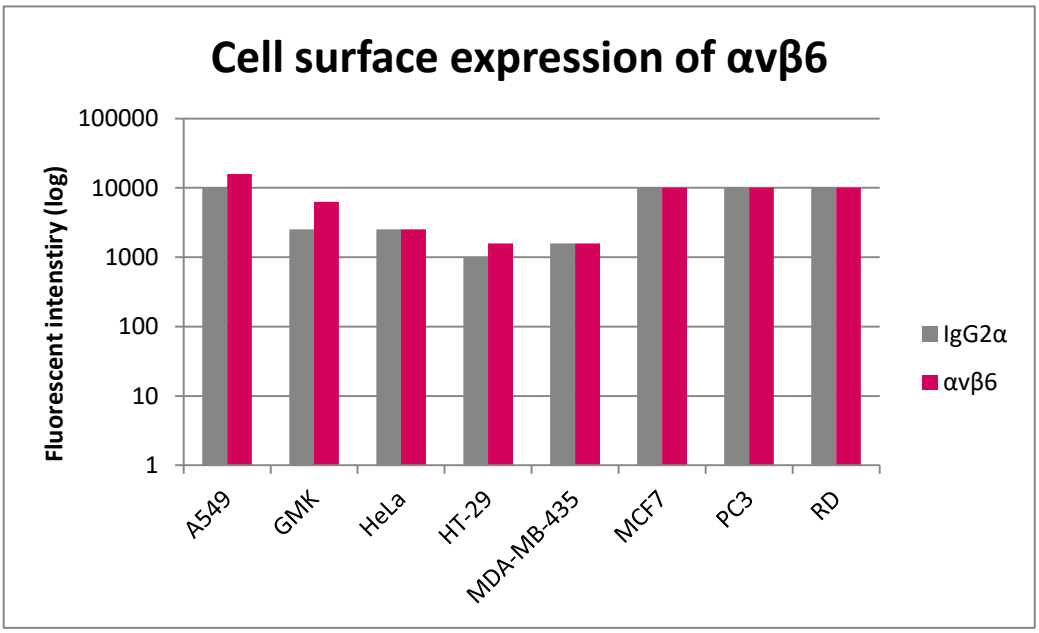
Cell surface expression of αvβ6
Fluorescent intenstiry (log)
100000
10000
1000
100
10
1
A549
GMK
HeLa
HT-29
MDA-MB-435
MCF7
PC3
RD
IgG2α
αvβ6

Figure 3.7: Flow cytometric analysis of αvβ3 and αvβ6 expression on the surface of different cell lines.

Cells were tested at a density of 5 x 105cells per ml. (**A**) Histograms show detection of 5 µg/ml PE mouse IgG1 or IGg2α Isotype controls (grey plots) and detection of integrins by 5 µg/ml PE- labelled anti-human αvβ3 or anti- human αvβ6/ PE- labelled goat anti- mouse IgG (pink plots). Results were generated and gated with a FACS (BD Accuri C6) machine then analysed with FlowJo software. (**B**) A chart shows a comparison of the mean fluorescence intensity given by the isotype and αvβ3 or αvβ6 antibodies on the different cell lines (logarithmic scale, base 10).

Table 3.1: Fluorescence intensity ratio of αvβ3 and αvβ6 antibody compared to the Isotype control. MFI ratio was obtained by the mean fluorescence intensity of the antibody divided by the mean fluorescence intensity of the isotype providing a numerical result of the expression of the integrin receptor. Ratios are used to define categories of expression for use in Figure 3.5.

</= 1 = no expression (white), then >1 -3 (light pink or purple), 3 -15 (darker purple), > 15 (darkest purple) increasing levels of expression.

Cell Lines	Tissue Origin	Murine mAbsFow Cytometry (MFI ratio)	
		αvβ3	αvβ6
A549	Lung	1,77	1.84
GMK	Kidney (Monkey)	13,75	1.13
HeLa	Cervical	1,84	0.79
HT-29	Colon	0.66	0.97
MCF-7	Mammary	1,18	1.09
MDA-MB-435	Mammary	3,01	0.61
PC3	Prostate	1,06	0.83
RD	Sarcoma (Skeletal)	2,26	1.16

	Infection															
Cell	**αvβ3**	**αvβ6**	RGDM	RGDL	RGDR	RGDA	RGDS	RGDT	RGDI	RGDG	RGDF	RGDD	RGDQ	d4	**αvβ3***	**αvβ6***
A549																
GMK															N.D	N.D
HeLa															N.D	N.D
HT29																
MCF-7																
MDA-MB-435															N.D	N.D
PC3																
RD															N.D	N.D

Key

αvβ3

- Highest Expression
- Low Expression
- No Expression

αvβ6

- Highest Expression
- Low Expression
- No Expression

CAV9 infection

- Efficient infection
- Partial infection
- Some plaques
- No infection

Figure 3.8: Schematic diagram of αvβ3 and αvβ6 expression on different cell lines compared with efficiency of infection by a panel of enteroviruses.

αvβ3 and αvβ6 expression is based on fluorescence intensity ration in Table 3.1.

- αvβ3* and αvβ6* expression is based on an analysis by (Goodman *et al.*, 2012).

3.4.Blocking of Viral Infection with Monoclonal Antibodies

From the flow cytometry analysis of integrins we showed that A549 cells expressed he highest level of αvβ6 and some αvβ3. In order to test whether infection of these cells by CAV9 mutants is related to either receptors, function- blocking antibodies against integrins αvβ6 and αvβ3, were used to block these molecules on A549 cells. A549 cells were grown on cover slips over night prior to treatment with 1.0 μg of PE mouse IgG2a or IgG1 Isotype controls and 1.0 μg of anti-integrin αvβ6 and αvβ3 antibodies. An equal amount of a selection of CAV9 mutant viruses (RGDM/L/F & d4) showing good (RGDM/L) or poor (RGDF, d4) growth on A549 cells were absorbed to the cells then incubated at 37˚C for 8 hours to allow infection to proceed. Infected cells were then detected using an antibody to CAV9 particles and a secondary antibody. Typical immunofluorescence images are shown in **Figures 3.9** & **3.10** and a graphical summary is shown in **Figure 3.11.**

As expected, from **Figures 3.4, 3.5** and **3.6** there is a big difference in infectivity of the different mutants. RGDM and RGDL gave many infected cells, while RGDF and d4 gave few. The αvβ3 antibody reduced infectivity of RGDM and RGDL only slightly suggesting that αvβ3 is not the main RGD- dependent receptor for CAV9, which agrees with previous work (Williams *et al.*, 2004; Heikkilä *et al.*, 2009). Despite the fact that treatment with αvβ6 antibody dramatically reduced the infection of RGDL mutant virus, other mutants were not affected as much suggesting that infection by RGDL is strongly dependent on αvβ6 integrin but this is not the case for other viruses, even the wild type RGDM. These results together with the ones from flow cytometry strongly suggest the

presence of a different molecule serving as receptor for CAV9 and possibly related with RGD+1 variation.

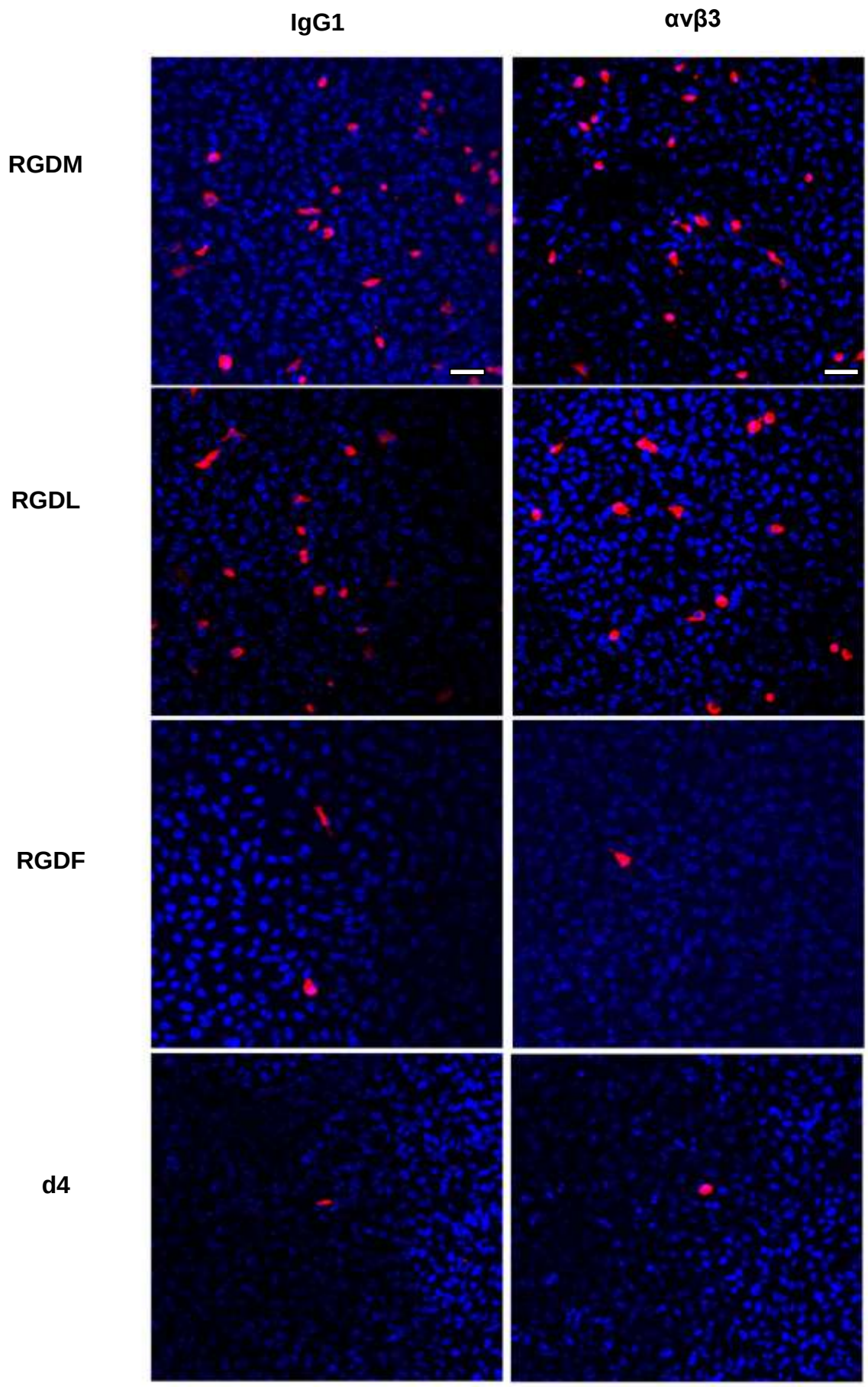
IgG1
αvβ3
RGDM
RGDL
RGDF
d4

Figure 3.9: αvβ3 and CAV9 infectivity on A549 cells.

1.0 µg of mouse IgG1 isotype control or 1.0 µg of anti-integrin αvβ3 antibody was used to pre-treat A549 cells (30 min, 37 °C) before infecting with an equal quantity of CAV9 RGDM, RGDL, RGDL or d4 and incubating at 37°C for 8 hours. Infected cells were detected using primary anti-CAV9 antibody and Alexafluor 555 goat anti- mouse IgG secondary. Nuclei were stained with DAPI in mounting medium. Images were visualized using a Nikon A1 si confocal microscope. Nuclei were observed using the DAPI channel (blue) and infected cells in the PE channel (red); scale bar: 100 µm.

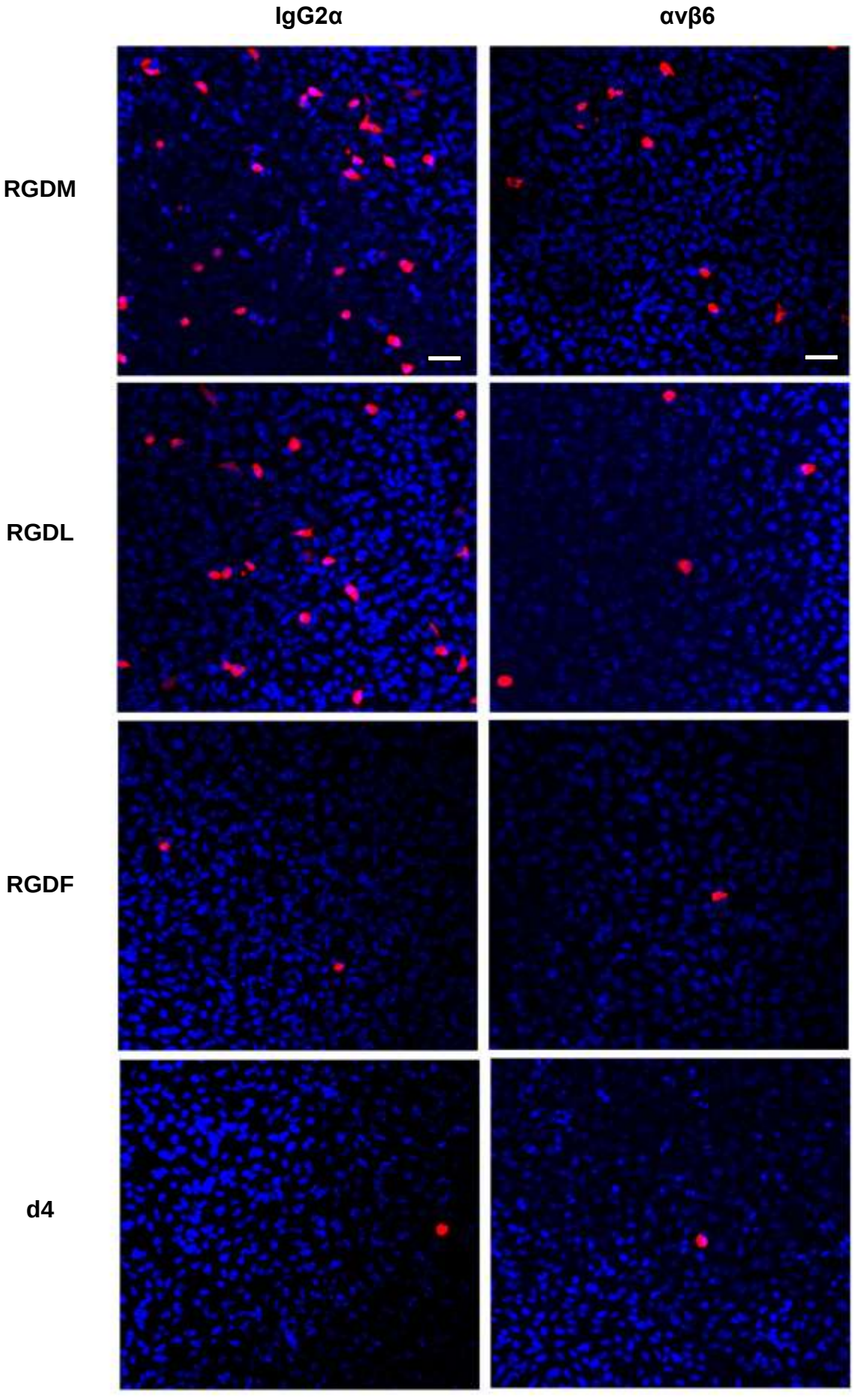
IgG2α
αvβ6
RGDM
RGDL
RGDF
d4

Figure 3.10: αvβ6 and CAV9 infectivity on A549 cells.

1.0 µg of mouse IgG2a isotype control or 1.0 µg of anti-integrin αvβ6 antibody was used to pre-treat A549 cells (30 min, 37 °C) before infecting with an equal quantity of CAV9 RGDM, RGDL, RGDL or d4 and incubating at 37°C for 8 hours. Infected cells were detected using primary anti-CAV9 antibody and Alexafluor 555 goat anti- mouse IgG secondary. Nuclei were stained with DAPI in mounting medium. Images were visualized using a Nikon A1 si confocal microscope. Nuclei were observed using the DAPI channel (blue) and infected cells in the PE (red); scale bar: 100 µm.

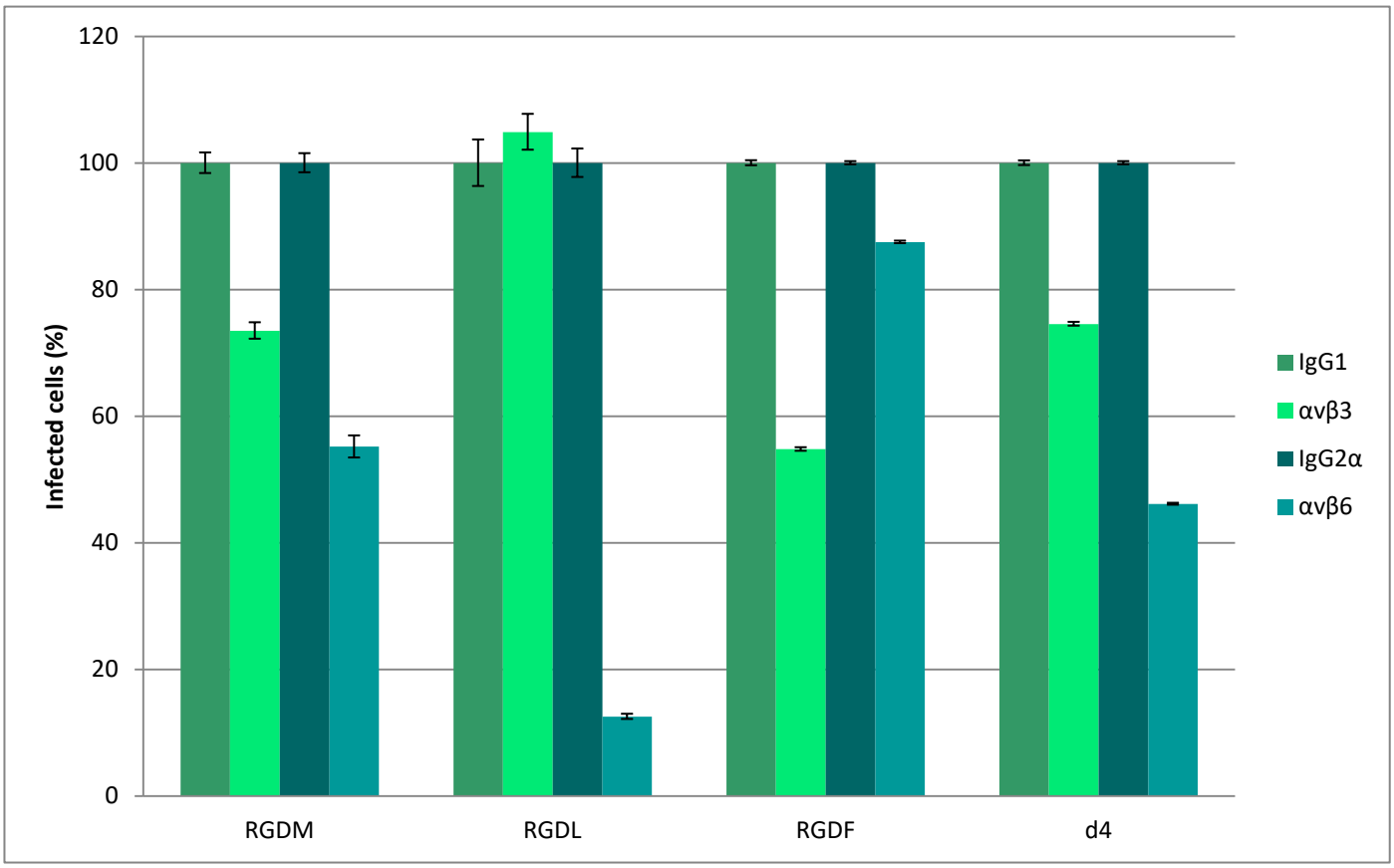

Figure 3.11: Effect of αvβ6 and αvβ3 antibodies on CAV9 infection of A549 cells.

1.0 µg of mouse IgG2a or IgG1 Isotype controls and 1.0 µg of anti-integrin αvβ6 and αvβ3 antibodies were used to pre-treat A549 cells (30 min, 37°C) before infecting with an equal quantity of CAV9 RGDM, RGDL, RGDF or d4. Infected cells were detected and counted using a CAV9 antibody and Alexafluor 555 labelled secondary. 20 random fields were counted in each case and the results are expresses as a percentage (%) of the count for the appropriate isotype which was set at 100%.

3.5. Analysis of EDTA resistant CAV9 infectivity

Phage display experiments to study the determinants of binding of ligands to integrins αvβ3 and αvβ6 found that, in addition to RGD-containing peptides, αvβ6 but not αvβ3 bound to peptides containing the motif DLXXL (Kraft *et al.*, 1999). This motif allowed binding of the peptides to αvβ6, without an RGD motif. Interestingly, the sequence DLXXL overlaps the RGD motif in many RGD-containing picornaviruses (**Figure 3.1, 3.2, 3.3**) where there is strong conservation of L residues at the RGD +1 and +4 positions (RGD**L**XX**L**, where the DLXXL motif is underlined and the conserved +1 and +4 positions are in bold). In previous experiments on FMDV it was found that the DLXXL motif overlapping the RGD motif plays an important role on integrin binding as it allows the virus to form a highly stable complex with the integrin after RGD binding (Dicara *et al.*, 2008). Since RGD binding to integrins is divalent cation- dependent, treatment with EDTA resulted in the inhibition of this process. However, when EDTA was added after binding, it was unable to displace FMDV suggesting that the DLXXL motif stabilizes the RGD/ integrin interactions.

Several CAV9 isolated contain the same DLXXL sequence as FMDV, although a number of them including the Griggs strain have the sequence RGDMXXL (**Figure 3.**1) Thus we wanted to examine whether CAV9 can also form a highly stable- EDTA resistant complex with integrins and if DMXXL can function in the same way, which may explain why L or M are frequently found at the +1 position in CAV9 isolates.

RGDM, RGDL RGDR and RGDF were chosen for study. To confirm that binding is cation- dependent, these viruses were bound to cells in the presence of growth

medium, which contains both Ca^{2+} and Mg^{2+} cations, TBS buffer containing Ca^{2+} and Mg^{2+}, or TBS-EDTA.

After the cells were allowed to bind to the CAV9 variants at 4 °C they were washed with growth medium and a plaque assay was performed to measure the infectivity of the viruses. The results are shown in **Figures 3.12 & 3.13** and indicate that there is some cell- type variation. In GMK cells, binding is severely affected by the presence of EDTA for both RGDM and RGDL, compared to binding in growth medium or TBS-CaMg, as expected for RGD-dependent binding, which requires divalent cations (**Figure 3.12**). In A549 cells, there is a small effect of EDTA on RGDM, but surprisingly RGDL binding is stimulated by EDTA. There is little effect of EDTA on binding of RGDF in both cell lines. RGDR binding is not affected by EDTA in GMK cells, but reduced in A549 cells. The RGDR and RGDF results are not surprising as the non-optimal RGDX amino acids presumably means that the inefficient infection of these cells is through a non-RGD-dependent interaction and therefore may not require divalent cations.

To investigate if the DLXXL or DMXXL motifs can give EDTA- resistant binding, the same experiment was performed except that binding was done in the presence of growth medium at 4˚ C and then cells were washed with either TBS-CaMg or TBS-EDTA, while control cells were washed with media. The results are shown in **Figure 3.13**. It was observed that in GMK cells CAV9 wt (RGDM) as well as CAV9 mutant RGDL can form a stable EDTA-resistant complex upon binding, as the presence of EDTA did not disassociate any significant number of viruses. Protection was complete for RGDL, but not as effective for RGDM. In A549 cells, EDTA washing did not have any effect on either virus. This is not surprising for RGDL, as performing binding in the

presence of EDTA did not have a substantial effect on plaque number (**Figure 3.9**), but for RGDM, where some reduction in binding was observed when performed in the presence of EDTA, binding before washing did seem to prevent this, suggesting that the DMXXL motif present in this virus may work in a similar manner to the DLXXL motif. In the presence of TBS- CaMg all the viruses show an increase in plaque formation, presumably because this solution had higher concentrations of calcium and magnesium ions than the control medium. Surprisingly, the RGDR mutant showed unexpected evidence of a stable, EDTA- resistant complex as well as better infectivity in the presence of TBS- CaMg and EDTA.

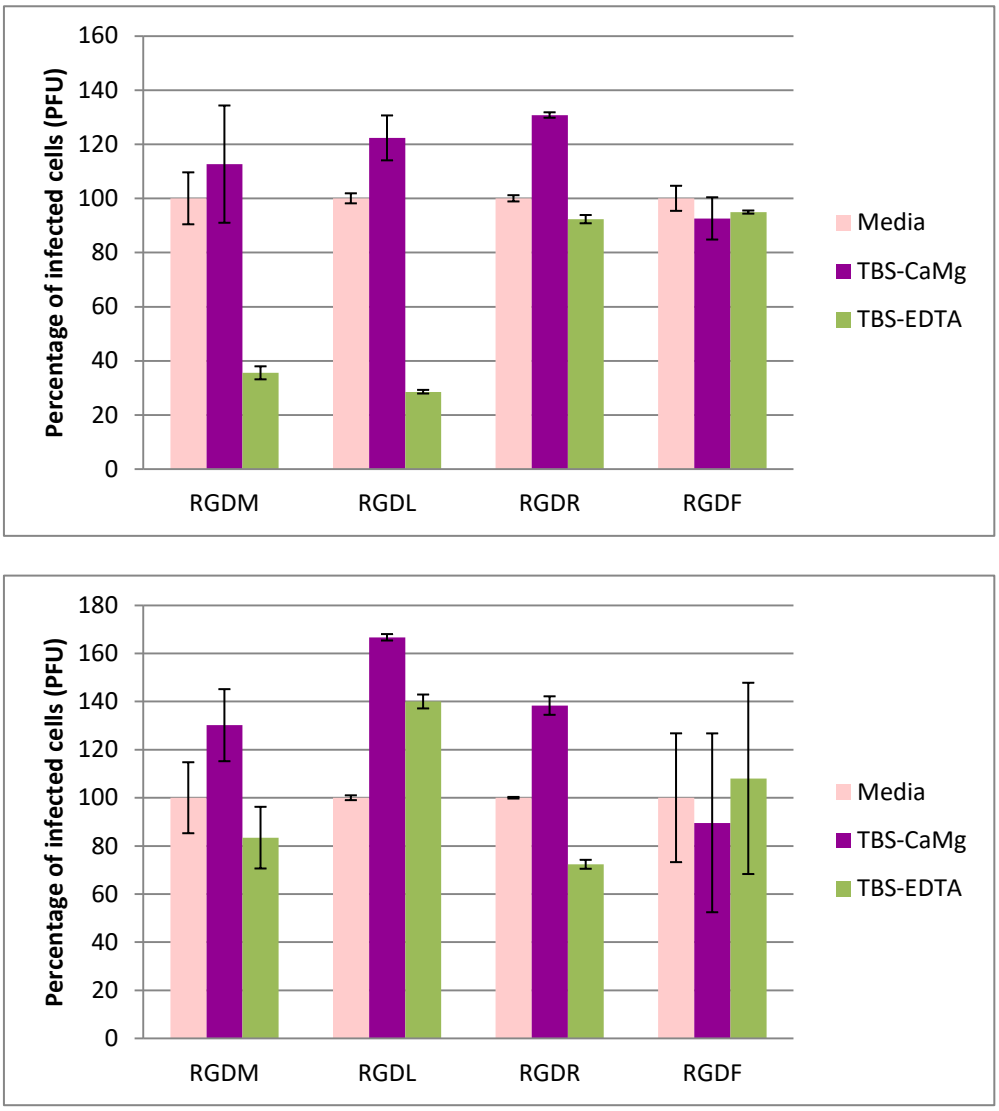

Figure 3.12: Effect of EDTA treatment on the infectivity of CAV9 mutants on A549 and GMK cell lines.

GMK (top) and A549 (bottom) cells were grown on 6- well plates. Monolayers were treated with either media, TBS- CaMg or TBS- EDTA and the viral mutants were added simultaneously and incubated for 1 h at 4˚C to allow binding to cells but not internalisation. Plaque assays were then performed followed by staining with Crystal Violet. The mean percentage of infected cells and standard error from triplicate experiments are shown.

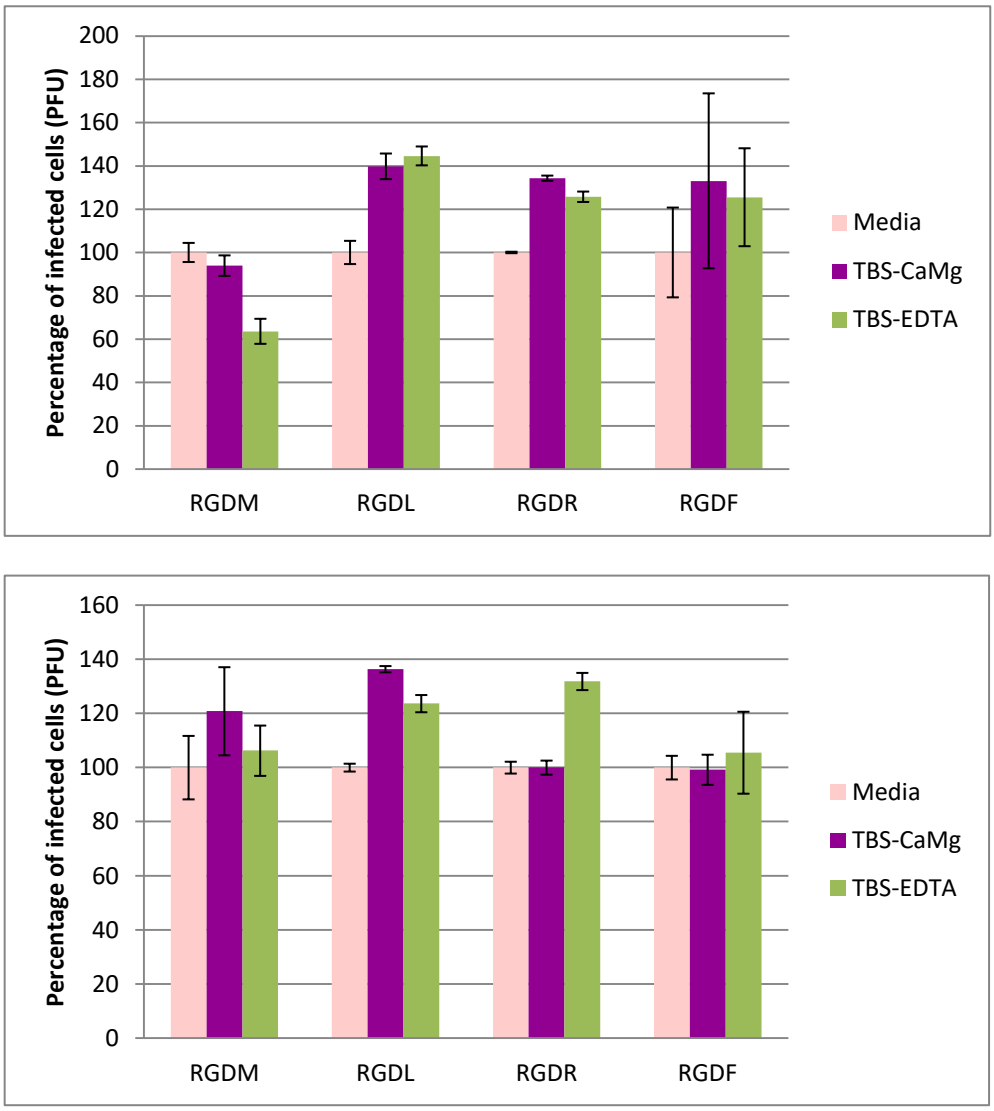

Figure 3.13: Effect of EDTA treatment post- infection of CAV9 mutants on A549 and GMK cell lines.

CAV9 mutants in medium were bound to GMK (top) and A549 (bottom) cell monolayers in a 6-well plate for 1 h at 4˚C to allow binding but not internalisation. Excess, unbound virus was removed and the cells were washed in the presence of either media, divalent cations (TBS-CaMg) or EDTA (TBS-EDTA).

3.6.Effects of chemical inhibitors of endocytosis on CAV9 infection

It has been reported that uncoating of the CAV9 particle is not dependent on endosomal acidification (Huttunen *et al.*, 2014). To start to understand if RGD-dependent and independent infection may proceed through different entry pathways and have different requirements, we investigated whether this lack of dependence on acidification is true for CAV9 mutants. The dependence of vesicle acidification for CAV9 entry was explored using ammonium chloride (**Figure 3.14**). Ammonium chloride is a lysosomotropic weak base that diffuses into the endosome thus inhibiting the acidification (Ohkuma & Poole, 1978). To investigate the effect of ammonium chloride on the virus infection, A549 and RD cells in a 6- well plate were treated with medium supplemented with 50 mM HEPES, pH 7.5 or 20 mM NH_4Cl or medium and 50 mM HEPES, pH 7.5 for 1 hour at 37 ˚C. Cells were then infected with CAV9- wt (RGDM), RGDF and d4 variants. In A549 cells, the treatment of NH_4Cl inhibited the infection of the d4 mutant suggesting that the d4 entry pathway is highly dependent on endosomal acidification. However, as expected, the presence of ammonium chloride did not affect the infectivity and entry of the wild type virus (RGDM). The RGDF variant was also not affected, suggesting that even though the +1 F is not ideal for the RGD motif (RGD-dependent cells) it is still internalised in the same manner and is not dependent on the acidification of endosomes. Meanwhile, infection in RD cells was slightly decreased by the treatment with ammonium chloride, more so in the case of the RGDM, showing that in these cells the acidification of endosomes might have more of an importance in the

efficiency of uncoating. Surprisingly, though the d4 variants was affected only slightly in RD cells.

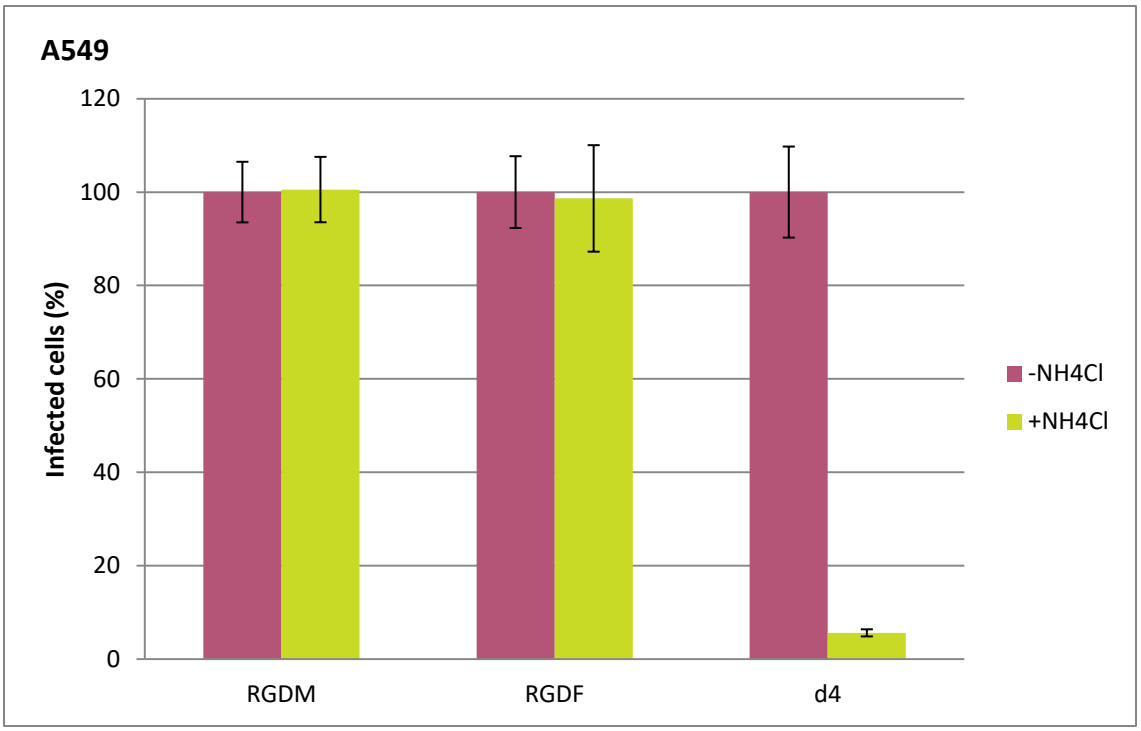
A549
120
100
80
60
40
20
0
Infected cells (%)
RGDM
RGDF
d4
-NH4Cl
+NH4Cl

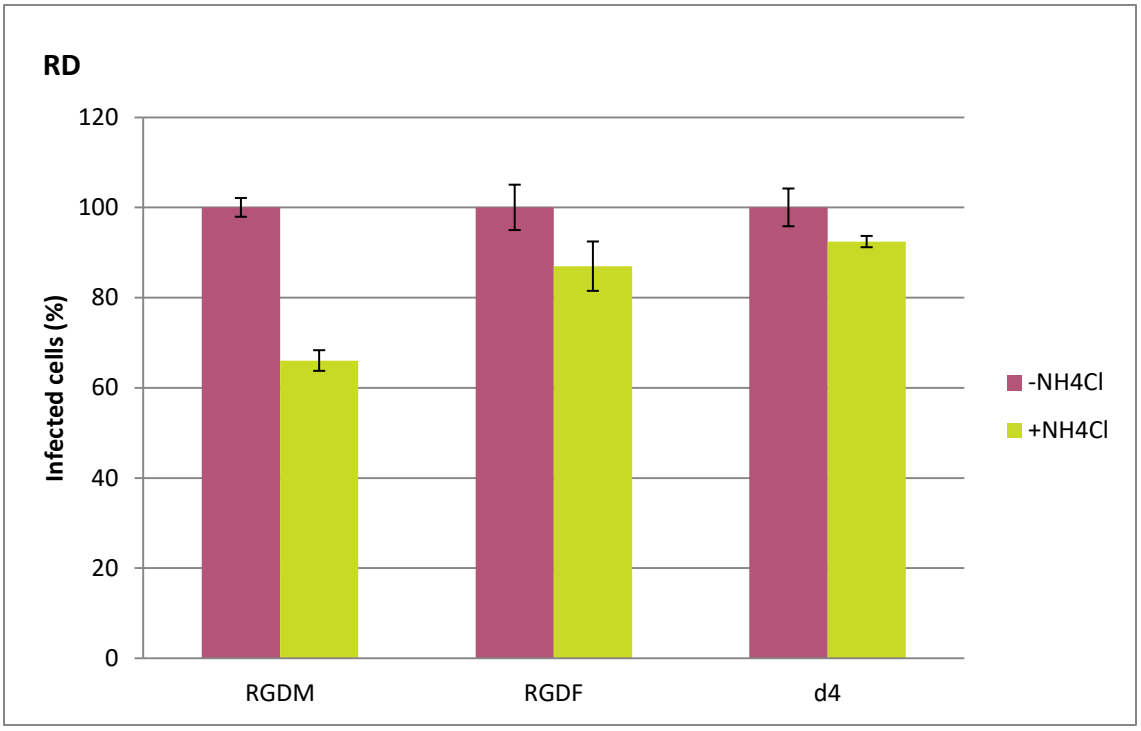
RD
120
100
80
60
40
20
0
Infected cells (%)
RGDM
RGDF
d4
-NH4Cl
+NH4Cl

Figure 3.14: The effect of ammonium chloride on CAV9 infection.

A549 and RD cells were grown on 6- well plates. Monolayers were treated with either medium containing ammonium chloride and HEPES buffer, or just HEPES buffer for 1h at 37˚C prior addition of CAV9 wt, RGDF and d4. Cells were stained after 4 days with Crystal Violet. The mean percentage of infected cells and standard error from triplicate experiments are shown.

3.7. Adaptation of RGDT to GMK and RD cells

In a number of previous studies it has been shown that cell- cultured viruses can mutate and adapt for better infectivity. The experiments described earlier in this chapter have indicated that infection of A549 and GMK cells is RGD- dependent and efficiency varies according to the RGDX position. To investigate the pressure on the RGDX position we selected the mutant virus RGDT that had poor infectivity on these cells. RGDT was chosen as a single mutation could give a change of the T codon present in the mutant (ACG) to M (AUG). RGDT virus was passaged 9 times in GMK cell line. We also passaged it in RD cells as a control, since infectivity on RD cells appeared to be RGD- independent and all mutated RGD viruses showed efficient infectivity on these cells (**Figure 3.4**). From the results obtained after 9 passages it can be seen that both cell adapted viruses reverted the RGDX (threonine) mutation to an RGDL (leucine).

The results are shown in **Figures 3.16 and 3.17**. Surprisingly, in RD cells where we expected no selection pressure, the RGD region in fact accumulated mutations (**Figure 3.16**). The initial virus has the expected ACG codon, but by passage 4 a small signal for U appeared in the second position in the codon, suggesting that a proportion of virus present now had the codon AUG, giving RGDM. There was also a weak signal for C in the third position of the codon. By the 6^{th} passage, the change to U in the centre position was almost complete, there was a majority of C in the third position and approximately 50 % of the viruses had a mutation of A to C in the first position. By the 9^{th} passage, there had been a complete change to the codon CUC, giving RGDL. This

implies that even in RD cells, there seems to be a selective pressure to change the RGDX position.

In the case of GMK cells the RGDT virus seemed to be under more ‘stress’ to replicate successfully and cause efficient infection than in RD cells (**Figure 3.16**). The final codon selected was the same as in RD cells (CUC, giving RGDL), but already by passage 4 this change is almost complete. Therefore, by passage 9 the virus had accumulated 3 nucleotide substitutions to change the sequence from RGDT to RGDL.

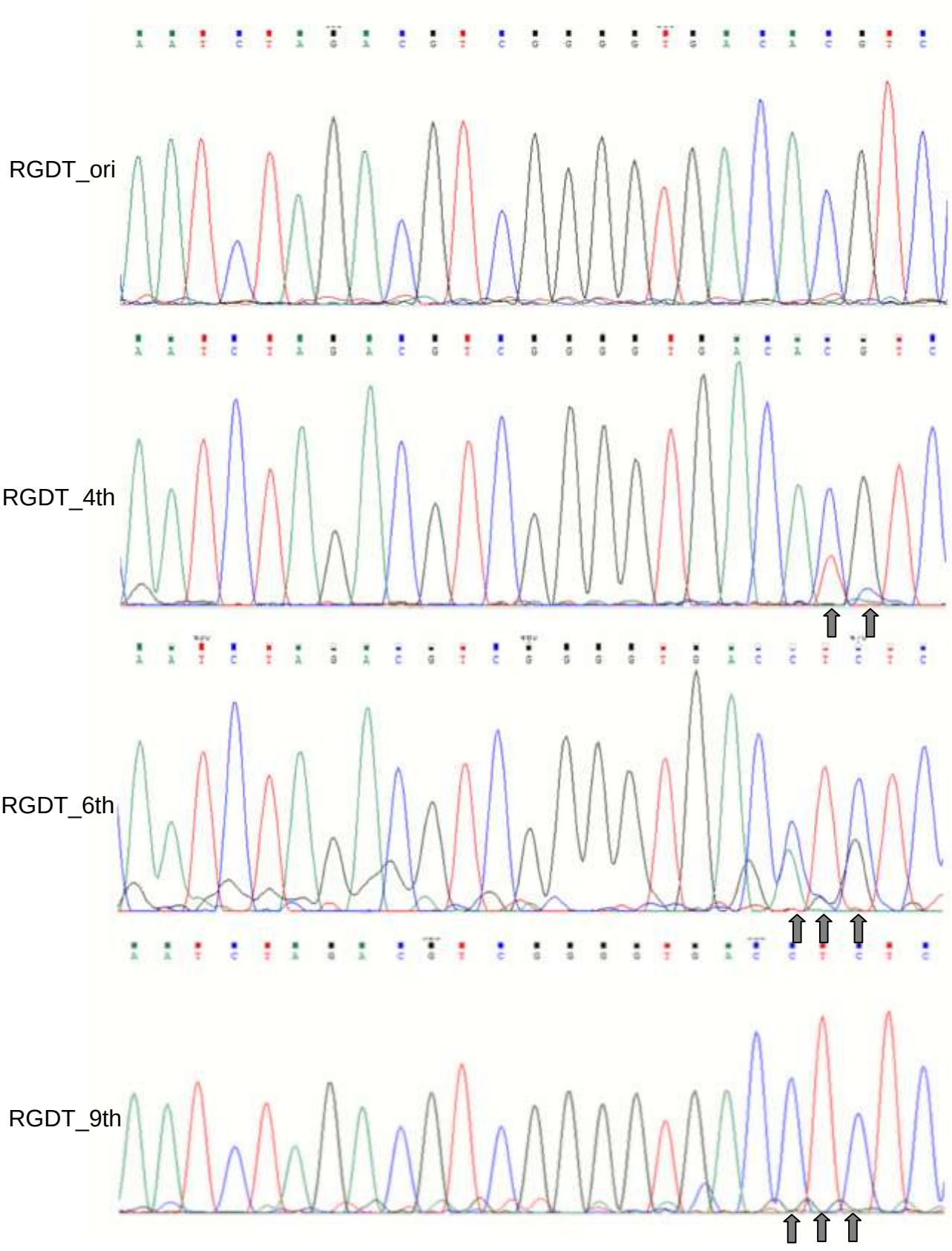
RGDT_ori
RGDT_4th
RGDT_6th
RGDT_9th

Figure 3.15: Histograms of the sequence analysis of the RD-adapted CAV9-RGDT mutant, passage 4, 6 and 9 using Chromas software.

RGDT was passaged 9 times on RD cells and the original virus and passages 4, 6 and 9 were analysed by RT-PCR and sequencing. The arrows indicate the nucleotide change to give T293L (T to L). Result shows that there are two peaks in the sequence of P4, a big T peak to form the AUG nucleotide and a small peak of C is starting to appear whereas, in P6 the T amino acid has now become dominant and two peaks of the C amino acid appeared forming the CTC nucleotide. By P9 the amino acid change has been completed and no more heterogeneity can be observed.

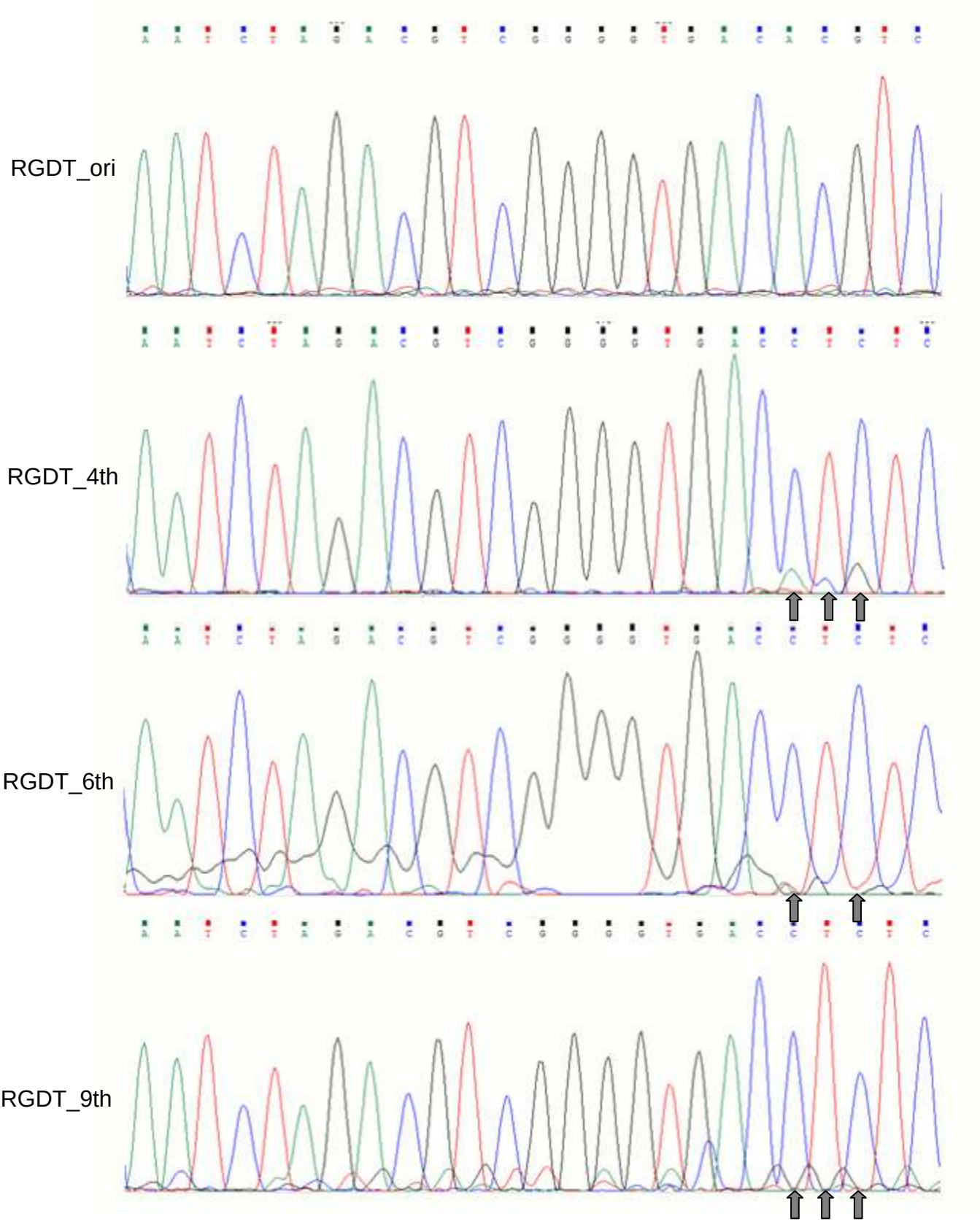
RGDT_ori
RGDT_4th
RGDT_6th
RGDT_9th

Figure 3.16: Histograms of the sequence analysis of the GMK-adapted CAV9-RGDT mutant, passage 4, 6 and 9 using Chromas software.

RGDT was passaged 9 times on GMK cells and the original virus and passages 4, 6 and 9 were analysed by RT-PCR and sequencing The arrows indicate the nucleotide change to give T293L (T to L). Result shows that there are three peaks in the sequence of P4, remains of ACG and the amino acid has completed its change to CTC.

3.8. Discussion

Understanding the cell tropism of a virus is critical for an understanding of diseases and design of drugs or vaccines to prevent diseases. In addition, there is growing interest in using the efficient infection by viruses to target cancer cells, through oncolytic virotherapy (Kaufman *et al.*, 2015). As well as direct cell killing, infection may also induce host anti-tumour immunity, making this a potentially powerful approach. Many cancer cells over-express molecules which are receptors for specific viruses and so oncolytic viruses could have a specific effect on cancer cells and less effect on normal cells. Integrin αvβ6 is over-expressed in a number of cancers and RGD-containing peptide lignds of αvβ6 are being explored in imaging and therapy (Man *et al.*, 2013).

Here, we have studied CAV9, a pathogenic enterovirus within the family *Picornaviridae* (Grist *et al.*, 1978; Tracy *et al.*, 2011; Hober *et al.*, 2013). A key point that affects cell tropism is the entry mechanism in which viruses interact with cell surface receptors to enter the cell and cause infection. Previously it was found that CAV9 utilizes an RGD motif that can be recognized by integrin receptors during cell entry. The RGD motif is localized on an insertion of 15 amino acids at the C- terminus of the VP1 capsid protein (Chang *et al.*, 1989, 1992). Interestingly, CAV9 utilizes at least two cellular entry pathways, one dependent on the RGD motif and one independent of its RGD motif (Chang *et al.*, 1989, 1992; Roivainen *et al.*, 1991; Hughes *et al.*, 1995). The RGD-dependent pathway has been reported to require integrins, although an older report suggested that CAV9 lacking an RGD motif could still bind to integrin αvβ3 (Triantafilou *et al.*, 2000b; Heikkilä, 2013). In addition to the RGD motif, different amino acids

substitutions found near the RGD motif of different picornaviruses have been shown to be important in receptor binding mechanisms (Jackson *et al.*, 2000; Boonyakiat *et al.*, 2001). CAV9 has been reported to interact with the integrin αvβ6 and as well as giving an understanding of the cell biology and tropism of CAV9, more information on the significance of the RGD motif and surrounding amino acids could be important for the development of anti- cancer therapies.

We started the study by using weblogo analysis of the available sequences of isolates of the RGD-containing picornaviruses CAV9, E9, HPeV and FMDV (**Figures 3.1, 3.2 and 3.3**). This highlighted the importance of L/M downstream of the RGD motif in all the viruses, except FMDV SAT 2, where R is found at this position. This suggests that all the viruses (except possibly FMDV SAT 2) interact with the same range of integrin receptors, as suggested by previous direct analysis (Jackson et al., 2003; Williams et al., 2004).

We have then greatly extended previous work using a panel of cells not previously used for CAV9 research and several novel variants with amino acids substitutions downstream of the RGD region specifically the RGD+1 position(RGDX) (**Figure 3.4**). We concluded that the infectivity of the cells seemed to fall into two groups; A549 and GMK were poorly infected with the viruses carrying amino acids other than M/L in the RGDX position and by a mutant with a complete RGD deletion. PC3 cells were not as efficiently infected as GMK and A549 cells and had a more relaxed preference for the RGD +1 amino acid. Only the wild type (RGDM) and RGDL mutants grew efficiently in these cells (RGD- dependent group). On the other hand all variants grew very efficiently on RD cells, suggesting an efficient RGD- independent mechanism. This is

confirmed by the efficient growth of the complete RGD deletion, d4. In the case of HeLa and MCF7 cells we concluded that infection is also RGD- independent although the growth was poor compared to RD cells. Similar results were obtained when an infectivity assay and virus yield assay was performed **(Figures 3.5 and 3.6)**. These highlighted the need for a functional RGD motif and M/L at the RGDX position in GMK and A549 cells, but not in HeLa, MCF7 and RD cells. Interestingly, CAV9 infects RD cells much more efficiently that the other cell lines, even though the RGD motif is perfectly conserved in all CAV9 isolates and so presumably is needed for natural infections and transmission, yet RD infection seems to be RGD-independent.

It is important to mention that all cellular studies related to CAV9 have been carried out in cancerous cell models in which the receptor expression may differ from primary cells. It may be the case that when infecting humans, CAV9 uses a range of different receptors in a tissue-specific manner, which allows the virus to survive in a multicellular environment (Heikkilä *et al.*, 2016). Since the RGD motif is conserved in clinical CAV9 isolates it likely plays a significant role in initiating the CAV9 life cycle in a multi-cellular environment.

RGD motifs can be recognized by different integrins, mainly those with αv chain, which the virus utilizes as receptors during viral binding and cell entry (Johnson *et al.*, 2009a). Most importantly, CAV9 has been reported to use integrins αvβ3 and αvβ6 as cellular receptors (Roivainen *et al.*, 1991; Vuorinen *et al.*, 1999; Williams *et al.*, 2004; Heikkilä *et al.*, 2009, 2010). It has been suggested that αvβ6 has a higher affinity for CAV9 than αvβ3 (Williams *et al.*, 2004; Heikkilä *et al.*, 2009, 2010). To investigate which of the cells used in our experiments express these integrins known to be used by CAV9, we

used flow cytometry detection of antibodies against αvβ3 and αvβ6. Our results (**Figure 3.7**) suggested that the expression of αvβ3 is very low, almost not existing on all cell lines except GMK cells. Although αvβ3 is not expressed, CAV9 still infects these cells efficiently suggesting that αvβ3 is not the receptor used to infect the cells (**Table 3.1**). As previously reported, αvβ6 was expressed on A549 cells, where it was previously found to be the RGD- dependent receptor, but the expression level is low (Heikkilä et al., 2009). Presumably, even low levels of this integrin are sufficient to allow CAV9 infection of A549 cells. In contrast, there seemed to be very little expression of αvβ6 on GMK cells, although as GMK cells were the only non-human cell line used (from green monkey), it is a possibility that the antibody used does not recognise the αvβ6 in these cells. However, PC3 cells also showed little or no αvβ6 expression even though CAV9 infection was RGD-dependent.

To understand which integrin is likely to be involved in entry into one of the RGD-dependent cell lines, A549, blocking antibodies against αvβ3 and αvβ6 were used (**Figure 3.11**). Neither antibody gave full protection, as has been reported previously (Williams *et al*., 2004; Heikkila *et al*., 2009). However, RGDL was blocked very efficiently by the anti- αvβ6, but not the anti- αvβ3 antibody. RGDM is blocked less efficiently by the anti- αvβ6. The incomplete blocking, particularly for RGDM suggests that other integrins can be involved in CAV9 entry.

To better understand the conservation of the M/L at the RGDX position, experiments with EDTA were performed. Since the initial CAV9/ integrin interaction is RGD mediated and is divalent cation- dependent, treatment with EDTA should result in the inhibition of this process. However for FMDV, once formed, the virus/ integrin complex

is rapidly stabilised (by the DLXXL motif) and becomes resistant to EDTA- mediated dissociation (Dicara *et al.*, 2008). Our results (**Figures 3.12 and 3.13**) are surprising in that infection of GMK and A549 cells have different features. As expected, in GMK cells incubating in the presence of EDTA, almost completely prevented infection of RGDM and RGDL, but there was significant infection in A549 cells, particularly for RGDL. This may suggest that in A549 cells, these viruses can bind to a non-integrin molecule in a cation- independent way and then interact with the integrin when the EDTA is removed. As expected, in GMK cells RGDL and RGDM infections are more resistant to EDTA after binding, presumably due to stabilization of the virus/integrin complex. The fact that RGDM/ integrin is only partially stabilised shows that DMXXL is probably also an integrin binding, stabilising motif, but may not be as efficient as DLXXL. This could be why the majority of isolates of CAV9, E9, HPeV and FMDV prefer L at the RGDX position (**Figures 3.1, 3.2 and 3.3**).

To put to the test the how much pressure there is on the RGD +1 position in RGD-dependent cells, RGDT variant were selected and passaged 9 times in GMK cells and in RD cells as a control. Our findings show that in both cell lines there is a preference of a leucine at the +1 position, as after 9 passages there was complete change to this amino acid through 3 nucleotide changes to the codon. This is a very surprising result as RD cells are infected in an RGD- independent pathway and all variants infected these cells very efficiently. The results may suggest that even in these cells there is some interaction with αvβ6integrin which then gives a pressure for RGDL to be selected or that a completely different integrin may be used in these cells and had a preference for a leucine at the +1 position downstream the RGD motif. The result on

GMK cells is less surprising, but shows a very strong selective pressure as the change to RGDL was complete after only 4 passages. It is interesting that a codon needing 3 changes was selected (L), rather than M which needed only a single change. This may suggest that there is a strong preference for RGDL over RGDM in these cells, which could be related to the more efficient DLXXL motif leading to stable binding of the virus to its receptor guaranteeing an efficient infection compared to the DMXXL motif. In addition, we suggest that the different amino acids at the RGD + position might affect the usage of receptor and a lower affinity receptor might be used by some of the variants, thus the virus by altering the amino acid to leucine ensures that the high affinity αvβ6 integrin is in use and a specific efficient entry pathway is followed. It is certainly the case that different amino acids are found at the RGDX position in ligands of different integrins (Springer, 2002).

This is the most extensive analysis of the RGDX position using mutant viruses. Other work has tended to use peptides with different mutations to block virus infection by competition. For example, a study of all the amino acids positions in the FMDV GH loop, using alanine scanning mutagenesis showed that in addition to the RGD, RGDX and the RGD +4 positions (L in both cases) were the only critical determinants of RGD function (Burman *et al.*, 2006). Peptides mutant at these positions were not able to interfere with FMDV binding to αvβ6, suggesting that the RGD is not fully functional without an intact DLXXL motif. In contrast, competition with FMDV for binding to αvβ3 was not affected. Given the pattern of conservation of the RGDX and RGD +4 positions, this is further evidence that αvβ3 is not an important receptor for FMDV and probably not for CAV9, in agreement with the antibody blocking experiments. Despite

the differences in the techniques used, the results we have obtained are comparable with those obtained for FMDV and using mutant viruses allows the interaction to be studied more directly as well as giving the possibility of monitoring the evolutionary pressure to change to a more favourable amino acid.

In addition to the importance of the RGDLXXL or RGDMXXL motifs, there may be a structural reason why M/L is preferred at the RGDX position. This position is located at a hinge position between the RGD and a downstream helix in both FMDV and cellular ligands of αvβ6 such as chromogranin (Curnis *et al.*, 2012; Howard *et al.*, 2013). In both cases the RGD motif is internal and the downstream helix seems to play a key role in binding to the integrin. The CAV9 RGD is located close to the C-terminus of the VP1 protein and so any helix formed will be shorter and less stable, but may still be important in binding and dependent on the RGDX position for optimal orientation.

Downstream of binding of the virus to the integrin, the virus must still enter the cell and uncoat. One possibility is that different receptor usage may lead to a different entry pathway. To investigate whether the amino acids at the + position of the RGD motif have an effect in the entry pathway we tested the infectivity of CAV9 wt, RGDF and d4 in the presence ammonium chloride, known to inhibit the acidification of endosomes. Our data shows that infection of A549 cells with the d4 variant is highly dependent on endosomal acidification, while infection with CAV9 wt and RGDF does not suggesting that these two variants are internalised in the same manner. Although RGDF is a variant that does not infect these cells very efficient due to the fact that A549 cells are RGD- dependent cell line, the variant might still be using the same integrin receptor as CAV9 wt and the difference in the number of plaques might be down to a more delayed

infection process. This preliminary assessment of the effect on the entry pathway needs to be built on by interfering with other pathways. In summary, we have used a large panel of CAV9 RGDX mutant to probe the significance of this position. It is clear that in some cells it plays an important role in RGD function and affects how efficiently the cell can be infected. The effect seems to be through the integrin αvβ6. In other cells, this position has no impact on infectivity and infection is RGD independent. The insights gained could be very important for the design of mutant viruses efficiently targeting specific cells e.g. cancer cells.

Chapter 4. The molecular basis of HSPG interaction with Coxsackie virus A9

Introduction

Successful virus infection is a multiple step process, which includes initial binding to the cell surface, internalization, replication, and egress. In the initial step of virus infection, viruses can bind to several different cellular surface molecules, like proteins, lipids, and carbohydrates. These molecules may function in mediating attachment (i.e., concentrating virus on the cell surface) or serve as receptors or co-receptors facilitating viral endocytosis, conformational changes, and the initiation of signaling pathways associated with infection (Olofsson & Bergström, 2005; Taube *et al.*, 2010).

Heparan sulfate proteoglycans (HSPGs) are glycoproteins found at the cell surface and in the extracellular matrix (ECM), where they interact with several different ligands (Sarrazin *et al.*, 2011; Zhu *et al.*, 2011). Heparan sulfate (HS) and the closely related molecule heparin have highly sulfated disaccharide repeats, and hence they are negatively charged. HS has been reported to interact and serve as a receptor for many human pathogenic viruses including herpes simplex viruses (HSV), swine vesicular disease virus (SVDV), human papillomavirus 16 (HPV16), human immunodeficiency virus (HIV), Theiler's murine encephalomyelitis virus (TMEV), Enterovirus 71 (EV-71), foot-and-mouth disease viruses (FMDV) and human rhinoviruses (HRV -89 and -54) (Shieh *et al.*, 1992; Mondor *et al.*, 1998; Shukla & Spear, 2001; Reddi & Lipton, 2002; Jackson *et al.*, 2003; Escribano-Romero *et al.*, 2004; Bender *et al.*, 2005; Vlasak *et al.*, 2005; Khan *et al.*, 2007). Cell culture adapted viruses have been frequently associated with gaining the ability to bind to HSPG through amino acid substitutions (Fry *et al.*, 1999; Maree *et al.*, 2011). McLeish et al., demonstrated that an amino acid difference at position 132 in CAV9 VP1 is associated with HSPG binding through symmetry-

related clusters of positive charges (McLeish *et al.*, 2012). It was demonstrated that non- binding isolates; CO62, CO87 and Griggs, possess a threonine (T) at this position while HSPG- binding isolates, CO79 and CO85, have the positively charged amino acid arginine (R) (McLeish *et al.*, 2012). Variants of some other *Enterovirus B* species viruses were found to have a similar polymorphism that correlated with HSPG binding.

Passaging CAV9 Griggs on A549 lung carcinoma cells generated a mutant (S2871R), S to R mutation at position 287 in VP1, which was shown to grow more efficiently than the original virus and whose infectivity could be blocked heparin (Williams et al., unpublished). This blocking by soluble heparin is suggested to occur due to the ability of the virus to bind to cell surface heparan sulfate proteoglycans (HSPG).

The aim of this chapter is to investigate other possible mechanisms for CAV9 to acquire the ability to bind to HS and whether this can contribute to a successful infection and influence cell tropism.

4.1. Inhibition of infection with soluble heparin

The results in Figure 3.4 show that of the range of RGDX mutants studied, only the RGDR mutant grew efficiently on MCF7 cells, although this effect was sometimes more evident than others and the reason for this variability is not known (data not shown). In addition, during checking of the sequence of the RGDX mutants (**Table 2.1**), it was found that one virus (Q2861R) had a mutation Q -> R at position 286 in VP1. In order for a virus to bind to negatively charged HSPG, it must have a positively charged area. As both these mutations lead to an extra positively charged amino acid, they were analyzed by using soluble heparin in an attempt to block infection. Plaque assays were performed on A549, HeLa, MCF7 and RD cell lines using CAV9 wt (RGDM), RGDR, S2871R, T1321R and Q2861R viruses in the presence and absence of heparin, an analogue of heparan sulfate (HS) (Skidmore *et al.*, 2008). The results are shown in **Figure 4.1**. On A549 cells the CAV9 WT gives more plaques after heparin treatment than the mock- treated as reported in previous work (McLeish *et al.*, 2012). In contrast heparin blocked all mutant viruses highly efficiently. Comparing the plaques on A549 and RD cells in the presence of heparin a slight increase in size of plaques can be observed (data not shown). On HeLa cells, the presence or absence of heparin does not give any significant difference in plaque number for CAV9 wt. CAV9 wt also grows poorly compared to the other mutants used in this experiment. The RGDR, S2871R, T1321R and Q2861R were completely blocked by heparin. In the case of MCF7 where the CAV9 WT again does not grow very efficiently, all mutants tested gave plaques and heparin showed significant blocking in infectivity suggesting that these mutants benefit

from the ability to bind to HSPG to promote infection. On RD cells as in the case of A549, CAV9 WT gives more plaques when treated with heparin rather than non-treated CAV9 WT. The S2871R and Q2861R viruses treated with heparin were completely blocked and no plaques were observed while the treated RGDR and T1321R were nearly completely blocked by heparin.

Thus in all these cell lines, infection of the mutant viruses was blocked by heparin, suggesting that they have the ability to bind to HSPG. So in addition, to the previously studied mutants, S2871R and T1321R, two new mutants able to bind to HSPG have been discovered, both with mutations close to the RGD motif.

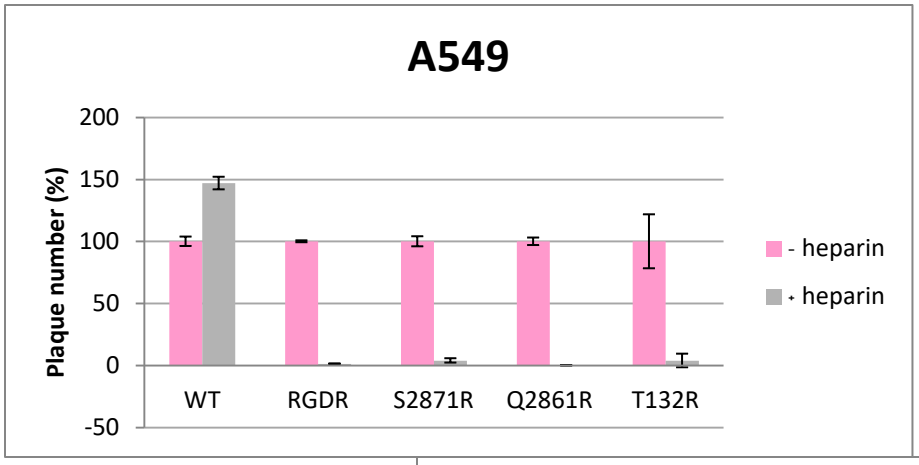
A549
Plaque number (%)
200
150
100
50
0
-50
WT
RGDR
S2871R
Q2861R
T132R
- heparin
+ heparin

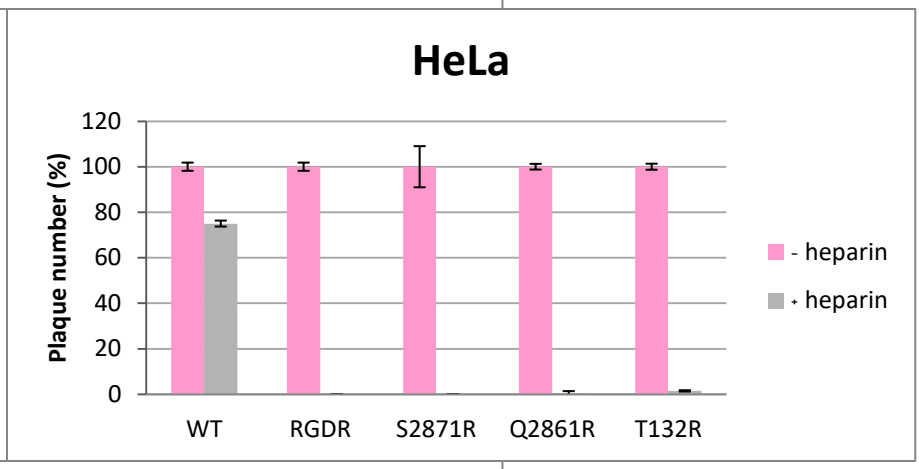
HeLa
Plaque number (%)
120
100
80
60
40
20
0
WT
RGDR
S2871R
Q2861R
T132R
- heparin
+ heparin

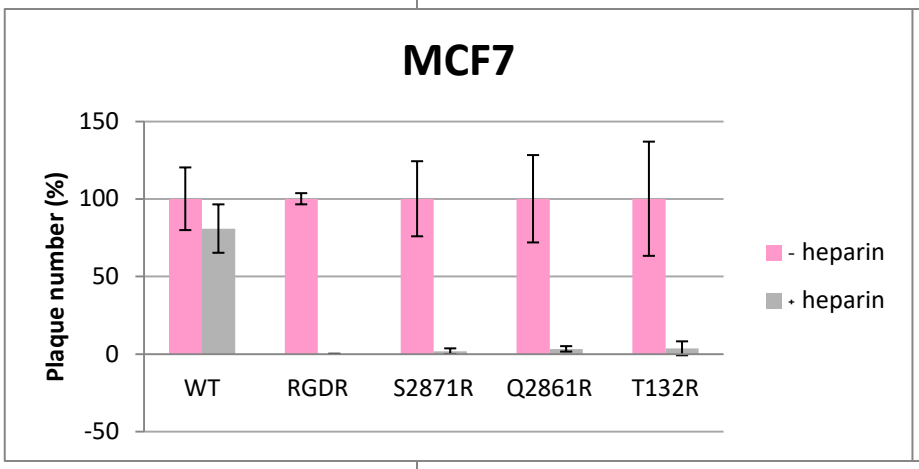
MCF7
Plaque number (%)
150
100
50
0
-50
WT
RGDR
S2871R
Q2861R
T132R
- heparin
+ heparin

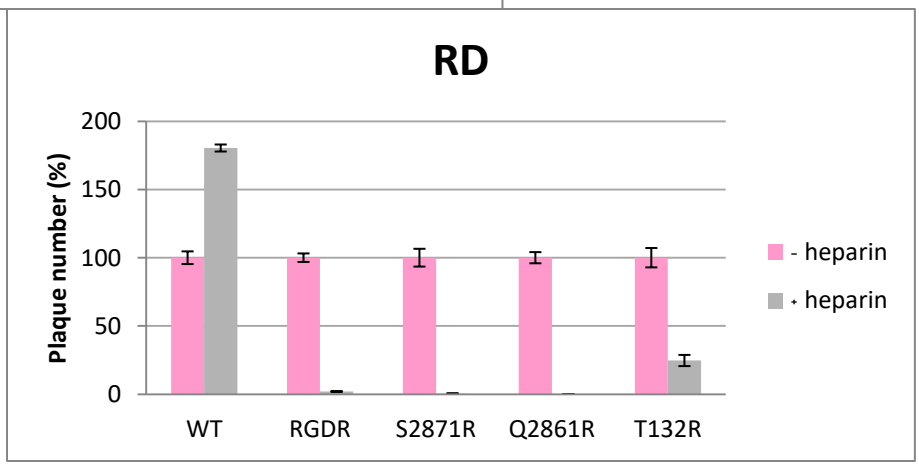
RD
Plaque number (%)
200
150
100
50
0
WT
RGDR
S2871R
Q2861R
T132R
- heparin
+ heparin

Figure 4.1: Heparin inhibits plaque formation of CAV9 mutants that have a positive amino acid substitution near the RGD motif in the VP1 capsid protein.

CAV9 mutants along with the parental strain (WT) were treated with heparin (5mg/ml) prior to plaque assay on four different cell lines, A549, HeLa, MCF7 and RD. In each case, the number of plaques obtained was expressed as a percentage of the number obtained in a no- heparin control (0 mg/ml). The values presented are means from three independent experiments and error bars represent the standard deviation between the three values.

4.2.Removal of viral particles using immobilised heparin

To further examine HSPG binding we examined whether CAV9 variants could directly bind to immobilised heparin. The virus was mixed with either heparin-agarose or just agarose. The supernatants were recovered from the slurry by centrifugation prior to plaque assay using A549 cells. Infection of T132R and S2871R supernatants were almost completely lost when heparin agarose was used compared to agarose, indicating that these viruses had bound to the immobilised heparin. Infection of RGDR and Q2861R supernatants was reduced, while CAV9 wt (RGDM) apparently retained full infectivity in the supernatant (**Figure 4.2**). To confirm that the loss of activity was due to virus binding to the immobilized heparin, this was treated with 0.5 M NaCl and the eluate was also subjected to plaque assay. Released infectivity from the slurry was observed in T132R, Q2861R and S2871R demonstrated that the virus particles were bound to the immobilised heparin and are therefore capable of binding to heparin. Surprisingly, some CAV9 wt infectivity was also released from the immobilised heparin in contrast to McLeish et al (2012), suggesting that this virus can potentially bind to heparin, although binding may be weaker that for the mutants.

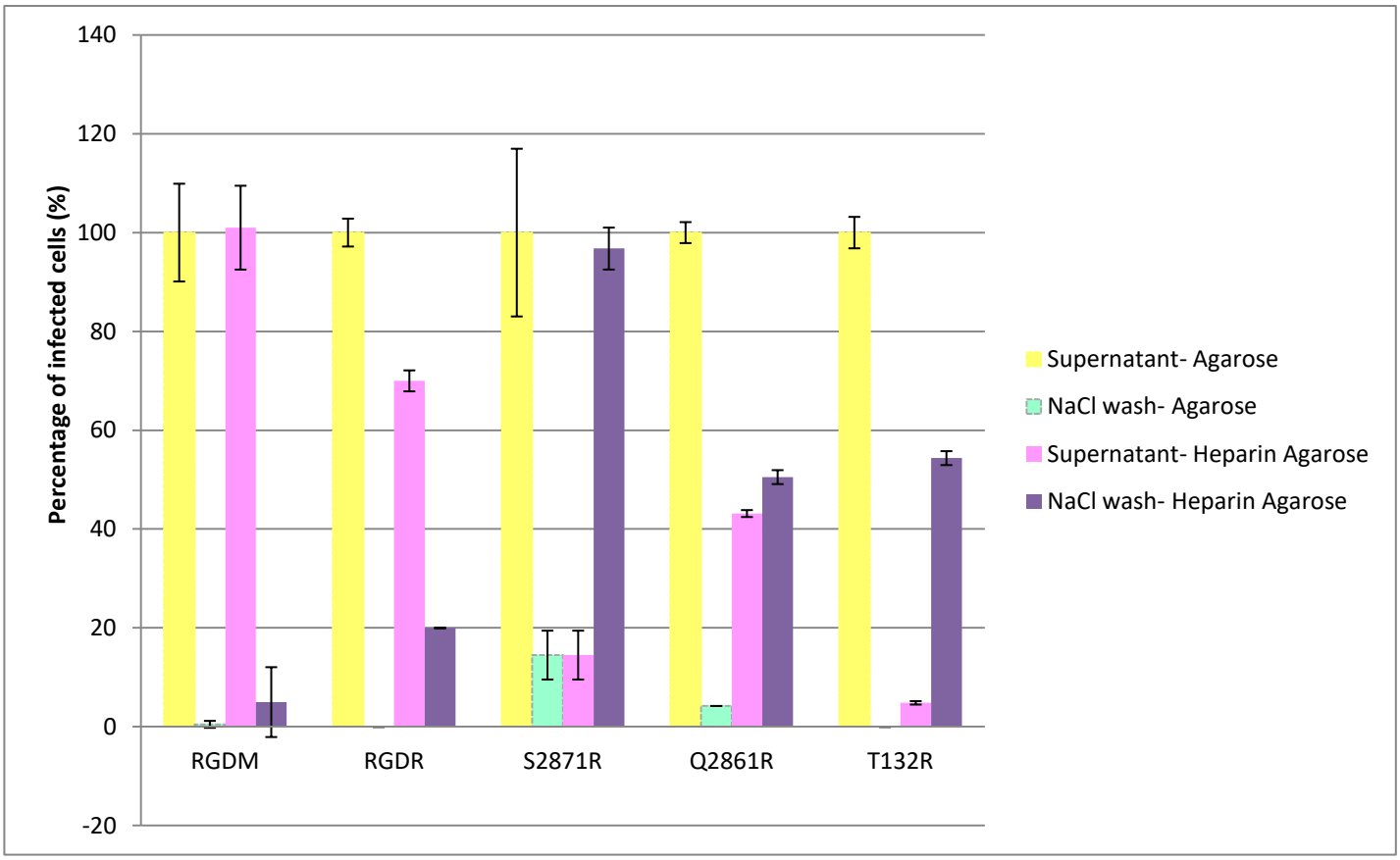

Figure 4.2: Binding to immobilised heparin.

CAV9 variants were incubated with agarose or heparin-agarose beads for 1 h and the supernatants subjected to plaque assays on A549 cells. Any bound viruses were eluted using 0.5 M $NaCl_2$ and again analysed by plaque assays. The results are the means of two independent experiments, and error bars indicate the variation between the two results.

4.3. Inhibition of Proteoglycan Sulfation with Sodium Chlorate

In order to study further the role of HS in cellular infection of CAV9 we followed the strategy of altering its biosynthesis. Plaque assays were performed on A549 and GMK cells grown in the presence of sodium chlorate, which acts as a metabolic inhibitor altering the biosynthesis of HS. Sodium chlorate was previously shown to inhibit human rhinovirus A54 (HRV A54) infection in RD cells by blocking a crucial stage in HSPG biosynthesis (Khan *et al.*, 2007). In addition, the presence of sodium chlorate also reduces infectivity to two CAV9 isolates, CO79 and CO85 (McLeish *et al.*, 2012) and was more recently found to inhibit CAV9-Griggs and HPeV-1 (Harris) (Merilahti *et al.*, 2016). This CAV9 result was in contrast to McLeish et al. (2012) who found that the infectivity of CAV9- Griggs was slightly increased when sodium chlorate was used.

A549 and GMK cells were grown for 3 days in medium with and without 50 mM sodium chlorate before they were infected with the viruses. The results are presented in **Figure 4.3 & 4.4.** In A549 cells (**Figure 4.3**) the presence of sodium chlorate completely blocked the infection of RGDR and Q2861R mutant viruses compared to the non-chlorate- treated control. CAV9 wt was not affected greatly by the treatment. Surprisingly, infection of S2871R and T132R appeared to be enhanced in the presence of sodium chlorate. Although the number of plaques observed did not change the larger phenotype of the plaques shows that the presence of sodium chlorate and thus the blocking of HSPG allows the virus to infect surrounding cells more efficiently following the initial infection, cells creating bigger plaques. GMK cells are also infected in a much more efficient way by several of the viruses, when HSPG sulfation is blocked by

sodium chlorate (**Figure 4.5**). Again, as for A549 cells, T132R and S287R give larger plaques in cells grown in the presence of sodium chlorate, but the effect is much more extreme. In GMK cells, the CAV9 wt also gives larger plaques in cells grown with sodium chlorate, which was not clearly seen in A549 cells. This suggests that HSPG binding may not be an advantage to the virus in GMK cells but rather interferes with efficient infection. The effect on the mutants RGDR and Q2861R are not as obvious, but these viruses, like the other variants are not blocked by treatment with sodium chlorate suggesting that they do not use HSPG during entry into GMK cells.

Together these results suggest that different mutants can infect different cells in even more different ways. We can see that in A549 cells, two of the mutants are completely dependent on functional HSPG expression and without it they cannot infect the cells. It is important to note that these mutants that depend on HSPG are the ones with an amino acid substitution at the +1 position downstream of the RGD motif (RGDR and RGDA [Q2861R]). In A549 cells then, it seems that the RGD motif made defective by these RGDX mutations does not allow infection, but that infection can be rescued by the presence of the mutation which allows an interaction with HSPG. If HSPG is not sulphated and is non-functional, these mutants cannot infect the cells. On the other hand wt, S2871R and T132R have a functional RGD motif with a methionine at the +1 position (RGDM) and although these viruses have the ability to bind to HSPG, blocking the interaction does not prevent infection since this can still go ahead through an RGD/ integrin interaction.

On the contrary, in GMK cells HSPG binding does not seem to benefit any of the viruses. RGDR and Q2861R both still infect cells, although giving smaller plaques,

despite the non-optimal RGDX probably making the interaction with integrins less efficient. This may suggest that the RGD/integrin is not as important as it is in A549 cell infection as there is a useful RGD- independent pathway not present in A549 cells. Instead, infection of several of the viruses is enhanced by blocking HSPG sulfation.

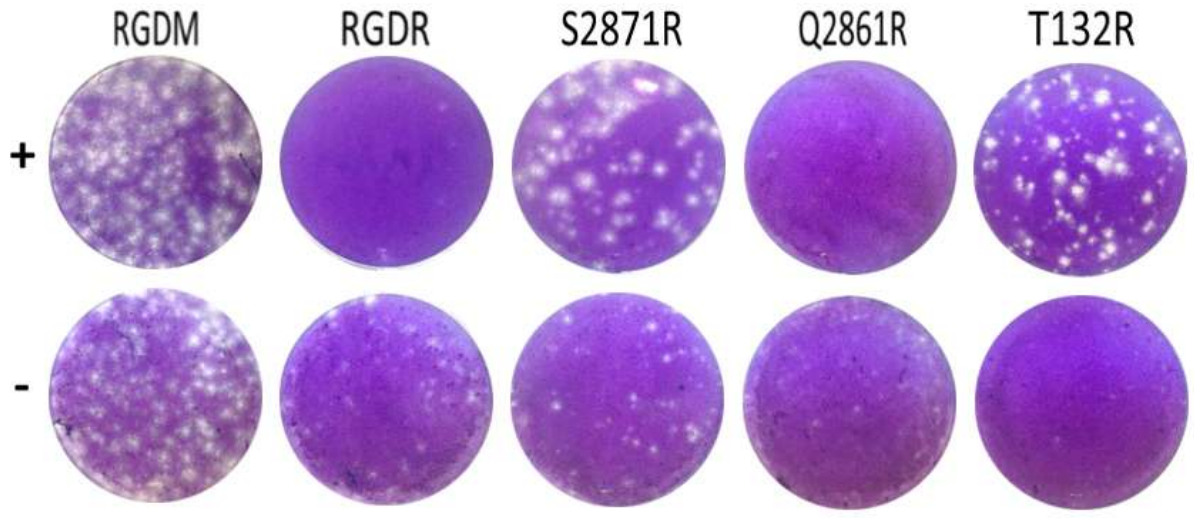

Figure 4.3: The effect of sodium chlorate on infection of A549 cells by CAV9 variants.

A549 cells were grown for 72h in the presence or absence of sodium chlorate ($NaClO_3$) prior to infection with CAV9-wt (RGDM), RGDR, CAV9-S2871R, CAV9-Q2861R and CAV9-T132R. Cells were incubated for 4 days followed by staining with Crystal Violet.

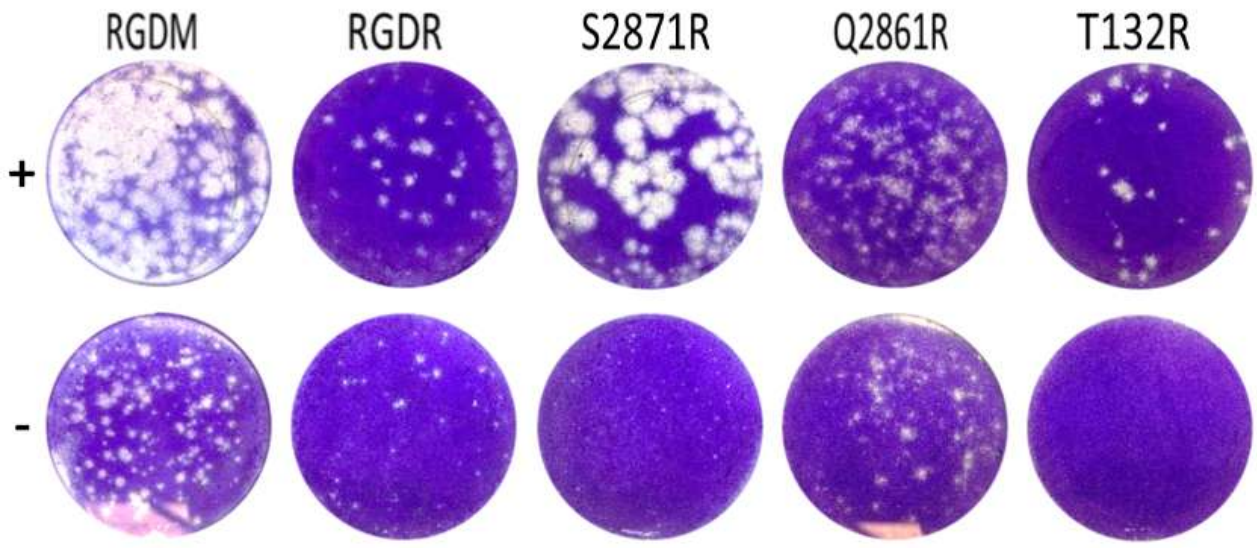

Figure 4.4: The effect of sodium chlorate on infection of GMK cells by CAV9 variants.

GMK cells were grown for 72h in the presence or absence of sodium chlorate ($NaClO_3$) prior to infection with CAV9-wt (RGDM), RGDR, CAV9-S2871R, CAV9-Q2861R and CAV9-T132R. Cells were incubated for 4 days followed by staining with Crystal Violet.

4.4.Inhibition of Binding to Cell Surface HSPG by Protamine Sulfate

To further analyse the role of HS in the life cycle of CAV9, protamine sulfate (PS) was used (Merilahti *et al.*, 2016). Protamine sulfate is a drug that reverses the anticoagulant effects of heparin by binding to it and has similar effect on cell surface HS. PS is an agent that contains clusters of positively charged amino acid residues and has the capacity to bind to negatively charged sulfate and carboxyl groups to antagonize protein interactions with heparin and HS.

A549 and GMK cells were incubated with protamine sulphate prior to virus infection. As indicated in **Figure 4.5**, in GMK cells treating with PS had little effect on plaque size or number of CAV9-wt, T1321R or Q2861R, but there was an increase in plaque number for RGDR and S2871R. This result correlates with the sodium chlorate data, which suggests that HSPG binding is not beneficial to CAV9 mutants in GMK cells.

On the other hand, in A549 cells PS shows an effect on all of the viruses (**Figure 4.6**). There is a dose-dependent blocking of RGDR and Q2861R infection, suggesting again that HSPG interactions are needed for infection of these cells. There is a slight inhibitory effect on CAV9-wt and a clearer inhibitory effect on S2871R. The effect on T1321R is more complex. At the lower PS concentration there is an increase in plaque size, while at the higher concentration there seems to be substantial inhibition of infection.

In summary, the results agree with those from the sodium chlorate experiment in showing the cell type differences in the importance of the interaction with HSPG for infection of A549 and GMK cells, when the Q2861R and RGDR mutants are

considered. The blocking of infection of S2871R and T1321R at high PS concentrations is more difficult to relate to the sodium chlorate data and suggests that HSPG binding could be an advantage to these viruses.

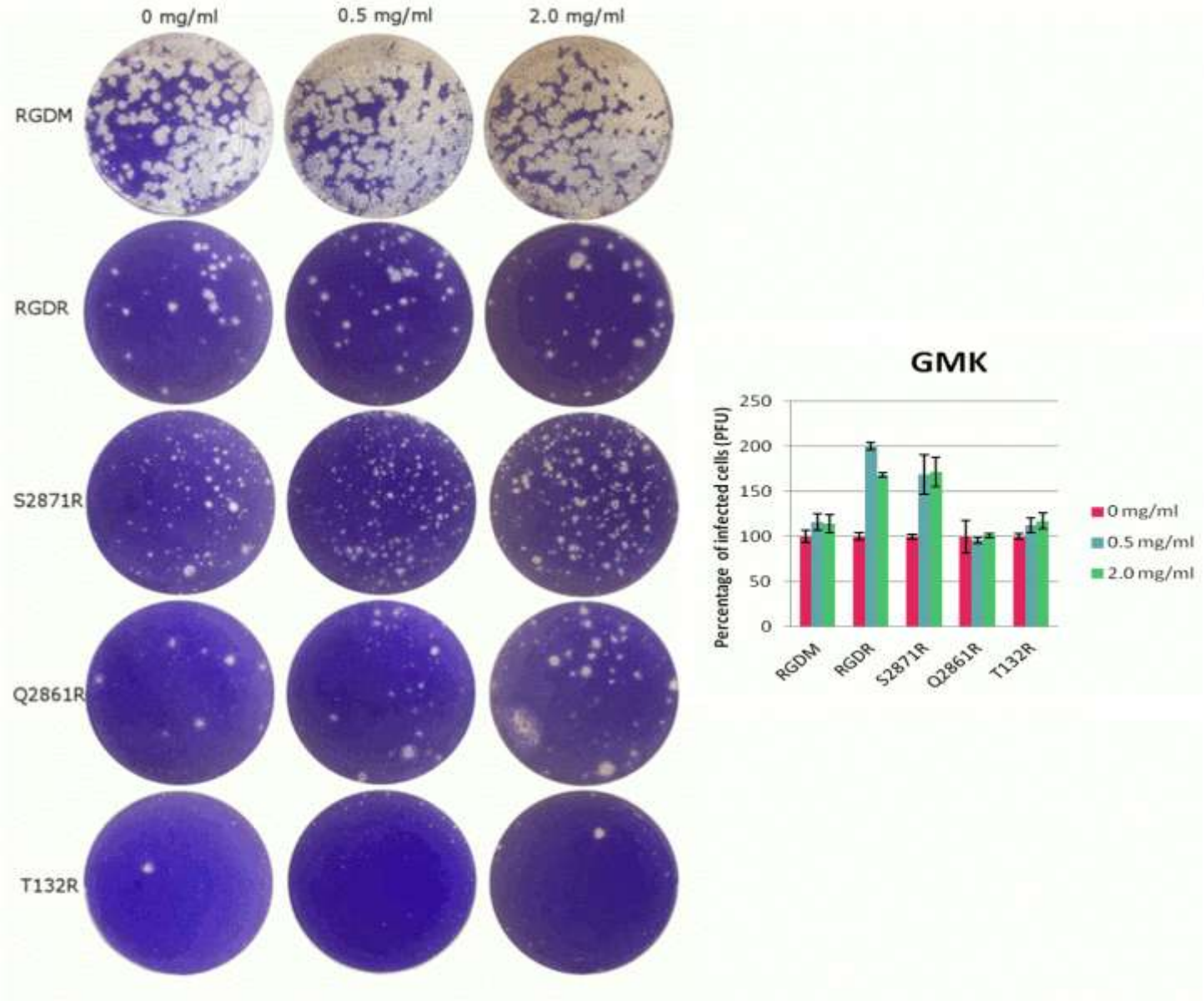

Figure 4.5: The effect of protamine sulfate on GMK cells.

GMK cells were grown for 2-3 days or until confluent. Cells were incubated with 0.5 and 2.0 mg/ml protamine sulfate (PS) for 2 h at 37°C prior to infectivity assay with CAV9-wt (RGDM), RGDR, CAV9-S2871R, CAV9-Q2861R and CAV9-T132R. Viruses were incubated in cells for 3-4 days followed by staining with Crystal Violet. In the panel, plaques were counted and the numbers expressed as a % of the number seen in the absence of PS. The experiment was performed three times and standard deviations are shown.

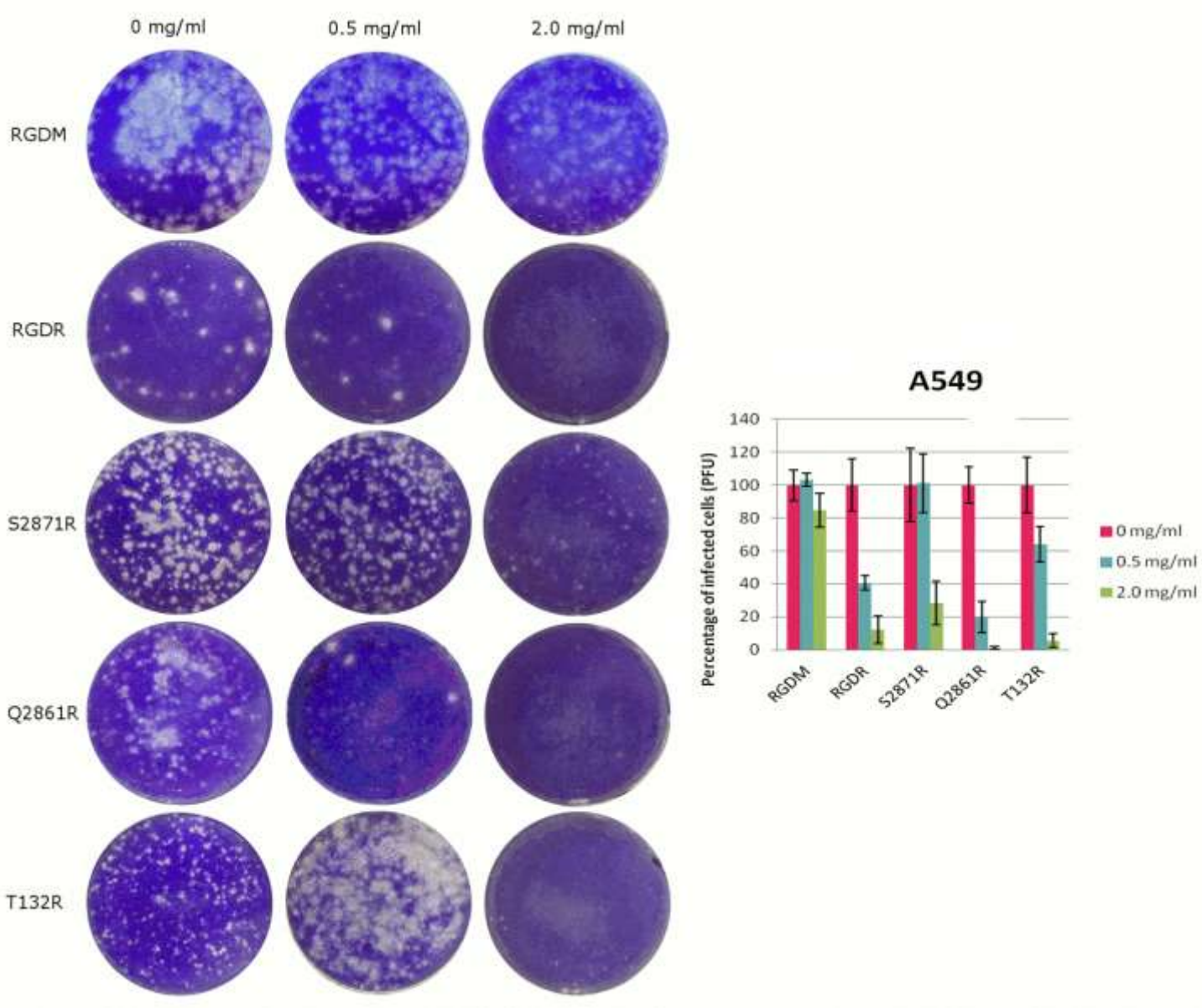

Figure 4.6: The effect of protamine sulfate on A549 cells.

A549 cells were grown for 2-3 days or until confluent. Cells were incubated with 0.5 and 2.0 mg/ml protamine sulfate (PS) for 2 h at 37°C prior to infectivity assay with CAV9-wt (RGDM), RGDR, CAV9-S2871R, CAV9-Q2861R and CAV9-T132R. Viruses were incubated in cells for 3-4 days followed by staining with Crystal Violet. In the panel, plaques were counted and the numbers expressed as a % of the number seen in the absence of PS. The experiment was performed three times and standard deviations are shown.

4.5. Discussion

Heparan sulfate (HS) is a glycosaminoglycan chain found in heparan sulfate proteoglycans (HSPG). HSPGs are abundant on cell surfaces and widely distributed in animal tissues as part of extracellular matrix as well as integral membrane components. HS has highly sulfated disaccharide repeats, and hence they are negatively charged. By binding to numerous ligands and signaling molecules the role of HS is to act in cell adhesion, migration, proliferation and differentiation (Turnbull *et al.*, 2001). HS also provides attachment sites and hence functions as attachment receptor for many human pathogenic viruses including herpes virus, human papillomavirus, hepatitis virus, human immunodeficiency virus, respiratory syncytial virus and alphavirus (Frankel & Pabo, 1988; Krusat & Streckert, 1997; Bender *et al.*, 2005; Johnson *et al.*, 2009b; Dasgupta *et al.*, 2011; Sarrazin *et al.*, 2011; Tiwari *et al.*, 2011). Among viruses that use HS in cellular infection are also several picornaviruses; variants of foot-and-mouth disease virus (FMDV), swine vesicular disease virus, coxsackievirus B3, Theiler´s murine encephalomyelitis virus, HRV54, variants of HRV89, some echoviruses and more recently EV-71 (Jackson *et al.*, 1996; Goodfellow *et al.*, 2001; Escribano-Romero *et al.*, 2004; Khan *et al.*, 2007). These viruses usually have other receptors and so HS is probably a co- receptor possibly giving some advantage by allowing the virus to bind to the abundant HS on the cell surface to make interactions with other receptors easier (Fry *et al.*, 1999; Feng *et al.*, 2011; Maree *et al.*, 2011). In the case of most picornaviruses, the site of HS binding is not known, but for FMDV a mutation in VP3 creates a basic pocket allowing HS binding and mutations at the 5-fold axis are involved in some cases (Fry *et al*., 1999; Maree *et al*., 2011). Similar

5-fold axis mutations in CAV9 were found to allow binding to HS, or at least to the related molecule heparin (McLeish *et al*., 2012). Previous work on CAV9 also identified a mutation upstream of the RGD motif (S2871R) that could allow HS binding (Williams, unpublished). This added a basic residue to an already basic region overlapping the RGD motif (giving RRRRGD) and it is likely that this creates enough of a basic patch to allow binding to HS.

During the experiments on RGDX mutants it was seen that two viruses, RGDR and RGDA (which was found to have an additional mutation (Q2861R)), often grew on MCF7 cells much better than other mutants, which had already been observed for S2871R. These mutants were therefore tested for blocking by heparin (**Figure 4.1**). Soluble heparin is a HS analogue displaying identical properties to heparan sulfate. HS analogues will occupy the free HS binding sites on viruses and prevent them binding to cell surface HS. We found that these mutants were indeed blocked by heparin, suggesting that they do have the ability to bind to HS. Thus, two new HS-binding mutants had been identified.

It is interesting that these mutants and the S2871R mutant are located close to the RGD motif. This could be significant as interactions may enhance the RGD/integrin interaction. On the other hand, this may be encouraged by the already basic nature of the RGD region in the CAV9 Griggs strain, which has the sequence RRRGD, so has three basic residues (R). Mutations giving extra basic amino acids in this region may therefore tend to give HS-binding strains. This may be a similar situation to that seen in CAV9 and some FMDV strains where a single amino acid change in VP1 near to the 5-

fold axis immediately gives a cluster of positive charges, due to the symmetry of the particle (McLeish et al., 2012; Maree et al., 2011).

The heparin binding experiment alone cannot verify if HSPG is indeed a functional receptor used for viral entry, since inhibition of infection can simply be down to the fact that the virus can aggregate on the molecule (as heparin has many potential binding sites) and can no longer be taken up by the cells because it is too big for entry.

In further confirmation of the role of HSPG in cell binding, the variants were tested on their ability to bind to immobilised heparin (**Figure 4.2**). The single amino acid substitutions found in these CAV9 variants allowed the virus to bind to the immobilised heparin with the only exception being RGDR. Interestingly, it was previously proposed that the prototype CAV9- wt (RGDM) does not bind to heparin (McLeish *et al.*, 2012). Our new findings show that CAV9- wt can partially bind to immobilised heparin, although less efficiently that the mutants. This is in agreement with another recent study (Merilahti *et al.*, 2016). The ability of CAV9 virus to bind not only to integrins but also to HSPG may be important for a successful infection when one or the other receptors is absent.

To confirm our findings and identify how important is the HSPG binding in cell infection cells were treated with sodium chlorate (**Figures 4.3 and 4.4**). Sodium chlorate inhibits sulfation reactions in the cells and thus letting the cells grow in its presence impairs the integrity of cell surface HSPG. Unfortunately, HeLa, MCF7 and RD cells did not respond well to the treatment and experiments were carried out using A549 and GMK cells only. We showed that in GMK cells, by removing the HSPG from the cell surface,

the virus can infect the cell in a more efficient way, as an increased number and size of plaques was observed. It seems that although the mutant viruses, and to a lesser extent the CAV9-wt, can bind to HSPG this may not be useful in infection of GMK cells. In fact this binding is not only unnecessary in these cells, but is actually a disadvantage. A possible explanation for our observations could be the fact that the virus has the opportunity to ‘’freely’’ move on the cell surface locating a useful receptor for efficient infection rather than being ‘’stuck’’ in a place where the receptor is not available by binding to HSPG.

On the other hand, in A549 cells the RGDR and Q286R mutants lack a ‘functional’ RGD because of the mutation in the downstream amino acids and the viruses rely on interactions with HSPG for efficient infection. In the case of A549 it seems that the binding to HSPG offers an advantage to the virus to infect certain cells. This result, together with cell type differences seen in the EDTA experiment (**Figures 3.12** and **3.13**), highlights the fact that even cells which seem to be similar in their behaviour in some ways (e.g. being infected by CAV9 in an RGD-dependent manner), may have subtle or more major differences in other properties, presumably due to different expression of surface molecules. It would be useful to investigate HS expression in these two cell lines.

Although sodium chlorate inhibits the sulfation of HSPG there is not enough research available on its effects on other sulfated molecules, such as sialic acid; a known receptor for Enterovirus- 70 (EV-70). In addition, humans and monkeys differ in the expression of sialic acid, and if this molecule is important for infection it could explain

the differences in infectivity between A549 cells (human) and GMK cells (monkey) (Varki *et al.*, 2011).

To analyse the role of HS further, CAV9 variants and the prototype were used in protamine sulphate cell blocking assays. Protamine sulphate (PS) is a drug that reverses the anticoagulant effects of heparin by binding to it. PS contains clusters of positive charged amino acids and has the capacity to bind to negatively charged sulphate of heparin and HS. In contrast with the sodium chlorate, protamine sulphate inhibited the infectivity of all CAV9 variants in A549 cells suggesting that heparan sulfate has a general role of CAV9 infection in A549 cells. In contrast, agreeing with the sodium chlorate results, GMK cells showed a slight increase in infectivity providing further evidence that the use of HSPG of the virus is not advantageous in efficient entry in these cells.

Overall, HS has a role in CAV9 infection at least in some cells such as A549, but alone is unlikely to be sufficient for virus infection. It is safe to assume that HS is part of complex network of different types of receptors which play important role in tissue tropism and the virus can switch between them according to different circumstances.

Chapter 5. General Discussion and Future Work

5.1.General Discussion

The purpose of this thesis was to understand the cell tropism of Coxsackie virus A9 (CAV9) and the importance of the RGD motif in infection and entry. We achieved this by analysing the infection in a panel of eight different cell lines using 12 different CAV9 variants at the RGD + 1 position and flow cytometry analysis on the two known receptors αvβ6 and αvβ3. These virus variants were used in an array of different experiments and these methods have helped us to better understand virus binding to the cell surface and to determine if any other possible mechanisms can be used by different cell lines. A detailed understanding of virus infection and cell surface receptors will help to establish the basis for antiviral drugs but also possibly exploit these viruses in oncolytic virus cancer treatment.

Interaction with the cell surface is the primary event in the infectious viral entry and it is generally believed that the binding of an enterovirus to the cell surface is mediated by the associations of one or more protein receptors and/or non-protein attachment factors (Fuchs & Blaas, 2010; Tuthill *et al.*, 2010). A successful cellular infection thus relies on both the attachment factors and true protein receptors that contribute to the binding of a virus to the cell surface and intracellular transport of virus particle (Mercer & Helenius, 2009). Chapter 3 is a chapter that investigates the ability of RGDX CAV9 variants to grow on different cell lines as well as expression of the known integrin receptors αvβ6 and αvβ3. Distinct patterns of infection were observed, agreeing with the already known RGD- dependent and RGD-independent pathways, but did not fully correlate with receptor expressions, suggesting that other determinants also help define tropism

of CAV9. To investigate this further, EDTA stability assays were performed. In previous studies peptides containing the DLXXL motif could bind to αvβ6 even in the absence of the RGD motif. This DLXXL plays an important role on integrin binding as it allows the virus to form a highly stable complex with the integrin after RGD binding (Dicara *et al.*, 2008). Since RGD binding to integrins is divalent cation- dependent, treatment with EDTA resulted in the inhibition of this process. However, when EDTA was added after binding, it was unable to displace CAV9 suggesting that the DLXXL motif stabilizes the RGD/ integrin interactions. Interestingly we showed that DMXXL can also stabilize these interactions. To further investigate the importance of the +1 position of the RGD motif, the RGDT variant was passaged on GMK and RD cells. In RD cells, over 9 passages the RGDT variant (codon ACG) seemed to have changed twice, firstly to AUG and later to UUC encoding the leucine amino acid (RGDL). There was rapid selection (complete by 4 passages) for a leucine codon in the case of GMK cells showing there is pressure for an optimal amino acid at the RGD position. The change observed in RD cells was very surprising as these cells seemed to be infected in an RGD- independent manner. This may suggest that there is some advantageous interaction with an integrin even in RD cells.

Chapter 4 contains an analysis of the molecular basis of the binding of HSPG affects infectivity of CAV9 variants on cells. To investigate CAV9 binding to HSPG, CAV9 wt, RGDR, S2871R, Q2861R and T132R were used in a series of different experiments. Firstly, viruses were blocked by soluble heparin and bound to immobilized heparin beads suggesting that they can attach to HSPG on the cell surface. Together with previous findings, the results suggest multiple potential mechanisms for HSPG binding

(McLeish *et al.*, 2012). Surprisingly, upon further investigating blocking of HSPG, we found that GMK cells are infected in more efficiently when HSPG binding was prevented raising questions whether the HSPG binding offers an advantage to the virus like previously thought or not.

5.2.Future Work

The work already performed has given new insights into how CAV9 infects different cell lines and the molecular determinants which underpin the interactions with integrins and HSPG. To extend the work a number of new experiments could be performed.

- The work on adapting CAV9 to different cell lines could be extended to different mutants and different cell lines representing RGD- dependent and RGD-independent infection, to investigate whether these RGD- dependent cells will give arise to the same mutation at the RGDX position, or if the preferred amino acid at the RGDX position is cell-type dependent. Similar experiments could be performed to study the RGD +4 position, the other key component of the DLXXL motif, and other surrounding amino acids. Information of this type could then be used to design viruses carrying optimal sequences as a first step to using them in oncolytic therapy.
- Another avenue to explore entry pathways of these virus variants to find whether the RGD +1 position and also HSPG binding affects the entry pathway of the virus into the cell. This could be performed using a panel of drugs targeting steps involved in different entry pathways, as well as dominant negative mutants or siRNA knock-down. How the RGD/integrin and HSPG binding influences the

involvement of other molecules thought to be needed for a post-binding step, e.g. GRP78 and β2- microglobulin (Heikkilä *et al.*, 2010), should also be explored.

- The experiments revealed that there may be other integrins involved in RGD interactions and antibody blocking assays with other known integrins which interact with RGD motifs could be used to identify if other integrins can be used as receptors by the virus.
- The experiments showed that RD cells, where infection appeared to be largely independent of integrins, are infected much more efficiently than GMK, A549 and PC3 cells, where infection uses the RGD motif. RD cells should therefore be a good model for the identification of the RGD-independent receptor for the RGD- independent mechanisms.
- The significance of CAV9 HSPG binding should be analyzed by using clinical isolates and investigating how many of these are capable of using this molecule, then using sequencing to identify the molecular basis of the interaction.

These experiments should give important new information on the significance of RGD/ integrin and HSPG binding in CAV9 and also in other viruses with an RGD motif, such as human parechoviruses and FMDV, which will underpin new strategies for their control.

Chapter 6. References

Adams MJ, Lefkowitz EJ, King AMQ et al. (2015) Ratification vote on taxonomic proposals to the International Committee on Taxonomy of Viruses (2015). *Archives of Virology*, **160**, 1837–1850.

Adams MJ, Lefkowitz EJ, King AMQ et al. (2016) Ratification vote on taxonomic proposals to the International Committee on Taxonomy of Viruses (2016). *Archives of Virology*, **161**, 2921–2949.

Adams MJ, Lefkowitz EJ, King AMQ et al. (2017) Changes to taxonomy and the International Code of Virus Classification and Nomenclature ratified by the International Committee on Taxonomy of Viruses (2017). *Archives of Virology*, **162**, 2505–2538.

Ahmedah HT, Patterson LH, Shnyder SD, Sheldrake HM (2017) RGD-binding integrins in head and neck cancers. *Cancers*, **9**.

Al-Sunaidi M, Williams CH, Hughes PJ, Schnurr DP, Stanway G (2007) Analysis of a new human parechovirus allows the definition of parechovirus types and the

identification of RNA structural domains. *Journal of Virology*, **81**, 1013–1021.

Aldabe R, Barco A, Carrasco L (1996) Membrane permeabilization by poliovirus proteins 2B and 2BC. *The Journal of biological chemistry*, **271**, 23134–7.

Baltimore D (1971) Expression of animal virus genomes. *Bacteriological reviews*, **35**, 235–241.

Baranowski E, Sevilla N, Verdaguer N, Ruiz-Jarabo CM, Beck E, Domingo E (1998) Multiple Virulence Determinants of Foot-and-Mouth Disease Virus in Cell Culture. *J. Virol.*, **72**, 6362–6372.

Baranowski E, Ruiz-Jarabo CM, Sevilla N, Andreu D, Beck E, Domingo E (2000) Cell recognition by foot-and-mouth disease virus that lacks the RGD integrin-binding motif: flexibility in aphthovirus receptor usage. *Journal of virology*, **74**, 1641–1647.

Barco A, Carrasco L (1995) A human virus protein, poliovirus protein 2BC, induces membrane proliferation and blocks the exocytic pathway in the yeast Saccharomyces cerevisiae. *The European Molecular Biology Organization*

Journal, **14**, 3349–64.

Barco A, Feduchi E, Carrasco L (2000) Poliovirus Protease 3Cpro Kills Cells by Apoptosis. *Virology*, **266**, 352–360.

Barczyk M, Carracedo S, Gullberg D (2010) Integrins. *Cell and tissue research*, **339**, 269–80.

Belsham GJ, Normann P (2008) Dynamics of picornavirus RNA replication within infected cells. *Journal of General Virology*, **89**, 485–493.

Belsham GJ, Sonenberg N (1996) RNA-protein interactions in regulation of picornavirus RNA translation. *Microbiological reviews*, **60**, 499–511.

Bender FC, Whitbeck JC, Lou H, Cohen GH, Eisenberg RJ (2005) Herpes simplex virus glycoprotein B binds to cell surfaces independently of heparan sulfate and blocks virus entry. *Journal of Virology*, **79**, 11588–11597.

Bergelson JM, Shepley MP, Chan BM, Hemler ME, Finberg RW (1992) Identification of the integrin VLA-2 as a receptor for echovirus 1. *Science (New York, N.Y.)*, **255**,

1718–1720.

Bergelson JM, Chan M, Solomon KR, St John NF, Lin H, Finberg RW (1994) Decay-accelerating factor (CD55), a glycosylphosphatidylinositol-anchored complement regulatory protein, is a receptor for several echoviruses. *Proceedings of the National Academy of Sciences of the United States of America*, **91**, 6245–6248.

Berryman S, Clark S, Monaghan P, Jackson T (2005) Early Events in Integrin alpha v beta 6-Mediated Cell Entry of Foot-and-Mouth Disease Virus. *Journal of Virology*, **79**, 8519–8534.

Bhella D, Goodfellow IG, Roversi P, Pettigrew D, Chaudhry Y, Evans DJ, Lea SM (2004) The structure of echovirus type 12 bound to a two-domain fragment of its cellular attachment protein decay-accelerating factor (CD 55). *The Journal of biological chemistry*, **279**, 8325–8332.

Boonyakiat Y, Hughes PJ, Ghazi F, Stanway G (2001) Arginine-glycine-aspartic acid motif is critical for human parechovirus 1 entry. *Journal of virology*, **75**, 10000–

10004.

Boros A, Nemes C, Pankovics P, Kapusinszky B, Delwart E, Reuter G (2012) Identification and complete genome characterization of a novel picornavirus in turkey (Meleagris gallopavo). *Journal of General Virology*, **93**, 2171–2182.

Büchen-Osmond C (2003) The universal virus database ICTVdB. *Computing in Science and Engineering*, **5**, 235–241.

Burman A, Clark S, Abrescia NG a, Fry EE, Stuart DI, Jackson T (2006) Specificity of the VP1 GH loop of Foot-and-Mouth Disease virus for alphav integrins. *Journal of virology*, **80**, 9798–9810.

Calandria C, Irurzun A, Barco Á, Carrasco L (2004) Individual expression of poliovirus 2Apro and 3Cpro induces activation of caspase-3 and PARP cleavage in HeLa cells. *Virus Research*, **104**, 39–49.

Cann AJ (2012) *Principles of Molecular Virology*, 5th edn. Elsevier, 315 pp.

Cardin AD, Weintraub HJ (1989) Molecular modeling of protein-glycosaminoglycan

interactions. *Arteriosclerosis (Dallas, Tex.)*, **9**, 21–32.

Carter JB, Saunders VA (2007) *Virology: Principles and Applications*, 2nd edn (eds Carter J, Saunders VA). John Wiley and Sons.

Castelló A, Álvarez E, Carrasco L (2011) The Multifaceted Poliovirus 2A Protease: Regulation of Gene Expression by Picornavirus Proteases. *Journal of Biomedicine and Biotechnology*, **2011**, 1–23.

Chan KP, Goh KT, Chong CY, Teo ES, Lau G, Ling AE (2003) Epidemic hand, foot and mouth disease caused by human enterovirus 71, Singapore. *Emerging Infectious Diseases*, **9**, 78–85.

Chang KH, Auvinen P, Hyypia T, Stanway G (1989) The nucleotide sequence of Coxsackievirus A9; Implications for receptor binding and enterovirus classification. *Journal of General Virology*, **70**, 3269–3280.

Chang KH, Day C, Walker J, Hyypia T, Stanway G (1992) The nucleotide sequences of wild-type coxsackievirus A9 strains imply that an RGD motif in VP1 is functionally

significant. *Journal of General Virology*, **73**, 621–626.

Chazal N, Gerlier D (2003) Virus entry, assembly, budding, and membrane rafts. *Microbiology and molecular biology reviews*, **67**, 226–37, table of contents.

Cicala C, Martinelli E, McNally JP et al. (2009) The integrin alpha4beta7 forms a complex with cell-surface CD4 and defines a T-cell subset that is highly susceptible to infection by HIV-1. *Proceedings of the National Academy of Sciences*, **106**, 20877–20882.

Coffin JM (2013) Virions at the Gates: Receptors and the Host–Virus Arms Race. *PLoS Biology*, **11**.

Curnis F, Gasparri AM, Longhi R et al. (2012) Chromogranin A binds to αvβ6-integrin and promotes wound healing in mice. *Cellular and Molecular Life Sciences*, **69**, 2791–2803.

Dalldorf G, Sickles GM (1948) An Unidentified, Filtrable Agent Isolated From the Feces of Children With Paralysis. *Science (New York, N.Y.)*, **108**, 61–62.

Dasgupta J, Bienkowska-Haba M, Ortega ME et al. (2011) Structural basis of oligosaccharide receptor recognition by human papillomavirus. *The Journal of biological chemistry*, **286**, 2617–2624.

Dicara D, Burman A, Clark S et al. (2008) Foot-and-mouth disease virus forms a highly stable, EDTA-resistant complex with its principal receptor, integrin alphavbeta6: implications for infectiousness. *Journal of Virology*, **82**, 1537–1546.

Donnelly MLL, Hughes LE, Luke G, Mendoza H, Ten Dam E, Gani D, Ryan MD (2001) The “cleavage” activities of foot-and-mouth disease virus 2A site-directed mutants and naturally occurring “2A-like” sequences. *Journal of General Virology*, **82**, 1027–1041.

Elder K, Baker D, Ribes J (2005) *Infections, Fertility and Assisted Reproduction*. Cambridge University Press, New York.

Escribano-Romero E, Jimenez-Clavero MA, Gomes P, García JA, Ley V (2004) Heparan sulphate mediates swine vesicular disease virus attachment to the host

cell. *Journal of General Virology*, **85**, 653–663.

Evans DMA, Dunn G, Minor PD et al. (1985) Increased neurovirulence associated with a single nucleotide change in a noncoding region of the Sabin type 3 poliovaccine genome. *Nature*, **314**, 548–550.

Faraj AA (2006) Poliomyelitis: Orthopaedic management. *Current Orthopaedics*, **20**, 41–46.

Feire AL, Roy RM, Manley K, Compton T (2010) The glycoprotein B disintegrin-like domain binds beta 1 integrin to mediate cytomegalovirus entry. *Journal of virology*, **84**, 10026–10037.

Feng Y, Broder CC, Kennedy PE, Berger EA (2011) HIV-1 entry cofactor: functional cDNA cloning of a seven-transmembrane, G protein-coupled receptor. *Journal of Immunology* , **186**, 6076–6081.

Fernández-Miragall O, Quinto SL d, Martínez-Salas E (2009) Relevance of RNA structure for the activity of picornavirus IRES elements. *Virus Research*, **139**, 172–

182.

Flint J, Enquist LW, Racaniello VR, Skalka AM (2009) *Principles of Virology*, 3rd Editio edn. American Society of Microbiology.

Frankel AD, Pabo CO (1988) Cellular uptake of the tat protein from human immunodeficiency virus. *Cell*, **55**, 1189–93.

Fry EE, Lea SM, Jackson T et al. (1999) The structure and function of a foot-and-mouth disease virus-oligosaccharide receptor complex. *The EMBO Journal*, **18**, 543–54.

Fuchs R, Blaas D (2010) Uncoating of human rhinoviruses. *Reviews in Medical Virology*, **20**, 281–297.

Gelderblom H (1996) Structure and classification of viruses. *Medical Microbiology*, 1–14.

Ghigo E (2010) A dilemma for viruses and giant viruses: which endocytic pathway to use to enter cells? *Intervirology*, **53**, 274–83.

Gofshteyn J, Cárdenas AM, Bearden D (2016) Treatment of Chronic Enterovirus Encephalitis With Fluoxetine in a Patient With X-Linked Agammaglobulinemia. *Pediatric Neurology*, **64**, 94–98.

Goldstein JL, Brown MS (2009) The LDL receptor. *Arteriosclerosis, Thrombosis, and Vascular Biology*, **29**, 431–438.

Gong P, Peersen OB (2010) Structural basis for active site closure by the poliovirus RNA-dependent RNA polymerase. *Proceedings of the National Academy of Sciences of the United States of America*, **107**, 22505–10.

Goodfellow IG, Sioofy AB, Powell RM, Evans DJ (2001) Echoviruses bind heparan sulfate at the cell surface. *Journal of virology*, **75**, 4918–21.

Goodman SL, Grote HJ, Wilm C (2012) Matched rabbit monoclonal antibodies against αv-series integrins reveal a novel αvβ3-LIBS epitope, and permit routine staining of archival paraffin samples of human tumors. *Biology Open*, **1**, 329–340.

Grant BD, Donaldson JG (2009) Pathways and mechanisms of endocytic recycling.

Nature reviews. Molecular cell biology, **10**, 597–608.

Grist NR, Bell EJ, Assaad F (1978) Enteroviruses in human disease. *Progress in medical virology. Fortschritte der medizinischen Virusforschung. Progrès en virologie médicale*, **24**, 114–57.

Grove J, Marsh M (2011) The cell biology of receptor-mediated virus entry. *The Journal of cell biology*, **195**, 1071–82.

Hansen CG, Nichols BJ (2009) Molecular mechanisms of clathrin-independent endocytosis. *Journal of cell science*, **122**, 1713–21.

Harvala H, Kalimo H, Stanway G, Hyypiä T (2003) Pathogenesis of coxsackievirus A9 in mice: Role of the viral arginine-glycine-aspartic acid motif. *Journal of General Virology*, **84**, 2375–2379.

Harvala H, Kalimo H, Bergelson J, Stanway G, Hyypiä T (2005) Tissue tropism of recombinant coxsackieviruses in an adult mouse model. *Journal of General Virology*, **86**, 1897–1907.

Hayer A, Stoeber M, Ritz D, Engel S, Meyer HH, Helenius A (2010) Caveolin-1 is ubiquitinated and targeted to intralumenal vesicles in endolysosomes for degradation. *The Journal of cell biology*, **191**, 615–29.

He Y, Lin F, Chipman PR et al. (2002) Structure of decay-accelerating factor bound to echovirus 7: a virus-receptor complex. *Proceedings of the National Academy of Sciences of the United States of America*, **99**, 10325–10329.

Heikkilä O (2013) *Receptors and Endocytosis of Coxsackievirus a9*.

Heikkilä O, Susi P, Stanway G, Hyypiä T (2009) Integrin αVβ6 is a high-affinity receptor for coxsackievirus A9. *Journal of General Virology*, **90**, 197–204.

Heikkilä O, Susi P, Tevaluoto T, Härmä H, Marjomäki V, Hyypiä T, Kiljunen S (2010) Internalization of coxsackievirus A9 is mediated by {beta}2-microglobulin, dynamin, and Arf6 but not by caveolin-1 or clathrin. *Journal of Virology*, **84**, 3666–3681.

Heikkilä O, Merilahti P, Hakanen M et al. (2016) Integrins are not essential for entry of coxsackievirus A9 into SW480 human colon adenocarcinoma cells. *Journal of*

Virology, **13**, 171.

Hendry E, Hatanaka H, Fry E et al. (1999) The crystal structure of coxsackievirus A9: New insights into the uncoating mechanisms of enteroviruses. *Structure*, **7**, 1527–1538.

Hewat EA, Neumann E, Conway JF, Moser R, Ronacher B, Marlovits TC, Blaas D (2000) The cellular receptor to human rhinovirus 2 binds around the 5-fold axis and not in the canyon: a structural view. *The EMBO Journal*, **19**, 6317–6325.

Hinton T, Ross-Smith N, Warner S, Belsham G, Crabb B (2002) Conservation of L and 3C proteinase activities across distantly related aphthoviruses. *Journal of General Virology*, **83**, 3111–3121.

Hober D, Alidjinou E (2013) Enteroviral pathogenesis of type 1 diabetes: queries and answers. *Current opinion in infectious diseases*, **26**, 263–269.

Hober D, Sauter P (2010) Pathogenesis of type 1 diabetes mellitus: interplay between enterovirus and host. *Nature reviews. Endocrinology*, **6**, 279–289.

Hober D, Sané F, Riedweg K, Moumna I (2013) Viruses and Type 1 Diabetes: Focus on the Enteroviruses. In: *Type 1 Diabetes*, pp. 25–69.

Hogle JM (2002) Poliovirus Cell Entry: Common Structural Themes in Viral Cell Entry Pathways. *Annual Review of Microbiology*, **56**, 677–702.

Hogle JM, Chow M, Filman DJ (1985) Three-dimensional structure of poliovirus at 2.9 A resolution. *Science (New York, N.Y.)*, **229**, 1358–1365.

Howard TP, Middelhaufe S, Moore K et al. (2013) Synthesis of customized petroleum-replica fuel molecules by targeted modification of free fatty acid pools in Escherichia coli. *Proceedings of the National Academy of Sciences*, **110**, 7636–7641.

Hughes PJ, Stanway G (2000) The 2A proteins of three diverse picornaviruses are related to each other and to the H-rev107 family of proteins involved in the control of cell proliferation. *Journal of General Virology*, **81**, 201–207.

Hughes PJ, Horsnell C, Hyypiä T, Stanway G (1995) The coxsackievirus A9 RGD motif

is not essential for virus viability. *Journal of virology*, **69**, 8035–8040.

Hussain KM, Leong KLJ, Ng MM-L, Chu JJH (2011) The essential role of clathrin-mediated endocytosis in the infectious entry of human enterovirus 71. *The Journal of biological chemistry*, **286**, 309–21.

Hussein HAM, Walker LR, Abdel-Raouf UM, Desouky SA, Montasser AKM, Akula SM (2015) Beyond RGD: virus interactions with integrins. *Archives of Virology*, **160**, 2669–2681.

Huttenlocher A, Horwitz AR (2011) Integrins in Cell Migration. *Cold Spring Harbor Perspectives in Biology*, **3**.

Huttunen M, Waris M, Kajander R, Hyypiä T, Marjomäki V (2014) Coxsackievirus A9 infects cells via nonacidic multivesicular bodies. *Journal of virology*, **88**, 5138–51.

Hyypia T, Stanway G (1993) Biology of coxsackie A viruses. *Advances in virus research*, **42**, 343–373.

Hyypia T, Hyypia T, Kallajoki M et al. (1993) Pathogenetic differences between

coxsackie A and B virus infections in newborn mice. *Virus Research*, **27**, 71–78.

Hyypia T, Hovi T, Knowles NJ et al. (1997) Classification of enteroviruses based on molecular and biological properties. *Journal of General Virology*, **78 (Pt 1)**, 1–11.

Jackson T, Ellard FM, Ghazaleh R a et al. (1996) Efficient infection of cells in culture by type O foot-and-mouth disease virus requires binding to cell surface heparan sulfate. *Journal of virology*, **70**, 5282–5287.

Jackson T, Blakemore W, Newman JWI, Knowles NJ, Mould AP, Humphries MJ, King AMQ (2000) Foot-and-mouth disease virus is a ligand for the high-affinity binding conformation of integrin α5β1: Influence of the leucine residue within the RGDL motif on selectivity of integrin binding. *Journal of General Virology*, **81**, 1383–1391.

Jackson T, King AM., Stuart DI, Fry E (2003) Structure and receptor binding. *Virus Research*, **91**, 33–46.

Jang SK, Kräusslich HG, Nicklin MJ, Duke GM, Palmenberg AC, Wimmer E (1988) A segment of the 5’ nontranslated region of encephalomyocarditis virus RNA directs

internal entry of ribosomes during in vitro translation. *Journal of virology*, **62**, 2636–43.

Jinno-Oue a, Oue M, Ruscetti SK (2001) A unique heparin-binding domain in the envelope protein of the neuropathogenic PVC-211 murine leukemia virus may contribute to its brain capillary endothelial cell tropism. *Journal of virology*, **75**, 12439–12445.

Joachims M, Harris KS, Etchison D (1995) Poliovirus Protease 3C Mediates Cleavage of Microtubule-Associated Protein 4. *Virology*, **211**, 451–461.

Johnson MS, Lu N, Denessiouk K, Heino J, Gullberg D (2009a) Integrins during evolution: Evolutionary trees and model organisms. *Biochimica et Biophysica Acta - Biomembranes*, **1788**, 779–789.

Johnson KM, Kines RC, Roberts JN, Lowy DR, Schiller JT, Day PM (2009b) Role of Heparan Sulfate in Attachment to and Infection of the Murine Female Genital Tract by Human Papillomavirus. *Journal of Virology*, **83**, 2067–2074.

Joki-Korpela P, Marjomäki V, Krogerus C, Heino J, Hyypiä T (2001) Entry of human parechovirus 1. *Journal of virology*, **75**, 1958–67.

Jokinen J, White DJ, Salmela M et al. (2010) Molecular mechanism of α2β1 integrin interaction with human echovirus 1. *The EMBO Journal*, **29**, 196–208.

Jonassen CM, Jonassen TØ, Grinde B (1998) Short Communication A common RNA motif in the 3' end of the genomes of astroviruses , avian infectious bronchitis virus and an equine rhinovirus. *Journal of General Virology*, **79**, 715–718.

de Jong AS, de Mattia F, Van Dommelen MM, Lanke K, Melchers WJG, Willems PHGM, van Kuppeveld FJM (2008) Functional Analysis of Picornavirus 2B Proteins: Effects on Calcium Homeostasis and Intracellular Protein Trafficking. *Journal of Virology*, **82**, 3782–3790.

Kaku Y, Chard LS, Inoue T, Belsham GJ (2002) Unique characteristics of a picornavirus internal ribosome entry site from the porcine teschovirus-1 talfan. *Journal of Virology*, **76**, 11721–11728.

Kaufman HL, Kohlhapp FJ, Zloza A (2015) Oncolytic viruses: a new class of immunotherapy drugs. *Nature Reviews Drug Discovery*, **14**, 642–662.

Kerkvliet J, Edukulla R, Rodriguez M (2010) Novel Roles of the Picornaviral 3D Polymerase in Viral Pathogenesis. *Advances in Virology*, **2010**, 1–9.

Khan AG, Pichler J, Rosemann A, Blaas D (2007) Human rhinovirus type 54 infection via heparan sulfate is less efficient and strictly dependent on low endosomal pH. *Journal of virology*, **81**, 4625–32.

King AMQ, Adams MJ, Carstens EB, Lefkowitz EJ (2011) *Virus taxonomy : classification and nomenclature of viruses : ninth report of the International Committee on Taxonomy of Viruses*. Elsevier.

Klose T, Kuznetsov YG, Xiao C, Sun S, McPherson A, Rossmann MG (2010) The three-dimensional structure of Mimivirus. *Intervirology*, **53**, 268–73.

Knowles NJ, Delwart E, Gorbalenya AE et al. (2012a) Picornaviridae : the ICTV Report and Beyond. 2808.

Knowles N, Hovi T, Hyypiä T (2012b) Picornaviridae. *… and nomenclature of ….*

Kraft S, Diefenbach B, Mehta R, Jonczyk A, Luckenbach GA, Goodman SL (1999) Definition of an unexpected ligand recognition motif for alphav beta6 integrin. *The Journal of biological chemistry*, **274**, 1979–85.

Krusat T, Streckert HJ (1997) Heparin-dependent attachment of respiratory syncytial virus (RSV) to host cells. *Archives of virology*, **142**, 1247–54.

Laquerre S, Argnani R, Anderson DB, Zucchini S, Manservigi R, Glorioso JC (1998) Heparan sulfate proteoglycan binding by herpes simplex virus type 1 glycoproteins B and C, which differ in their contributions to virus attachment, penetration, and cell-to-cell spread. *Journal of Virology*, **72**, 6119–6130.

Lim JP, Gleeson PA (2011) Macropinocytosis: an endocytic pathway for internalising large gulps. *Immunology and Cell Biology*, **89**, 836–843.

Lin X (2004) Functions of heparan sulfate proteoglycans in cell signaling during development. *Development*, **131**, 6009–6021.

Lin J-Y, Chen T-C, Weng K-F, Chang S-C, Chen L-L, Shih S-R (2009) Viral and host proteins involved in picornavirus life cycle. *Journal of biomedical science*, **16**, 103.

van der Linden L, Wolthers KC, van Kuppeveld FJM, Linden L, Wolthers KC, van Kuppeveld FJM (2015) Replication and Inhibitors of Enteroviruses and Parechoviruses. *Viruses*, **7**, 4529–4562.

La Linn M, Eble JA, Lübken C, Slade RW, Heino J, Davies J, Suhrbier A (2005) An arthritogenic alphavirus uses the α1β1 integrin collagen receptor. *Virology*, **336**, 229–239.

Liu Y, Wang C, Mueller S, Paul A V., Wimmer E, Jiang P (2010) Direct Interaction between Two Viral Proteins, the Nonstructural Protein 2CATPase and the Capsid Protein VP3, Is Required for Enterovirus Morphogenesis. *PLoS Pathogens*, **6**, e1001066.

Lwoff A, Horne R, Tournier P (1962) A System of Viruses. *Cold Spring Harbor Symposia on Quantitative Biology*, **27**, 51–55.

Mahy BWJ, Van Regenmortel MH V. (2010) *Desk encyclopedia of general virology*. Academic Press, 644 pp.

Major RH (1954) *A History of Medicine: volume 2.*, First Edit edn (ed Thomas C). Springfield.

Man YKS, DiCara D, Chan N et al. (2013) Structural Guided Scaffold Phage Display Libraries as a Source of Bio-Therapeutics. (ed Han Z). *PLoS ONE*, **8**.

Maree FF, Blignaut B, Aschenbrenner L, Burrage T, Rieder E (2011) Analysis of SAT1 type foot-and-mouth disease virus capsid proteins: influence of receptor usage on the properties of virus particles. *Virus research*, **155**, 462–72.

Marsh M, Helenius A (1989) Virus Entry into Animal Cells. *Advances in Virus Research*, **36**, 107–151.

Marsh M, Helenius A (2006) Virus entry: open sesame. *Cell*, **124**, 729–40.

Martínez-Salas E (2008) The impact of RNA structure on picornavirus IRES activity. *Trends in Microbiology*, **16**, 230–237.

Mateu MG, Luz Valero M, Andreu D, Domingo E (1996) Systematic replacement of amino acid residues within an Arg-Gly-Asp-containing loop of foot-and-mouth disease virus and effect on cell recognition. *Journal of Biological Chemistry*, **271**, 12814–12819.

McKnight KL, Lemon SM (1998) The rhinovirus type 14 genome contains an internally located RNA structure that is required for viral replication. *RNA (New York, N.Y.)*, **4**, 1569–84.

McLeish NJ, Williams CH, Kaloudas D, Roivainen MM, Stanway G (2012) Symmetry-Related Clustering of Positive Charges Is a Common Mechanism for Heparan Sulfate Binding in Enteroviruses. *Journal of Virology*, **86**, 11163–11170.

McMinn PC (2002) An overview of the evolution of enterovirus 71 and its clinical and public health significance. *FEMS microbiology reviews*, **26**, 91–107.

Mercer J, Helenius A (2009) Virus entry by macropinocytosis. *Nature cell biology*, **11**, 510–20.

Mercer J, Schelhaas M, Helenius A (2010) Virus entry by endocytosis. *Annual review of biochemistry*, **79**, 803–33.

Merilahti P, Koskinen S, Heikkilä O, Karelehto E, Susi P (2012) Endocytosis of integrin-binding human picornaviruses. *Advances in Virology*, **2012**.

Merilahti P, Karelehto E, Susi P (2016) Role of Heparan Sulfate in Cellular Infection of Integrin-Binding Coxsackievirus A9 and Human Parechovirus 1 Isolates. *PloS one*, **11**, e0147168.

Miller EH, Obernosterer G, Raaben M et al. (2012) Ebola virus entry requires the host-programmed recognition of an intracellular receptor. *The EMBO Journal*, **31**, 1947–1960.

Mirmomeni MH, Hughes PJ, Stanway G (1997) An RNA Tertiary Structure in the 3 J Untranslated Region of Enteroviruses Is Necessary for Efficient Replication. *Journal of virology*, **71**, 2363–2370.

Mondor I, Ugolini S, Sattentau QJ (1998) Human immunodeficiency virus type 1

attachment to HeLa CD4 cells is CD4 independent and gp120 dependent and requires cell surface heparans. *Journal of Virology*, **72**, 3623–3634.

Moreau B, Bastedo C, Michel RP, Ghali P (2011) Hepatitis and encephalitis due to Coxsackie virus A9 in an adult. *Case Reports in Gastroenterology*, **5**, 617–622.

Muckelbauer JK, Kremer M, Minor I et al. (1995) The structure of coxsackievirus B3 at 3.5 A resolution. *Structure (London, England : 1993)*, **3**, 653–667.

Nelsen-Salz B, Eggers HJ, Zimmermann H (1999) Integrin αvβ3 (vitronectin receptor) is a candidate receptor for the virulent echovirus 9 strain Barty. *Journal of General Virology*, **80**, 2311–2313.

Nisole S, Saïb A (2004) Early steps of retrovirus replicative cycle. *Retrovirology*, **1**, 9.

Oberste MS, Maher K, Kilpatrick DR, Pallansch M a (1999) Molecular evolution of the human enteroviruses: correlation of serotype with VP1 sequence and application to picornavirus classification. *Journal of Virology*, **73**, 1941–1948.

Oh MD, Park S, Choi Y et al. (2003) Acute hemorrhagic conjunctivitis caused by

coxsackievirus A24 variant, South Korea, 2002. *Emerging Infectious Diseases*, **9**, 1010–1012.

Ohkuma S, Poole B (1978) Fluorescence probe measurement of the intralysosomal pH in living cells and the perturbation of pH by various agents. *Proceedings of the National Academy of Sciences of the United States of America*, **75**, 3327–31.

Olofsson S, Bergström T (2005) Glycoconjugate glycans as viral receptors. *Annals of Medicine*, **37**, 154–172.

Pabbaraju K, Wong S, Chan ENY, Tellier R (2013) Genetic characterization of a Coxsackie A9 virus associated with aseptic meningitis in Alberta , Canada in 2010. *Virology Journal*, **10**, 1–9.

De Palma AM, Vliegen I, De Clercq E, Neyts J (2008) Selective inhibitors of picornavirus replication. *Medicinal research reviews*, **28**, 823–84.

Palmenberg a, Neubauer D, Skern T (2010) Genome Organization and Encoded Proteins. *The Picornaviruses*, 3–17.

Pathak HB, Arnold JJ, Wiegand PN, Hargittai MRS, Cameron CE (2007) Picornavirus genome replication: assembly and organization of the VPg uridylylation ribonucleoprotein (initiation) complex. *The Journal of biological chemistry*, **282**, 16202–13.

Paul A, Rieder E, Kim D, van JB, Wimmer E (2000) Identification of an RNA hairpin in poliovirus RNA that serves as the primary template in the in vitro uridylylation of VPg. *Journal of Virology*, **74**, 10359–10370.

Paul A V, Peters J, Mugavero J, Yin J, van Boom JH, Wimmer E (2003) Biochemical and genetic studies of the VPg uridylylation reaction catalyzed by the RNA polymerase of poliovirus. *Journal of virology*, **77**, 891–904.

Pelkmans L, Helenius A (2002) Endocytosis via caveolae. *Traffic (Copenhagen, Denmark)*, **3**, 311–20.

Pelletier J, Sonenberg N (1985) Insertion mutagenesis to increase secondary structure within the 5’ noncoding region of a eukaryotic mRNA reduces translational

efficiency. *Cell*, **40**, 515–26.

Pellinen T, Ivaska J (2006) Integrin traffic. *Journal of cell science*, **119**, 3723–3731.

Pitkäranta A, Arruda E, Malmberg H, Hayden FG (1997) Detection of rhinovirus in sinus brushings of patients with acute community-acquired sinusitis by reverse transcription-PCR. *Journal of clinical microbiology*, **35**, 1791–3.

Plevka P, Hafenstein S, Harris KG et al. (2010) Interaction of decay-accelerating factor with echovirus 7. *Journal of Virology*, **84**, 12665–12674.

Plevka P, Perera R, Cardosa J, Kuhn RJ, Rossmann MG (2012) Crystal Structure of Human Enterovirus 71. *Science*, **336**, 1274–1274.

Plevka P, Perera R, Yap ML, Cardosa J, Kuhn RJ, Rossmann MG (2013) Structure of human enterovirus 71 in complex with a capsid-binding inhibitor. *Proceedings of the National Academy of Sciences of the United States of America*, **110**, 5463–7.

Racaniello VR (1990) Cell receptors for picornaviruses. *Current topics in microbiology and immunology*, **161**, 1–22.

Reddi H V, Lipton HL (2002) Heparan sulfate mediates infection of high-neurovirulence Theiler's viruses. *Journal of Virology*, **76**, 8400–8407.

Ren J, Wang X, Hu Z et al. (2013) Picornavirus uncoating intermediate captured in atomic detail. *Nature Communications*, **4**, 1009–1034.

Richards AL, Jackson WT (2012) Intracellular vesicle acidification promotes maturation of infectious poliovirus particles. *PLoS pathogens*, **8**, e1003046.

Robertson MP, Igel H, Baertsch R, Haussler D, Ares M, Scott WG (2004) The Structure of a Rigorously Conserved RNA Element within the SARS Virus Genome. *PLoS Biology*, **3**, 86–94.

Rohll JB, Percy N, Ley R, Evans DJ, Almond JW, Barclay WS (1994) The 5'-untranslated regions of picornavirus RNAs contain independent functional domains essential for RNA replication and translation. *Journal of Virology*, **68**, 4384–91.

Roivainen M, Klingel K (2009) Role of enteroviruses in the pathogenesis of type 1 diabetes. *Diabetologia*, **52**, 995–996.

Roivainen M, Hyypiä T, Piirainen L, Kalkkinen N, Stanway G, Hovi T (1991) RGD-dependent entry of coxsackievirus A9 into host cells and its bypass after cleavage of VP1 protein by intestinal proteases. *Journal of virology*, **65**, 4735–4740.

Rossmann MG, Arnold E, Erickson JW et al. (1985) Structure of a human common cold virus and functional relationship to other picornaviruses. *Nature*, **317**, 145–153.

Rossmann MG, He Y, Kuhn RJ (2002) Picornavirus- receptor interactions. *Trends in Microbiology*, **10**, 324–331.

Ruiz-Sáenz J, Goez Y, Tabares W, López-Herrera a. (2009) Cellular receptors for foot and mouth disease virus. *Intervirology*, **52**, 201–212.

Ruoslahti E (1991) Integrins. *Journal of Clinical Investigation*, **87**, 1–5.

Ruoslahti E, Pierschbacher MD (1987) New perspectives in cell adhesion: RGD and integrins. *Science (New York, N.Y.)*, **238**, 491–497.

Ryan MD, Flint M (1997) Virus-encoded proteinases of the picornavirus super-group. *Journal of General Virology*, **78**, 699–723.

Salguero FJ, Sánchez-Martín MA, Díaz-San Segundo F, de Avila A, Sevilla N (2005) Foot-and-mouth disease virus (FMDV) causes an acute disease that can be lethal for adult laboratory mice. *Virology*, **332**, 384–396.

Sanders B, Koldijk M, Schuitemaker H (2015) Inactivated Viral Vaccines. In: *Vaccine Analysis: Strategies, Principles, and Control* (eds Nunnally BK, Turula VE, Sitrin RD), pp. 45–80. Springer.

Santti J, Harvala H, Kinnunen L, Hyypiä T (2000) Molecular epidemiology and evolution of coxsackievirus A9. *Journal of General Virology*, **81**, 1361–1372.

Sarrazin S, Lamanna WC, Esko JD (2011) Heparan sulfate proteoglycans. *Cold Spring Harbor perspectives in biology*, **3**.

Sasaki J, Nagashima S, Taniguchi K (2003) Aichi virus Leader protein is involved in viral RNA replication and encapsidation. *Journal of virology*, **77**, 10799–10807.

Sawyer MH (2002) Enterovirus infections: diagnosis and treatment. *Seminars in pediatric infectious diseases*, **13**, 40–7.

Schelhaas M (2010) Come in and take your coat off - how host cells provide endocytosis for virus entry. *Cellular microbiology*, **12**, 1378–88.

Seitsonen J, Susi P, Heikkilä O, Sinkovits RS, Laurinmäki P, Hyypiä T, Butcher SJ (2010) Interaction of alphaVbeta3 and alphaVbeta6 integrins with human parechovirus 1. *Journal of virology*, **84**, 8509–8519.

Shafren DR, Gardner J, Mann VH, Antalis TM, Suhrbier A (1999) Picornavirus receptor down-regulation by plasminogen activator inhibitor type 2. *Journal of Virology*, **73**, 7193–7198.

Shakeel S, Seitsonen JJT, Kajander T, Laurinmäki P, Hyypiä T, Susi P, Butcher SJ (2013) Structural and functional analysis of coxsackievirus A9 integrin αvβ6 binding and uncoating. *Journal of virology*, **87**, 3943–51.

Shieh MT, WuDunn D, Montgomery RI, Esko JD, Spear PG (1992) Cell surface receptors for herpes simplex virus are heparan sulfate proteoglycans. *The Journal of cell biology*, **116**, 1273–1281.

Shingler KL, Yoder JL, Carnegie MS, Ashley RE, Makhov AM, Conway JF, Hafenstein S (2013) The Enterovirus 71 A-particle Forms a Gateway to Allow Genome Release: A CryoEM Study of Picornavirus Uncoating. (ed Rey FA). *PLoS Pathogens*, **9**.

Shukla D, Spear PG (2001) Herpesviruses and heparan sulfate: An intimate relationship in aid of viral entry. *Journal of Clinical Investigation*, **108**, 503–510.

Sieczkarski SB, Whittaker GR (2002) Influenza virus can enter and infect cells in the absence of clathrin-mediated endocytosis. *Journal of Virology*, **76**, 10455–10464.

Skidmore MA, Guimond SE, Rudd TR, Fernig DG, Turnbull JE, Yates EA (2008) The activities of heparan sulfate and its analogue heparin are dictated by biosynthesis, sequence, and conformation. *Connective tissue research*, **49**, 140–4.

Smith KM (1943) *Beyond the Microscope* (eds Beales HL, Williams WE). Penguin Books, 9-17 pp.

Smyth MS, Martin JH (2002) Picornavirus uncoating. *Molecular pathology*, **55**, 214–9.

Solomon T, Lewthwaite P, Perera D, Cardosa MJ, McMinn P, Ooi MH (2010) Virology, epidemiology, pathogenesis, and control of enterovirus 71. *The Lancet Infectious Diseases*, **10**, 778–790.

Spiller OB, Goodfellow IG, Evans DJ, Hinchliffe SJ, Morgan BP (2002) Coxsackie B viruses that use human DAF as a receptor infect pig cells via CAR and do not use pig DAF. *Journal of General Virology*, **83**, 45–52.

Springer TA (2002) Predicted and experimental structures of integrins and β-propellers. *Current Opinion in Structural Biology*, **12**, 802–813.

Stanway G (1990) Structure , function and evolution of picornaviruses. *Journal of General Virology*, **71**, 2483–2501.

Stanway G, Hyypiä T (1999) Parechoviruses. *Journal of virology*, **73**, 5249–5254.

Stanway G, Kalkkinen N, Roivainen M et al. (1994) Molecular and biological characteristics of echovirus 22, a representative of a new picornavirus group. *Journal of Virology*, **68**, 8232–8238.

Stanway G, Joki-Korpela P, Hyypia T (2000) Human parechoviruses - biology and clinical significance. *Reviews in Medical Virology*, **10**, 57–69.

Stanway G, Brown F, Christian P et al. (2005) *Family Picornaviridae. In: "Virus Taxonomy. Eighth Report of the International Committee on Taxonomy of Viruses".*, 8th edn (eds Fauquet CM, Mayo MA, Maniloff, J., Desselberger U, Ball LA). Elsevier/Academic Press, London, 757-778 pp.

Stergiou L, Bauer M, Mair W et al. (2013) Integrin-Mediated Signaling Induced by Simian Virus 40 Leads to Transient Uncoupling of Cortical Actin and the Plasma Membrane. (ed Johannes L). *PLoS ONE*, **8**.

Stewart PL, Nemerow GR (2007) Cell integrins: commonly used receptors for diverse viral pathogens. *Trends in Microbiology*, **15**, 500–507.

Strikas RA, Anderson LJ, Parker RA (1986) Temporal and geographic patterns of isolates of nonpolio enterovirus in the United States, 1970-1983. *The Journal of infectious diseases*, **153**, 346–51.

Sweeney TR, Cisnetto V, Bose D et al. (2010) Foot-and-mouth disease virus 2C is a hexameric AAA+ protein with a coordinated ATP hydrolysis mechanism. *The Journal of Biological Chemistry*, **285**, 24347–59.

Takei K, Haucke V (2001) Clathrin-mediated endocytosis: membrane factors pull the trigger. *Trends in cell biology*, **11**, 385–91.

Tapparel C, Siegrist F, Petty TJ, Kaiser L (2013) Picornavirus and enterovirus diversity with associated human diseases. *Infection, genetics and evolution : journal of molecular epidemiology and evolutionary genetics in infectious diseases*, **14**, 282–93.

Taube S, Jiang M, Wobus CE (2010) Glycosphingolipids as Receptors for Non-Enveloped Viruses. *Viruses*, **2**, 1011–1049.

Teterina NL, Pinto Y, Weaver JD, Jensen KS, Ehrenfeld E (2011) Analysis of poliovirus protein 3A interactions with viral and cellular proteins in infected cells. *Journal of virology*, **85**, 4284–96.

Thomas GJ, Nyström ML, Marshall JF (2006) αvβ6 integrin in wound healing and cancer of the oral cavity. *Journal of Oral Pathology and Medicine*, **35**, 1–10.

Tiwari V, Liu J, Valyi-Nagy T, Shukla D (2011) Anti-heparan Sulfate Peptides That Block Herpes Simplex Virus Infection *in Vivo*. *Journal of Biological Chemistry*, **286**, 25406–25415.

Todd S, Semler BL (1996) Structure- infectivity analysis of the human rhinovirus genomic RNA 3 ′ non-coding region. *Mutagenesis*, **24**, 2133–42.

Tracy S, Drescher KM, Chapman NM (2011) Enteroviruses and type 1 diabetes. *Diabetes/Metabolism Research and Reviews*, **27**, 820–823.

Triantafilou M, Triantafilou K, Wilson KM, Takada Y, Fernandez N, Stanway G (1999) Involvement of β2-microglobulin and integrin α(v)β3 molecules in the coxsackievirus A9 infectious cycle. *Journal of General Virology*, **80**, 2591–2600.

Triantafilou M, Triantafilou K, Wilson KM (2000a) A 70 kDa MHC class I associated protein (MAP-70) identified as a receptor molecule for coxsackievirus A9 cell

attachment. *Human Immunology*, **61**, 867–878.

Triantafilou K, Triantafilou M, Takada Y, Fernandez N (2000b) Human parechovirus 1 utilizes integrins alphavbeta3 and alphavbeta1 as receptors. *Journal of Virology*, **74**, 5856–62.

Triantafilou K, Fradelizi D, Wilson K, Triantafilou M (2002) GRP78, a coreceptor for coxsackievirus A9, interacts with major histocompatibility complex class I molecules which mediate virus internalization. *Journal of Virology*, **76**, 633–643.

Turnbull J, Powell A, Guimond S (2001) Heparan sulfate: decoding a dynamic multifunctional cell regulator. *Trends in cell biology*, **11**, 75–82.

Turner RB (2007) Rhinovirus: More than Just a Common Cold Virus. *The Journal of Infectious Diseases*, **195**, 765–766.

Tuthill TJ, Groppelli E, Hogle JM, Rowlands DJ (2010) Picornaviruses. *Current Topics Microbiol ogy and Immunology*, **343**, 43–89.

Varki NM, Strobert E, Dick EJ, Benirschke K, Varki A (2011) Biomedical Differences

Between Human and Nonhuman Hominids: Potential Roles for Uniquely Human Aspects of Sialic Acid Biology. *Annual Review of Pathology: Mechanisms of Disease*, **6**, 365–393.

Villarreal LP (2004) Are viruses alive? *Scientific American*, **291**, 100–105.

Vlasak M, Goesler I, Blaas D (2005) Human Rhinovirus Type 89 Variants Use Heparan Sulfate Proteoglycan for Cell Attachment Human Rhinovirus Type 89 Variants Use Heparan Sulfate Proteoglycan for Cell Attachment. *Journal of Virology*, **79**, 5963–5970.

Vuorinen T, Vainionpaa R, Heino J, Hyypia T (1999) Enterovirus receptors and virus replication in human leukocytes. *Journal of General Virology*, **80 (Pt 4)**, 921–927.

Ward T, Powell RM, Pipkin PA, Evans DJ, Minor PD, Almond JW (1998) Role for beta2-microglobulin in echovirus infection of rhabdomyosarcoma cells. *Journal of virology*, **72**, 5360–5.

Whitton JL, Cornell CT, Feuer R (2005) Host and virus determinants of picornavirus

pathogenesis and tropism. *Nature Reviews Microbiology*, **3**, 765–776.

Wildenbeest JG, van den Broek PJ, Benschop KS et al. (2011) Pleconaril revisited: clinical course of chronic enteroviral meningoencephalitis after treatment correlates with in vitro susceptibility. *Antiviral Therapy*, **17**, 459–466.

Williams CH, Kajander T, Hyypiä T, Jackson T, Sheppard D, Stanway G (2004) Integrin alpha v beta 6 is an RGD-dependent receptor for coxsackievirus A9. *Journal of Virology*, **78**, 6967–6973.

Woo PCY, Lau SKP, Li T et al. (2015) A novel dromedary camel enterovirus in the family Picornaviridae from dromedaries in the Middle East. *Journal of General Virology*, **96**, 1723–1731.

Wu KX, Ng MML, Chu JJH (2010) Developments towards antiviral therapies against enterovirus 71. *Drug Discovery Today*, **15**, 1041–1051.

Xia H, Wang P, Wang G-C et al. (2015) Human Enterovirus Nonstructural Protein 2CATPase Functions as Both an RNA Helicase and ATP-Independent RNA

Chaperone (ed Semler BL). *PLOS Pathogens*, **11**, e1005067.

Xiao C, Bator CM, Bowman VD et al. (2001) Interaction of coxsackievirus A21 with its cellular receptor, ICAM-1. *Journal of Virology*, **75**, 2444–2451.

Yin-Murphy M, Almond JW (1996) Picornaviruses.

Ypma-Wong MF, Dewalt PG, Johnson VH, Lamb JG, Semler BL (1988) Protein 3CD is the major poliovirus proteinase responsible for cleavage of the P1 capsid precursor. *Virology*, **166**, 265–70.

Zhou Y, Vedantham P, Lu K et al. (2015) Protease inhibitors targeting coronavirus and filovirus entry. *Antiviral Research*, **116**, 76–84.

Zhu W, Li J, Liang G (2011) How does cellular heparan sulfate function in viral pathogenicity? *Biomedical and environmental sciences : BES*, **24**, 81–87.